Report No. K-TRAN: KSU-12-6 ▪ FINAL REPORT ▪ August 2016

Influence of Rock Salt Impurities on Limestone Aggregate Durability

Kyle A. Riding, Ph.D., P.E.
Jonathan Varner
Cale Armstrong

Kansas State University Transportation Center

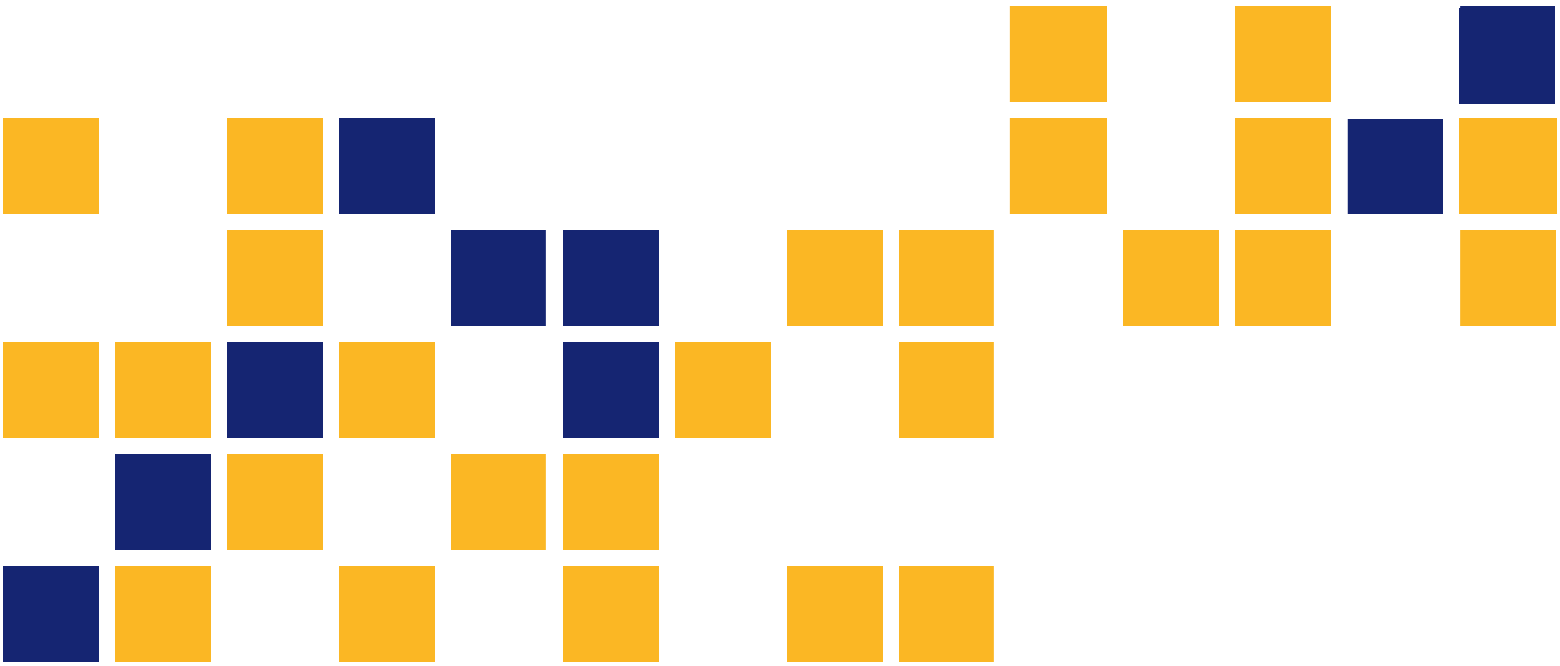

Kansas Department of Transportation

1 Report No. K-TRAN: KSU-12-6	**2 Government Accession No.**	**3 Recipient Catalog No.**
4 Title and Subtitle Influence of Rock Salt Impurities on Limestone Aggregate Durability		**5 Report Date** August 2016 **6 Performing Organization Code**
7 Author(s) Kyle A. Riding, Ph.D., P.E., Jonathan Varner, Cale Armstrong		**7 Performing Organization Report No.**
9 Performing Organization Name and Address Kansas State University Transportation Center Department of Civil Engineering 2118 Fiedler Hall Manhattan, Kansas 66506		**10 Work Unit No. (TRAIS)** **11 Contract or Grant No.** C1913
12 Sponsoring Agency Name and Address Kansas Department of Transportation Bureau of Research 2300 SW Van Buren Topeka, Kansas 66611-1195		**13 Type of Report and Period Covered** Final Report January 2012–December 2015 **14 Sponsoring Agency Code** RE-0575-01
15 Supplementary Notes For more information write to address in block 9.		

Non-durable coarse aggregate in concrete pavement can break down under repeated freeze-thaw cycles. Application of rock salt may increase the severity of exposure conditions because of trace compounds, such as calcium sulfate, in rock salt. Concrete and saw-cut limestone specimens were also subjected to wet-dry cycles in varying salt solutions to examine the influence of trace compounds in rock salt. Subsequently, limestone aggregate in concrete was subjected to freeze-thaw cycling in two methods: salt-treating the aggregate before batching concrete, and half-immersing concrete specimens in rock salt solution during freeze-thaw cycling. The wet-dry testing of cut limestone was not severe enough to determine the effects of trace compounds in salt solution. Preliminary experiments showed that salt-treating the aggregates before batching concrete showed more promise in differentiating aggregate quality or in gaining insights into concrete pavement performance. Concrete prisms were made using 12 different salt-treated aggregates and were tested according to Kansas Test Method KTMR-22 (2006) and additionally ASTM C666 (2008) using Method A. Companion prisms were made using the same aggregates without salt treatment and were tested using the same two freeze-thaw test methods.

Use of saw-cut limestone prisms for testing the freeze-thaw durability of concrete aggregates is not recommended as crushing limestone may change its properties, prisms from the same source have variable quality, and prisms are labor-intensive to make. Further testing should be conducted to validate the potential use of ASTM C666 Method A as a method to achieve similar freeze-thaw acceptance results as Method B in fewer freeze-thaw cycles. Freeze-thaw tests of concrete made with aggregates presoaked in salt brine could provide a good method to test the effects of salt exposure on internal freeze-thaw distress on the paste portion of the concrete. However, salt treatment may not be an effective method to use for coarse aggregate qualification.

17 Key Words Rock Salt, Limestone Aggregate, Aggregate Durability, Freeze-Thaw Cycles		**18 Distribution Statement** No restrictions. This document is available to the public through the National Technical Information Service www.ntis.gov.	
19 Security Classification (of this report) Unclassified	**20 Security Classification (of this page)** Unclassified	**21 No. of pages** 162	**22 Price**

Form DOT F 1700.7 (8-72)

This page intentionally left blank.

Influence of Rock Salt Impurities on Limestone Aggregate Durability

Final Report

Prepared by

Kyle A. Riding, Ph.D., P.E.
Jonathan Varner
Cale Armstrong

Kansas State University Transportation Center

A Report on Research Sponsored by

THE KANSAS DEPARTMENT OF TRANSPORTATION
TOPEKA, KANSAS

and

KANSAS STATE UNIVERSITY TRANSPORTATION CENTER
MANHATTAN, KANSAS

August 2016

PREFACE

The Kansas Department of Transportation's (KDOT) Kansas Transportation Research and New-Developments (K-TRAN) Research Program funded this research project. It is an ongoing, cooperative and comprehensive research program addressing transportation needs of the state of Kansas utilizing academic and research resources from KDOT, Kansas State University and the University of Kansas. Transportation professionals in KDOT and the universities jointly develop the projects included in the research program.

NOTICE

The authors and the state of Kansas do not endorse products or manufacturers. Trade and manufacturers names appear herein solely because they are considered essential to the object of this report.

This information is available in alternative accessible formats. To obtain an alternative format, contact the Office of Public Affairs, Kansas Department of Transportation, 700 SW Harrison, 2nd Floor – West Wing, Topeka, Kansas 66603-3745 or phone (785) 296-3585 (Voice) (TDD).

DISCLAIMER

The contents of this report reflect the views of the authors who are responsible for the facts and accuracy of the data presented herein. The contents do not necessarily reflect the views or the policies of the state of Kansas. This report does not constitute a standard, specification or regulation.

Abstract

Non-durable coarse aggregate in concrete pavement can break down under repeated freeze-thaw cycles. Application of rock salt may increase the severity of exposure conditions because of trace compounds, such as calcium sulfate, in rock salt. Concrete and saw-cut limestone specimens were also subjected to wet-dry cycles in varying salt solutions to examine the influence of trace compounds in rock salt. Subsequently, limestone aggregate in concrete was subjected to freeze-thaw cycling in two methods: salt-treating the aggregate before batching concrete, and half-immersing concrete specimens in rock salt solution during freeze-thaw cycling. The wet-dry testing of cut limestone was not severe enough to determine the effects of trace compounds in salt solution. Preliminary experiments showed that salt-treating the aggregates before batching concrete showed more promise in differentiating aggregate quality or in gaining insights into concrete pavement performance. Concrete prisms were made using 12 different salt-treated aggregates and were tested according to Kansas Test Method KTMR-22 (2006) and additionally ASTM C666 (2008) using Method A. Companion prisms were made using the same aggregates without salt treatment and were tested using the same two freeze-thaw test methods.

Use of saw-cut limestone prisms for testing the freeze-thaw durability of concrete aggregates is not recommended as crushing limestone may change its properties, prisms from the same source have variable quality, and prisms are labor-intensive to make. Further testing should be conducted to validate the potential use of ASTM C666 Method A as a method to achieve similar freeze-thaw acceptance results as Method B in fewer freeze-thaw cycles. Freeze-thaw tests of concrete made with aggregates presoaked in salt brine could provide a good method to test the effects of salt exposure on internal freeze-thaw distress on the paste portion of the concrete. However, salt treatment may not be an effective method to use for coarse aggregate qualification.

Acknowledgements

The advice and assistance of Joshua Welge, Kyle Larson, Will Lindquist, and other KDOT personnel for providing aggregate samples, making concrete prisms with salt-treated aggregates, as well as information on standard procedures such as salt application practices of various districts is gratefully acknowledged.

Table of Contents

List of Tables

List of Figures

Chapter 1: Introduction

1.1 Background

Concrete pavements in Kansas are subjected to repeated cycles of freezing and thawing during the winter. In order to remove ice and maintain safe driving conditions, these roadways are often exposed to high concentrations of deicer compounds. However, deicers increase the severity of the freeze-thaw exposure conditions. Rock salt, which can contain substances other than sodium chloride, is a common deicer containing impurities that may increase the severity of pavement exposure conditions. These exposure conditions are common in Kansas and cause concrete pavement deterioration, especially if non-durable coarse aggregate is used.

1.2 Problem Statement

Certain non-durable coarse aggregates in concrete pavement degrade under freeze-thaw action. Deicing salt application increases the severity of exposure conditions and severity may be further increased by the presence of impurities in deicers. Thus, certain non-durable coarse aggregates in concrete may degrade with deicer application, causing premature deterioration of concrete pavement.

1.3 Objectives

1. Determine if a concrete freeze-thaw test using impure rock salt can differentiate durable and non-durable coarse aggregates.
2. Determine the effects of impure rock salt on limestone aggregate without freeze-thaw action.
3. Analyze rock salt for the presence of potentially deleterious substances.
4. Determine if the use of Method A instead of Method B in KTMR-22 (2006) testing could reduce the number of cycles required to determine acceptance.
5. Determine if the use of salts in freeze-thaw testing could better differentiate between marginal and quality aggregates.

1.4 Scope of Research

Various experiments were conducted to examine the influence of rock salt impurities. For Phase I of this study, concrete containing limestone aggregate was subjected to two methods of freeze-thaw testing: treating coarse aggregate with impure rock salt prior to casting concrete and half-immersing concrete specimens in impure rock salt during freeze-thaw cycling. Wet-dry testing of both saw-cut limestone prisms and concrete containing limestone aggregate in impure rock salt was also conducted. The chemistry of rock salt was studied using inductively coupled plasma analysis and X-ray diffraction. Rock salt samples from individual storage sheds throughout Kansas were analyzed for composition variations.

Phase II of this study involved freeze-thaw testing of 12 sets of concrete prisms, each with a different source of limestone coarse aggregate. Half of the prisms batched in each set contained aggregates that were treated with salt brine prior to freeze-thaw testing.

Chapter 2: Literature Review

Frost durability of stone for use as concrete aggregate or dimension stone has been extensively studied. Durability is not "an intrinsic property" of the material and depends on the exposure conditions (Pigeon & Pleau, 1995).

2.1 D-Cracking

The quality of coarse aggregate influences the frost durability of concrete pavement. D-cracking results from the use of frost-susceptible aggregate that degrades under freeze-thaw conditions and damages the surrounding cement paste. Pavement cracks appear on the surface parallel to joints, generally preceded by cracking at the bottom of the slab. The aggregate must be sufficiently saturated with water for damage to occur (Koubaa, Snyder, & Janssen, 2002).

2.2 Kansas Department of Transportation Practices

2.2.1 Kansas Department of Transportation Deicing Salt Practices

The Kansas Department of Transportation (KDOT) divides Kansas into six districts that use varying methods of salt application and salt sources. District One uses magnesium chloride ($MgCl_2$) in the Topeka and Kansas City metro areas, as well as sodium chloride (NaCl) in solid form or applied as brine. Other parts of the district use NaCl in either form. Brine concentration used in Kansas is 23% salt as measured by a hydrometer. Salt used by District One comes from Hutchinson Salt, Independent Salt, Cargill, or Central Salt (Jaci Vogel, KDOT District Maintenance Engineer, personal communication, October 27, 2011).

District Two also applies NaCl as brine (23% salt solution) or solid form with salt originating from Independent Salt or the Hutchinson Salt Company (James Roudybush, KDOT District Maintenance Engineer, personal communication, November 2, 2011). Salt application rates are varied based on temperature and precipitation. The amount of salt, either in brine or solid form, applied per lane mile increases with increasing severity of a freezing event.

District Three uses a "salt sand mix," pretreats with salt brine, and purchases salt from Hutchinson, KS (Joseph Finley, KDOT District Maintenance Engineer, personal communication,

November 4, 2011). District Four uses NaCl brine for pre-treatment and deicing and purchases "medium graded salt" from the Cargill or Hutchinson salt companies (John Hrenak, KDOT District Maintenance Engineer, personal communication, November 2, 2011). District Five also uses NaCl in a 23% salt brine and purchases salt from the Hutchinson Salt Company or from Cargill's mine in Lyons, KS (Scott Koopmann, KDOT District Maintenance Engineer, personal communication, November 2, 2011). District Six uses NaCl in a 23% brine solution with salt from Central Salt in Lyons, KS, and Hutchinson Salt Company in Hutchinson, KS (Ron Hall, KDOT District Maintenance Engineer, personal communication, November 2, 2011).

2.2.2 Deicing Salt Impurities

Rock salt applied to Kansas roads is not pure NaCl and the composition varies based on the salt source. For example, one chemical analysis showed salt to be 98.7% NaCl, in addition to sulfate, calcium, magnesium, and sodium ferrocyanide decahydrate, also called yellow prussiate of soda (Lloyd Cady, QA Mine Manager for Cargill, personal communication, December 1, 2011). Another analysis found the salt to be 95.25% NaCl with varying amounts of impurities, such as calcium or sodium sulfate and magnesium (Todd Hamer, Area Sales Manager for Central Salt, personal communication, November 17, 2011).

2.3 Frost Damage to Concrete

2.3.1 Crystallization Pressure Theory

Scherer and Valenza (2005) state ice crystallization pressure causes internal frost damage. Ice crystals form within pores and are separated from pore walls by a narrow film of liquid. The film arises because of repulsion between the crystal and pore wall which allows the crystal to grow toward of the pore wall, exerting pressure. The resulting pressure causes damage in the material surrounding the pore. In mortar, entrained air voids counteract this pressure by nucleating ice in the air voids which causes removal of water from the pore network. Sun (2010) also discusses frost damage in the presence of entrained air voids. Ice forms in the air voids, drawing water out of the capillary voids and causing contraction.

2.3.2 Critical Degree of Saturation of Concrete

Frost damage to concrete requires sufficient saturation (Li, Pour-Ghaz, Castro, & Weiss, 2012). Li et al. studied air-entrained mortar in freeze-thaw and moisture sorption tests. In moisture sorption tests, greater air content increased the amount of water absorbed but reduced the degree of saturation reached due to additional volume provided by the air entrainment. Samples were also subjected to freeze-thaw tests at varying degrees of vacuum saturation. Damage, measured by changes in the relative elastic modulus using active acoustic emission, decreased as saturation was reduced. The critical degree of saturation was determined as 88%, which Li et al. state "appears to be independent of the air content." Accordingly, greater air content does not change the critical degree of saturation but increases the time required for critical saturation to occur as there is more total volume to be filled with water. Li et al. also noted that greater air content did not prevent damage above the critical degree of saturation.

2.4 Frost Damage to Aggregate

2.4.1 Hydraulic Pressure Theory

Verbeck and Landgren (1960) studied effects of aggregate on concrete frost durability based on the hydraulic pressure theory, which states that damage occurs from water movement caused by ice formation. They investigated the time needed to reach critical saturation of the aggregate and resulting behavior once saturated. Aggregates require time to saturate sufficiently for frost damage to occur based on pore size distribution and porosity. With a greater amount of smaller pores, the required time to critical saturation decreases as moisture is both absorbed and retained more readily at lower relative humidity levels compared to a pore system with larger pores. The time to critical saturation for a given pore size distribution increases with greater porosity. Properties of the paste surrounding the aggregate also influences the time to critical saturation by decreasing permeability and increasing cover thickness to increase the time to critical saturation. Verbeck and Landgren also examined instantaneous freezing of a critically saturated aggregate, but this is unlikely to occur in concrete outside the lab.

Damage during freezing of a critically saturated aggregate can be a function of aggregate size (Verbeck & Landgren, 1960). At lower freezing rates, ice formation causes water movement

through the aggregate. The resulting pressure depends on freezing rate and porosity, size, and permeability of the aggregate. “Critical size” refers to the aggregate size below which hydraulic pressure can be sustained by the aggregate. The combination of “moderate” porosity and low permeability can lead to a lower critical size value. Expulsion of water from the aggregate can also damage the surrounding paste. The amount of water expelled into the paste increases with increasing aggregate size and porosity, subsequently increasing the volume of air-entrained paste needed to “accommodate” the expelled water. Increased entrained air content can reduce the required paste volume. Verbeck and Landgren also note that the freezing point is lowered if the pore solution contains “water-soluble salts and cement alkalies.” Ice formation is also reduced if water is adsorbed or in very fine pores. The lower freezing point or decreased ice formation reduces hydraulic pressures.

2.4.2 Aggregate Pore Size Effects

The size of an aggregate’s pores influences its durability (Hudec, 1987). Hudec states that “The shape of the pore is not as important as the size of the shortest direction. It determines most of the properties of that pore space.” Hudec also notes that capillary transport can cause expansion or contraction, depending on pore size. Very small pores ($<4\times10^{-5}$ in.) can lead to expansion from osmosis between the pores and external water. Contraction can occur in stones containing capillary pores (4×10^{-5} to 0.04 in.) due to capillary tension, but the stone may return to original size upon full saturation. Deicing salt leads either to contraction by increased capillary tension or expansion due to osmosis if the external solution becomes more dilute than the pore solution. As a result of these effects, wetting and drying may be sufficient to break down the stone, particularly for stones containing mostly pores smaller than 4×10^{-5} inches. Adsorption also affects pore solution as bound water will have a lower vapor pressure. Dissolved ions in the pore solution tend to increase adsorption effects. Hudec also notes that osmotic effects from deicing salts are likely the cause of increased damage in freeze-thaw in salt solution.

Collins (1988) found small pores to be detrimental. He studied aggregate durability by freeze-thaw testing of concrete, mercury porosimetry, and optical petrography. Comparison of aggregate freeze-thaw performance, porosity, and strength showed that pore size distribution and

strength are related to durability. Frost susceptibility was greater as the amount of pores smaller than 8×10^{-6} inches increased. The author also noted that the effect of smaller pores could be offset by a sufficient volume of pores larger than 8×10^{-6} inches. For a given pore size distribution, increased strength resulted in greater durability. However, Collins noted limitations to mercury porosimetry, which Pitt, Schluter, Lee, and Dubberke (1987) also describe as the "ink bottle" effect. In the case of a large pore with a narrow entry, mercury porosimetry categorizes the pore according only to the radius of the entry. Collins (1988) also used petrography to study the aggregate, identifying larger pores as well as various durable attributes of the stone. Collins also observed that a relatively impervious matrix could surround susceptible elements in the aggregate.

2.4.3 Combined Effect of Pore Network and Minerology

Hudec (1987) notes that stone mineralogy also has a significant influence on durability since some minerals, such as clays or chert, are more active than others and cause increased adsorption within aggregate pores. Dunn and Hudec (1966) studied durability of carbonate stone based on its clay fraction, noting that stone durability depends on porosity and mineralogy. Stones reaching the lowest degree of vacuum saturation after 24 hours immersion were more durable. Differential thermal analysis indicated that less water froze in non-durable stones to the extent that no freezing was detected in some stones, even at temperatures as low as -40 °F. This result was attributed to water binding to clay minerals. The authors noted that damage may occur from expansion of this unfrozen water as temperature decreases. Clay distribution within the stone also affects durability, as concentrated and water-accessible clay could make a stone non-durable. The authors noted that dolomite may not bind to clay during stone formation, leading to concentration of clay and reducing durability. Conversely, calcite may bind to clay, causing clay dissemination throughout the stone and no durability reduction.

2.5 Influence of Salt on Concrete

2.5.1 Salt Crystallization Pressure

Damage to porous masonry can occur from crystallization of salt, as described by Scherer (2004). First, salt crystals are precipitated from solution. Crystal growth exerts pressure against pore walls because a 4 to 8×10^{-8} inch layer of solution exists between the crystal and pore wall, allowing the crystal to grow toward the pore wall. Crystal formation requires super-saturation of the solution, and the location of super-saturation depends on solution movement through porous material.

2.5.2 Moisture Transport of Salt Solutions in Concrete

Salt affects moisture transport in concrete. Spragg et al. (2011) measured moisture sorption and desorption of concrete and mortar in dilute and concentrated solutions of NaCl, $MgCl_2$, and calcium chloride ($CaCl_2$). Concrete samples were immersed in the solutions according to ASTM C1585. Dilute NaCl solution (0.7%) slightly increased the amount of fluid absorbed, but other salt solutions, including 23% NaCl, decreased the amount of fluid absorbed compared to deionized water. The absorbed amount varied based on salt type, but increasing the salt concentration reduced absorbed fluid for all salt types. Reduced absorption in salt solution was attributed to increasing viscosity (η) and surface tension (γ) occurring from increased salt concentration. Spragg et al. used "the square root of the ratio of surface tension and viscosity of the fluid $((\gamma/\eta))^{(1/2)}$" to compare water and salt solutions. As the $((\gamma/\eta))^{(1/2)}$ value of a salt solution decreases relative to water, the relative absorption also decreases.

Following solution absorption, Spragg et al. (2011) then dried the samples at 50% relative humidity (RH) and 73 °C. Samples containing salt solutions lost less water, particularly those treated in concentrated solution, compared to deionized water. Increased salt concentration increased disparity, but the 0.7% NaCl solution increased water loss. The rate of moisture loss during drying was slower than the rate of moisture uptake during wetting. The authors noted, therefore, "concrete is more likely to become preferentially increasingly wet over time."

Absorption of deionized water into the samples was then measured (Spragg et al., 2011). Again, treatment with salt solution reduced the amount of water absorbed compared to deionized

water, even for 0.7% NaCl. However, the absorbed fluid amount increased for all samples as compared to the initial sorption test, even when deionized water was used for both tests. Spragg et al. also conducted ASTM C1585 on concrete stored in various states ranging from oven-dry to vacuum saturated. The drier the storage environment, the more moisture was absorbed.

Spragg et al. (2011) also measured mass during drying of mortar saturated in concentrated solutions of NaCl, $CaCl_2$, and $MgCl_2$, as well as deionized water. RH of the drying environment was gradually reduced from 97.5% to 0%. The salt-treated samples gained mass at the first step (97.5% RH) and then gradually lost water as RH was decreased. Sample mass dropped below initial saturated weight only when RH dropped below the equilibrium RH of the salt solution.

2.5.3 Frost Damage to Concrete in Salt Solution

Litvan (1976) studied cement paste in freeze-thaw in various concentrations of NaCl. Length change measurements showed an increased net expansion in dilute solutions that decreased as solution concentration increased. The author used differential thermography that showed ice formed at the freezing point of the "eutectic" solution and the salt solution. The eutectic solution consistently froze at approximately -8 °F, and was preceded by freezing of the salt solution at a higher temperature. The difference between the two temperatures decreased as salt concentration increased. Differential thermography showed ice formation at one point for specimens in water or 26% NaCl.

Dunn and Hudec (1966) also subjected various stones to freezing in NaCl solution. Differential thermal analysis showed freezing point depression, slower freezing rate, and reduced ice formation compared to freezing in water.

Shi, Fay, Peterson, and Yang (2010) tested non-air-entrained concrete in freeze-thaw cycles in deionized water and various dilute (approximately 3%) solutions of deicers. Samples were tested according to Chappelow et al. (1992) using concrete samples placed on a sponge immersed in various solutions subjected to 10 freeze-thaw cycles. The 3% by mass NaCl solution significantly increased mass loss of the concrete sample compared to deionized water. Chemical alteration of the paste was also observed by SEM/EDX methodology. The authors

stated, “We hypothesize that the exposure of the cement paste to sodium chloride led to the preferential dissolution of silicate-rich type I C-S-H and the releasing of calcium sulfate ($CaSO_4$) from AFm and AFt phases.”

2.5.4 Sodium Salt Attack of Concrete

Haynes, O’Neill, Neff, and Mehta (2008) observed salt weathering of concrete exposed to sodium sulfate (Na_2SO_4), using river gravel for coarse aggregate and Type II cement with 5% tricalcium aluminate. Cylinders were partially immersed in a 5% by mass solution of Na_2SO_4, tap water, or kept dry. Exposure conditions varied to include constant temperature and relative humidity as well as cyclic exposure to varying temperature and/or relative humidity. Samples were kept in the exposure conditions for approximately 3 years, although 1.5 years in relative humidity levels were reduced to increase damage. Damage was thought to occur primarily from salt crystallization rather than chemical sulfate attack, although some chemical sulfate attack was observed. Loss of scaled material primarily occurred below the evaporation front and above the solution level. The authors attributed salt damage to formation of mirabilite, the hydrous form of Na_2SO_4, rather than anhydrous thernardite. The authors observed mirabilite crystallization in environmental conditions where thernardite only was expected. The authors also noted that alkali-silica gel appeared, though they did not list it as a primary cause of damage.

Haynes, O’Neill, Neff, and Mehta (2010) also researched the effect of sodium carbonate (Na_2CO_3) and NaCl on concrete, using the same concrete and environmental conditions as the study published in 2008. NaCl was found to be less destructive than Na_2CO_3 and both were found to be less destructive than Na_2SO_4. NaCl caused negligible scaling when compared to the other two salts. Damage from NaCl and Na_2CO_3 was primarily due to salt crystallization, in particular the formation of hydrous Na_2CO_3, according to the authors. Chemical alteration of the paste occurred with sodium carbonate and NaCl leading to slight depletion of sulfur dioxide and increased sodium oxide levels near the solution level. The authors also noted that symptoms of alkali-silica reaction appeared for specimens treated with Na_2CO_3, which may have contributed to damage.

2.5.5 Concrete Durability in Wet/Dry Cycles in Salt

Darwin, Browning, Gong, and Hughes (2007) subjected concrete prisms to cyclical wetting and drying in deicing salt solutions. NaCl, $MgCl_2$, $CaCl_2$, and calcium-magnesium-acetate (CMA) were used in 1.06 and 6.04 molal concentrations, as well as air and distilled water for control specimens. The NaCl grade was not explicitly stated, but since distilled water was used to make the solutions it is probable that the NaCl was either technical or reagent grade. Damage was monitored by relative dynamic modulus of elasticity, referred to as $P_{w/d}$, similar to measurements used in ASTM C666 (2008) freeze-thaw testing. The results of the specimens subjected to concentrated deicers are given in Figure 2.1 (Darwin, Browning, Gong, & Hughes, 2008). The dilute and concentrated NaCl solutions initially increased the $P_{w/d}$, which was attributed to moisture absorption or pore filling by salt. After reaching a maximum value, $P_{w/d}$ decreased over time in the concentrated NaCl solution, but did not appreciably decrease for dilute NaCl. The time to reach the maximum $P_{w/d}$ was greater for concentrated NaCl than for dilute NaCl. Surface scaling was noted in concentrated NaCl and "few signs of damage" were noted for specimens in dilute NaCl (Darwin et al., 2007).

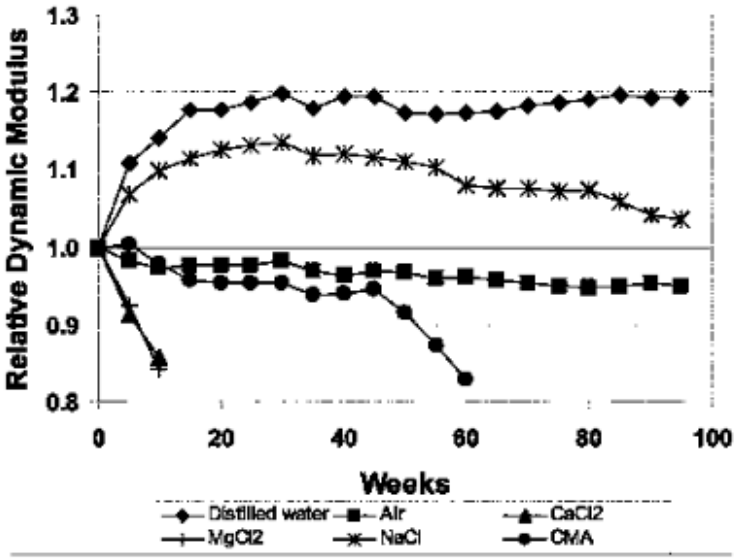

Fig. 1—Relative dynamic modulus of elasticity (wet-dry) $P_{w/d}$ versus number of weekly wet-dry cycles for specimens exposed to 6.04 molal ion concentration deicer solutions.

Figure 2.1: Relative Dynamic Modulus of Concrete Exposed to Various Deicer Salts
Source: Darwin et al. (2008), with permission from American Concrete Institute

Wang, Nelsen, and Nixon (2006) tested paste and concrete samples subjected to wet/dry cycles in deicing salt solutions, including NaCl and distilled water as a control. Freeze-thaw cycles were also conducted using these solutions. In wet/dry cycles, mass change was similar when samples were immersed in NaCl or water. Scaling was also negligible for samples in both solutions, though in NaCl solution compressive strength decreased slightly as the number of wet/dry cycles increased. In freeze-thaw cycles, scaling was slightly more severe for NaCl than water. However, with increasing freeze-thaw cycles, compressive strength increased slightly for samples in NaCl as compared to an initial increase followed by a slight decrease for samples in water.

2.5.6 Chemical Attack on Concrete from NaCl

Sutter et al. (2008) conducted an extensive study of concrete durability, examining chemical attack and scaling resistance in various concentrated deicers. Various test methods were employed, including ASTM C666 Method A with 3×3×11-inch concrete prisms in concentrated salt solutions. In almost all of the tests, NaCl was found to be relatively benign to concrete (corrosion was not considered), although NaCl affected concrete chemistry through formation of Friedel's salt and depletion of calcium hydroxide. The exception was a non-standard freeze-thaw test including oven-drying and exposure to deicing solutions. Increased damage was attributed to physical effects of the salt, including increased moisture retention, salt crystallization, and thermal expansion. An analysis of the NaCl solution used showed trace amounts of sulfur and other ions in addition to sodium and chloride.

2.6 Salt Impact on Aggregate Frost Durability

2.6.1 Effect of Deicing Salt on Aggregate

Crumpton, Smith, and Jayaprakash (1989) conducted a study on concrete “cups” made by taking concentric cores of field concrete, some with the inner core off-center to create variable thickness. These cores were filled with a 15% salt solution made with a locally used Kansas deicing salt, indicating impurities were present in the NaCl. The cups were then subjected to a number of wetting and drying cycles and damage was assessed by observation. The hygroscopic

nature of the salt solution was observed by the cups adsorbing sufficient water to keep the exterior damp at high humidity. The authors noted that “On days when it was raining outdoors, the moisture buildup on the outside of the cups was often great enough to dissolve some of the salt deposits.” Capillary sorption was also noted as the tops of the cups became coated with salt although the solution level was approximately one half-inch below the top of the cup. Salt crystallized on the cup exterior most rapidly in cracks (including those in the aggregate) and then aggregate-paste boundaries. The rate of moisture transport through individual aggregates varied, and was more rapid in aggregates that became coated in salt.

Concrete performance varied in the study (Crumpton et al., 1989). In several cups, the paste was scaled more than the aggregate but in other cups aggregate scaled more than the paste. The authors described scaled material of paste or aggregate as “oatmeal-sized” flakes, although one aggregate lost “a bean-shaped flake” 0.6 inches long. The authors also tested a sealer that led to cup cracking after the first cycle, indicating lower durability since the cups without the sealer did not crack even after 12 cycles (a cycle was 14 days). The authors also included “clinical observations” of field performance of aggregate as influenced by deicing salt, such as increased severity of alkali-aggregate reaction. Other observations included salt deposits in limestone and chemical degradation of aggregate leading to formation of sulfate salts.

2.6.2 Chemical Attack in Salt Solution

Gillott (1978) examined a number of quartzite and limestone samples for length change in continuous immersion in water and salt solutions. Limestone composition varied in amount and formation of dolomite or calcite as well as grain size range. Dilute and concentrated solutions of NaCl, $CaCl_2$, and magnesium sulfate ($MgSO_4$) were used. Length change varied based on stone composition, occurring for some stones only in sulfate solutions but in other stones only noticeably in chloride salt solutions. Electron micrographs of limestone before and after testing showed rounding of surfaces, indicating stone damage. Scaling or dissolution of the stones occurred, limiting observation of a consistent location over time using an electron microscope. The author noted that chemical attack from salt solutions occurred particularly at discontinuities in the stone matrix, such as cleavages or grain boundaries.

Gillott (1980) used scanning electron microscopy to study additional stones subjected to immersion in salt solutions of $CaCl_2$ and $MgSO_4$. He noted the carbonate fraction of the stones was most susceptible to salt attack. Damage effects were scaling and disintegration.

2.6.3 Interaction of Deicing Salt and Carbonate Stones

Hudec (1980) reported results of two studies examining carbonate stones for length change and absorption, testing stones that had been dried after immersion in 3% NaCl. More silica (mostly clay and chert) in the stone corresponded to increased absorption and increased loss in a freeze-thaw test of bare aggregate and $MgSO_4$ soundness test. NaCl treatment increased absorption at 92% RH for stones with low absorption, although absorption decreased or was unchanged for stones of high absorption. At 45% RH, NaCl treatment had little effect on absorption. Stone expansion during absorption was also measured, showing NaCl treatment increased expansion in stones of low expansion without NaCl and decreased expansion when the expansion was high without NaCl.

2.7 Effect of Salt Impurities on Concrete

Pitt et al. (1987) conducted a series of experiments examining the effect of deicing salt impurities on concrete frost durability. Samples were treated in various ways with saturated salt brines containing NaCl and comparatively small amounts of gypsum and then subjected to freeze-thaw testing.

Pitt et al. (1987) first tried four ways of applying salt brine to mortar cylinders over a 28-day period and then subjected the cylinders to freeze-thaw testing according to ASTM C666 Method A. None of the four methods caused noticeable damage without freeze-thaw testing. The first (“Method 1”) and most damaging method was to immerse the cylinders halfway in salt solution for 28 days. The second method filled an indentation in the cylinders. The third method alternated between 4 days total immersion in solution followed by 3 days drying. The last method was total immersion. During freeze-thaw testing, samples that were half-immersed in solutions containing 1.57% and 3.10% gypsum by weight of solute cracked below solution level. These samples, as measured by “pulse velocity ratio” according to ASTM C597, were the only

cylinders to deteriorate significantly during freeze-thaw testing. Half-immersion in salt solution also reduced splitting tensile strength, even in samples immersed only in NaCl. Loss for treatment with NaCl alone was approximately 10%, and gypsum addition caused greater loss. Mercury porosimetry was used to compare samples treated in NaCl with samples treated with NaCl solution containing 3.1% gypsum. The addition of gypsum increased porosity at the solution level and reduced porosity above and below the solution level. The authors noted reduced pore size could have led to increased freeze-thaw damage. Chemical tests run on the samples showed that the addition of gypsum had a varying effect on chloride and sulfate contents, depending on the gypsum amount added and location of the sample tested. For example, chloride content increased below solution level but decreased at the sample midpoint with the addition of gypsum.

Pitt et al. (1987) ran a further set of experiments on samples exposed to freeze-thaw cycles while half-immersed in salt brines containing NaCl and varying amounts of gypsum. Half-immersion during freeze-thaw increased the rate of damage and reduced the number of cycles. Below the solution level, cracks “perpendicular to the longitudinal axis of the cylinders” were initially observed but became more disordered with time. The authors observed a pessimum effect of gypsum content as the damage measured by pulse velocity ratio increased and then decreased with increasing gypsum content. However, brine composition data indicated that while gypsum content increased, NaCl content decreased, indicating an overall drop in solution concentration. Tensile strength of samples subjected to freeze-thaw cycles was determined and varied with increasing gypsum content in a manner similar to that observed for pulse velocity ratio readings. Mercury porosimetry indicated pore filling with the addition of NaCl and gypsum, the extent of which increased then decreased with increasing gypsum content, similar to results of tensile strength and freeze-thaw testing. X-ray diffraction data indicated that treatment with NaCl solution without gypsum led to increased formation of ettringite as well as formation of Friedel’s salt. Gypsum addition increased formation of ettringite and Friedel’s salt, thus causing pore filling. The authors also indicated that Friedel’s salt, which “does not contain the sulfate radical found in ettringite,” is more responsible than ettringite for pore-filling due to decreased sulfate concentrations in freeze-thaw treated samples. The authors noted that less than 0.5%

sulfate (by weight of solute) influenced mortar durability, and the primary damage mechanism was pore filling by Friedel's salt and possibly ettringite.

Pitt et al. (1987) also examined cores of concrete from an intersection of two roads, one heavily salted and the other not. Away from the intersection on the un-salted road, the chloride concentration decreased and the sulfate concentration increased slightly, correlating with laboratory testing. Chloride concentration was also higher at joints and lower at mid-points of slabs.

2.8 ASTM C666 using Salt Solutions

Salt solutions have been used to modify the ASTM C666 (2008) test method. Results and methods of a number of modified ASTM C666 tests are described.

2.8.1 Iowa DOT Salt-Treated Aggregates Study

Dubberke and Marks (1985) tested aggregate durability by salt treating coarse aggregate used to make concrete tested by ASTM C666 Method B with a 90-day moist curing time. NaCl was used because of reduced field performance of aggregate as the amount of deicing salt applied on roads increased. Aggregate was oven-dried at 230 °F for 24 hours and then soaked in a saturated solution of NaCl for 24 hours with the solution dumped over the aggregate upon removal from the oven. The process was repeated five times and the aggregate rinsed before mixing. Salt-treatment increased test severity. A reduction in "initial sonic modulus" was noted, indicating some damage occurred to the concrete before testing. However, test results correlated well with field performance. Durable aggregates were relatively unaffected by the test, lasting 300 freeze-thaw cycles with slight reduction in durability factor (DF) compared to the test run on untreated aggregate. Non-durable aggregates were severely impacted by salt-treatment and failed the test within 100 cycles. Untreated, DF of the non-durable aggregates after 300 cycles was greater than 90. The effect of salt-treatment on a non-durable aggregate is shown in Figure 2.2, where "NaCl only" refers to the salt-treatment method. One aggregate, "a low-porosity, fine-grained Farmington Stone," was severely damaged by the salt-treatment, with cracking in the aggregate that was not present without salt-treatment. The authors pointed out possible

mechanisms for the severity, including retention of water due to the salt, depressed freezing point, or salt crystallization. Aggregate chemistry was also examined, showing that increased sulfur content correlated to reduced durability, "especially when magnesium is present." Iron content could also be a factor, as the authors noted the possibility of a deleterious reaction in concrete when a "porous pyritic dolomite" is used as aggregate. The grade of NaCl used was not mentioned (i.e., rock salt, food, or reagent grade).

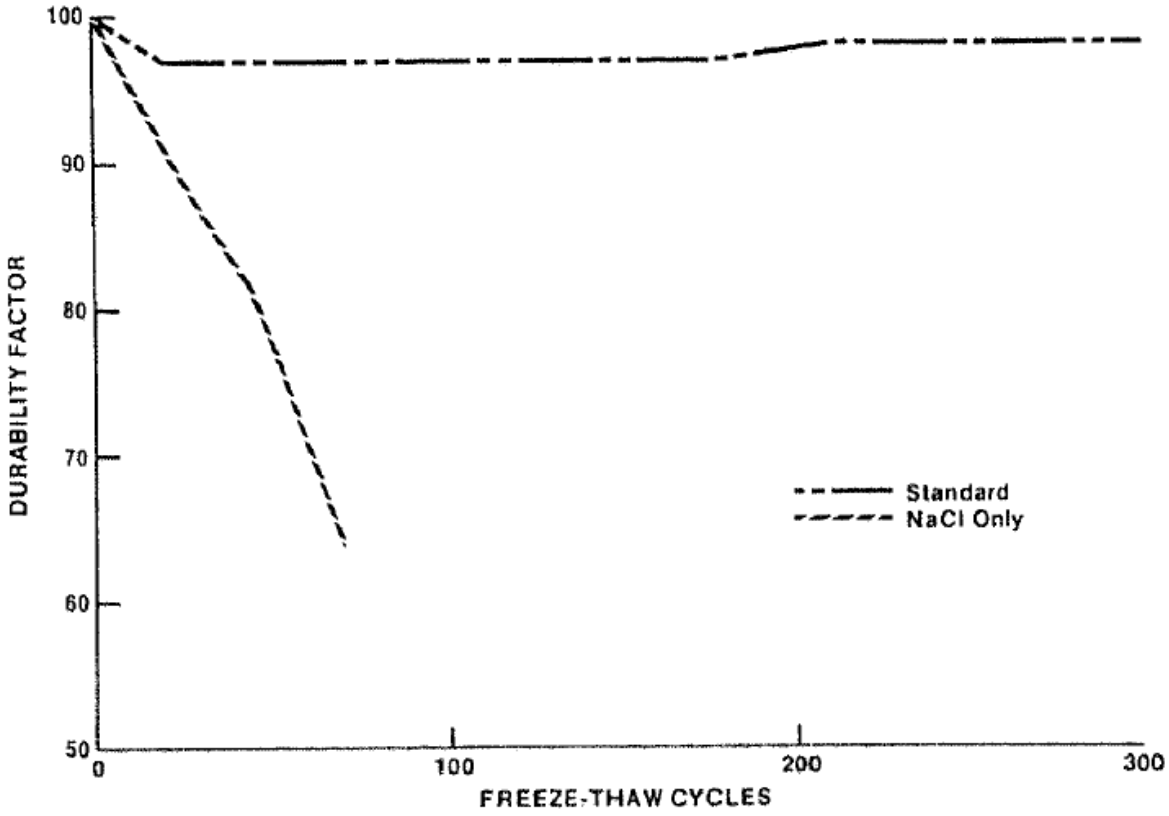

FIGURE 5 Smith durability factors.

Figure 2.2: Iowa DOT Salt-Treated Aggregate Results
Source: Dubberke and Marks (1985), with permission from the Transportation Research Board

2.8.2 Further ASTM C666 Testing using Salt-Treated Aggregates

Koubaa and Snyder (1996) evaluated aggregate durability using three variations of ASTM C666 Method B, the Washington hydraulic fracture test, and the Virginia Polytechnic

Institute single-cycle slow-freeze test. The three ASTM C666 Method B variations were, in order of increasing severity: unmodified, prisms wrapped in cloth, or salt-treated aggregate. In this study, “durable” and “marginal to non-durable” aggregates were not significantly impacted by salt-treatment. Non-durable aggregates were affected, with lower DF values and greater expansion than unmodified Procedure B method. Not all non-durable aggregates were equally affected, as the drop in DF varied between seven and 73. A similar pattern held for increased expansion, although a slight reduction in DF did not necessarily correspond to a minimal increase in expansion. The authors noted that the salt-treated aggregate procedure correlated best with field performance. Koubaa, Snyder, and Peterson (1997) also published this data in greater detail in a report for the Minnesota DOT.

Koubaa et al. (2002) also used the salt-treated coarse aggregate test method to assess frost durability of several coarse aggregates using various mitigation measures. Some measures included reducing water to cement ratio, blending durable and non-durable aggregates, and reducing coarse aggregate size.

2.8.3 Virginia DOT ASTM C666 Testing in Salt Solution

The Research Council of the Virginia Department of Highways and Transportation (VDH&T) compared results of ASTM C666 Method A using water or NaCl solution (Newlon, 1978). The concrete was moist-cured for 14 days and then dried for 7 days in the lab with a relative humidity between 35% and 45% prior to testing. Salt solutions of 2%, 3%, and 4% were used to study the effect of solution concentration on test results. Durable aggregates were used in the study, and air content and cementitious material were varied. The average DF of concrete with air content of 3.5% and 8% decreased with the addition of salt solution, but did not drop below 95 regardless of concentration. Variability increased as indicated by larger standard deviations. Without air entrainment, the average DF was 5.8 in a 2% salt solution. Type II, IP, and I cement with fly ash were used as replacement for Type I portland cement, and were moist-cured for 67 days without a drying period prior to testing (due to equipment failure). DF values for alternate cementitious materials were lower even in water. The addition of salt solution to the test reduced DF slightly except for the batch containing fly ash, in which the average DF

increased by approximately 12. However, variability with fly ash when tested in water was high as the standard deviation was approximately 14.

2.8.4 ASTM C666 Testing in Salt Solution Containing Gypsum

Detwiler and Powers-Couche (1999) tested concrete according to ASTM C666 Procedure A in 3% salt solution. The solute was NaCl or NaCl with 5% replacement with gypsum. Specimens were also examined by petrography and a scanning electron microscope was used to observe ettringite formation in air voids. Concrete was made using siliceous river gravel and varying cement types. Gypsum was added to the cement for some batches. Concrete fresh air content (by ASTM C231) was about 2% or 4%. In concrete with low air content, ettringite formation was not observed in air voids, but with higher air content, ettringite and/or calcium hydroxide formation was noted in air voids. For Type I cement, ettringite formation occurred earlier when gypsum was present in the salt solution compared to only NaCl. When gypsum was added to Type I cement, ettringite formation was limited to near the surface. For Type II cement in NaCl solution, ettringite was observed near the scaled surface and in small air voids near the surface of the concrete, although calcium hydroxide formation was more prevalent. These effects were not appreciably affected by gypsum addition to NaCl solution. The authors noted freeze-thaw action was the primary damage mechanism and ettringite formation was an effect.

2.9 Dimension Stone Durability

Dimension stone performance under freeze-thaw action or salt weathering cycles has been extensively studied.

2.9.1 Critical Degree of Saturation of Building Stone

Chen, Yeung, and Mori (2004) examined a welded tuff for critical degree of saturation using a freezing rate of 59 °F/h. Samples were saturated by immersion “in distilled water under vacuum condition for 72 h.” After one freeze-thaw cycle, compressive strength, P-wave velocity, and change in porosity were measured. The critical degree of saturation was determined to be 70%, the lowest saturation level in which loss of compressive strength and P-wave velocity were observed. Increased porosity was observed beginning at a 70% saturation level. Above 78%

saturation, surface cracks appeared, increasing in width with increasing saturation level. Two saturated samples were also examined for water movement during the test. One sample was frozen by immersion in liquid nitrogen, and the other frozen in a chamber at 0 °F. In the nitrogen-frozen sample, saturation was comparatively consistent between the surface and center of the specimen, but for the sample frozen at 0 °F, the saturation level was higher towards the sample exterior. The authors noted the results indicate water movement towards the specimen surface during freezing.

2.9.2 Stone in Freeze-Thaw in Salt Solution

Wessman (1996) studied the effect of salt on frost durability of stone, observing the critical degree of saturation and length change based on salt type and concentration. Wessman found the critical degree of saturation to be approximately 90%, regardless of salt type or concentration. Sodium sulfate slightly increased deformations between 100% and 90% saturation levels when compared to NaCl. Deformation at 100% saturation in salt solution was approximately equal regardless of salt type or concentration, although the addition of salt increased the deformation in comparison to water. However, only 1% and 0.5% salt solutions were used in the study.

McGreevy (1982) subjected limestone to freeze-thaw cycles in water, NaCl, $MgSO_4$, and Na_2SO_4 solutions of varying concentrations. The author found that increased concentration reduced mass loss, although the use of dilute NaCl increased the damage compared to water. The author also compared solution uptake of limestone in water and in salt solutions, showing that limestone absorbed less salt solution.

2.9.3 Salt Influence on Drying

Gonçalves, Pel, and Rodrigues (2007) used magnetic resonance imaging (MRI) to observe moisture movement during drying of masonry with and without NaCl. The samples used were made of plaster, mortar, and stone. Drying occurred initially from the sample surface, but over time the evaporation front progressed into the sample interior. The addition of salt decreased the overall evaporation rate of the samples, thereby maintaining an evaporation front at the sample surface for more time. Reduced evaporation in salt solution was attributed to the

influence of equilibrium RH (RH_{eq}) of the salt solution as it decreased the "driving RH gradient for vapour transport," with the evaporation rate decreasing as salt concentration near the surface increased during the drying period. The authors also noted subsequent salt crystallization at the surface may impede evaporation as well.

2.9.4 Comparison of Salt Type in Stone Weathering

Benavente, Garcia del Cura, Garcia-Guinea, Sanchez-Moral, and Ordonez (2004) studied crystallization of salt in pores, comparing NaCl and Na_2SO_4, the latter of which caused more stone damage. NaCl crystallized at the stone surface, whereas hydrous and anhydrous forms of Na_2SO_4 crystallized within the stone. Crystallization was also observed in glass capillary tubes, showing that NaCl formed at the water/vapor interface and Na_2SO_4 formed below the interface. Rodriguez-Navarro and Doehne (1999) also noted these effects in their glass capillary tube experiment.

Ruiz-Agudo, Mees, Jacobs, and Rodriguez-Navarro (2007) conducted a salt comparison study of Na_2SO_4 and $MgSO_4$ in limestone. Location of salt crystallization varied for the two salts as solution uptake was slower for $MgSO_4$ compared to Na_2SO_4. $MgSO_4$ crystallized deeper within the stone and caused cracking, whereas Na_2SO_4 crystals formed underneath the surface and caused scaling. However, both salts produced hydrated and anhydrous forms so it was unclear precisely how salt crystallization produces damage.

Cardell, Benavente, and Rodríguez-Gordillo (2008) studied the influence of dilute and concentrated solutions of calcium, magnesium, potassium, and sodium sulfates as well as various combinations of these salts. Moisture transport was more rapid with dilute solutions, though concentrated solutions led to more damage. Increased viscosity of concentrated solution slowed capillary rise, moving the evaporation front within the stone and causing salt crystallization. Damage was observed as limestone dissolution and formation of "microfissures." Furthermore, calcium and magnesium carbonate formation at the surface from dissolved constituents was noted. Salt type also altered damage symptoms because sodium solutions led to scaling, whereas magnesium solutions generated cracks. The authors also reported that mixing salts reduced damage.

2.9.5 Influence of Evaporation Rate on Sodium Salt Crystallization

Rodriguez-Navarro and Doehne (1999) found that salt crystallization is influenced by the salt type and environment, specifically RH changes. NaCl crystals formed in drops of salt solution showed different NaCl crystals based upon location within the drop. Salt crystallization within limestone showed that NaCl mostly formed efflorescence at the surface with minor scaling occurring under the efflorescence at low RH. These results were attributed to an increased evaporation rate allowing damaging crystal formation within the stone. Small pores were filled with NaCl, hindering capillary rise of the salt solution. The authors noted that NaCl crystal formation was slower compared to Na_2SO_4, which may have reduced damaging crystallization pressure.

2.9.6 Variations in Stone Permeability During Salt Weathering

McCabe, McKinley, Gomez-Heras, and Smith (2011) studied permeability of stone subjected to salt weathering in a combined solution of NaCl and $MgSO_4$. The authors used geostatistics to plot variation in permeability values over the stone surface over the course of the experiment. Permeability measurements were taken from numerous points on the sample surface. Permeability measurements reflected the influence of salt deposition, as permeability decreased due to salt crystallization in surface pores and then increased when salt removed material from the surface, exposing pores not yet filled with salt. This process occurred non-uniformly over the stone surface, which the authors explained using the concept of “dynamic instability,” or when initial material variations are “exploited” by the weathering process causing variable rates of decay over the stone surface.

Buj, Gisbert, McKinley, and Smith (2011) used similar methods on two limestone types subjected to salt weathering in NaCl or $MgSO_4$ solutions. The authors noted that differences in stone morphology govern the weathering process, relating high or low permeability values to particular features of the stone. The authors also noted that salt crystallization can reduce permeability by pore filling yet also increase it by expanding or creating cracks.

2.10 Summary

Durability of an aggregate depends heavily on its mineralogy and the size and distribution of pores. Smaller pores are typically more detrimental, either from generating increased hydraulic pressure during freeze-thaw action or osmotic and sorption effects. The presence of certain minerals, such as clay or chert, may indicate greater susceptibility to deterioration. Exposure conditions also affect durability, as deicer application can increase damage during freeze-thaw exposure. Effects of deicers include depression of the freezing point, increased moisture retention, and generating osmotic effects. Deicing salts can also degrade concrete due to chemical attack or salt crystallization, depending on salt type. When rock salt is used, the sulfate content may damage concrete more than pure NaCl due to increased formation of ettringite or Friedel's salt.

Chapter 3: Materials

3.1 Aggregates

Various limestone coarse aggregates, all provided through KDOT, were the principal object of study. Only one fine aggregate source was used for all concrete batching.

3.1.1 Coarse Aggregate

For Phase I of this study, six limestone coarse aggregate samples were examined. All but one limestone sample were from sources that typically pass KDOT specifications for aggregate durability of having a relative dynamic modulus of elasticity higher than 95% after 660 cycles of freezing and thawing in ASTM C666 (2008) Procedure B. The low-grade limestone sample was from the Plattsmouth ledge of Hamm's Lawrence quarry (Joshua Welge, KDOT Engineer of Tests, various personal communications between 2011 and 2013). Designations and sources of coarse aggregate samples are given in Table 3.1. The designation L1 was used for a sample of Hamm's Lawrence Toronto ledge limestone that was used only to make saw-cut limestone prisms.

The saturated-surface-dry (SSD) specific gravity (SPG), bulk SPG, and absorption of the coarse aggregates were determined according to Kansas Test Method KT-6 (2007). Results are given in Table 3.2.

Twelve different limestone coarse aggregates were examined during Phase II of this study. Two mixes were batched for each of the twelve aggregates. In one of the two mixes, the coarse aggregate was treated with salt brine prior to batching. The coarse aggregate was not salt treated for the other mix. Phase II coarse aggregate sources and SSD specific gravity values are provided in Table 3.3.

Table 3.1: Phase I Coarse Aggregate Designations and Sources

Rock Type	Designation	Source
Limestone	L2	Hamm's Lawrence Plattsmouth ledge
Limestone	L3	Zeandale
Limestone	L4	Severy
Limestone	L5	Desoto
Limestone	L6	LeLoup
Limestone	L7	Coffeyville

Table 3.2: Phase I Coarse Aggregate Properties

Aggregate	SSD SPG	Bulk SPG	Absorption (%)
L2	2.56	2.49	2.6
L3	2.60	2.54	2.3
L4	2.57	2.50	2.7
L5	2.60	2.55	1.9
L6	2.61	2.55	2.3
L7	2.53	2.44	3.8

Table 3.3: Phase II Coarse Aggregate Destinations and Sources

Agg. ID No.	Quarry Number	Bed(s)	Geology Class	Producer	SSD SPG	Mix ID	Salt Treatment
1	4-030-05-LS	8,9,10,11	SPGH	Penny's Aggregates, Inc.	2.58	3143	Yes
						3144	No
2	CO-001-SG	PIT	PIT	Eastern Colorado Aggregates	2.6	3189	No
						3190	Yes
3	MO-043-LS	1	WRSW	Jasper Stone, LLC	2.65	3199	No
						3201	Yes
4	2-031-04-LS	1,2	TWND	Bayer Construction Co.	2.62	3200	No
						3202	Yes
5	2-021-16-LS	2,3	EVCK	Hamm WB	2.45	3204	Yes
						3205	No
6	1-046-04-LS	9	FRLY	Mid-States Materials – Edgerton	2.61	3206	No
						3207	Yes
7	1-070-11-LS	3	RKBF	Mid-States Materials – Plummer's Creek	2.66	3220	No
						3221	Yes
8	1-070-11-LS	4	AVOC	Mid-States Materials – Plummer's Creek	2.64	3222	No
						3223	Yes
9	2-057-05-LS	1,2	FTRILEY	Florence	2.28	3227	No
						3228	Yes
10	4-050-06-LS	1,2	WRLD	Midwest Minerals, Inc. – Parsons	2.65	3234	No
						3235	Yes
11	4-006-03-LS	6,7,8	MCKS	Midwest Minerals, Inc. – Fort Scott	2.59	3236	No
						3237	Yes
12	4-025-03-LS	1,2,3	EVCK	Cornejo Stone	2.57	3238	No
						3239	Yes

3.1.2 Fine Aggregate

Kaw River sand was used as the fine aggregate in all concrete samples as required by KTMR-22 (2006). Kansas State University (KSU) determined fine aggregate specific gravity (SPG) and absorption for Phase I. KDOT measured these values for Phase II. To determine SPG, mass of a volumetric flask is measured when empty, filled with water, and filled with water and saturated-surface-dry (SSD) fine aggregate. Absorption is determined by comparing the oven-dry mass and SSD mass of the fine aggregate sample. KSU used the cone test to determine when the

fine aggregate was at SSD. KDOT used the procedure outlined in KT-6 (2007) to bring sand to SSD condition. This procedure involved transferring sand between two drying pans with rusted bottoms to indicate the presence of surface moisture. For Phase I, the bulk specific gravity was determined to be 2.61 and the absorption was 0.5%. These values varied for the mixes batched in Phase II as can be seen in Table 3.4.

Table 3.4: Phase II Fine Aggregate Properties

Mix ID	SSD SPG	Absorption (%)
3143	2.614	0.5
3144		
3189	2.602	0.7
3190		
3199	2.602	0.7
3201		
3200	2.602	0.7
3202		
3204	2.602	0.7
3205		
3206	2.602	0.7
3207		
3220	2.598	0.7
3221		
3222	2.598	0.7
3223		
3227	2.598	0.7
3228		
3234	2.598	0.7
3235		
3236	2.598	0.7
3237		
3238	2.598	0.7
3239		

3.2 Cement

Monarch Type I/II cement was used in all concrete samples, as stipulated by KTMR-22 (2006).

3.3 Concrete Admixtures

Air-entraining admixture (AEA) was the only concrete admixture used in the concrete samples. The type used for Phase I was Daravair 1000, a "saponified rosin formulation" (W.R. Grace & Co., 2007). The exact amount varied as a new sample of the admixture was used after batching some of the earlier concrete samples. Daravair 1400 was used for Phase II mixes.

3.4 Rock Salt

Rock salt samples from 13 storage sheds in Kansas were provided by KDOT. These samples were subjected to inductively coupled plasma (ICP) analysis by KDOT as well as X-ray diffraction. One large sample from a storage shed in the Manhattan, KS, area provided the rock salt to make all the rock salt brine used in testing of limestone or concrete specimens.

3.5 Limestone Prisms

Large rock samples of limestone, provided by KDOT, were used to make 2×2×9-inch stone prisms subjected to various testing methods. The prisms were cut to within $\pm^{1}/_{16}$ inch of stated dimensions using a slab saw. The prisms were generally cut with the long dimension approximately parallel to the bedding, though as-received rocks were cut to maximize the number of samples that could be cut out of the rock, resulting in several prisms cut perpendicular to the bedding. Prism dimensions were determined based on the maximum length that could be cut and size of rock samples.

Limestone came from three quarries, but one quarry provided limestone from two different ledges so that samples were treated as coming from four separate sources. Quarries were located near Lawrence, Severy, and Zeandale, Kansas, and provided coarse aggregate for use in concrete samples. The Lawrence quarry provided material from the Toronto and Plattsmouth ledges, though only the Plattsmouth ledge provided additional concrete coarse aggregate. Designations and sources for the different limestone sources are given in Table 3.5 (Joshua Welge, KDOT Engineer of Tests, various personal communications between 2011 and 2013).

Table 3.5: Limestone Prism Designations and Sources

Rock Type	Designation	Source
Limestone	L1	Hamm's Lawrence Toronto ledge
Limestone	L2	Hamm's Lawrence Plattsmouth ledge
Limestone	L3	Zeandale
Limestone	L4	Severy

3.6 Batch Design

The batch design specified in KTMR-22 was used for all concrete samples in this project. Cement content was 601.6 lbs/yd^3. Water to cement (w/c) ratios for Phase I and II mixes were 0.39 and 0.40, respectively. Design air content was 6.0%. Aggregate proportions were determined by the absolute volume method, using fine aggregate to fill 50% of aggregate volume and coarse aggregate the remaining 50%. Varying SPG values of coarse aggregates caused slight variations in batch weights. Specified slump and fresh air content values were 2 ± $^1/_2$ inches and 6.0 ± 1.0%, respectively. Phase II plastic properties are provided in Table 3.6.

In compliance with KTMR-22 (2006), coarse aggregate was split evenly into two size fractions before batching: -$^3/_4$ in. + $^1/_2$ in. and -$^1/_2$ in. + $^3/_8$ in. Separate fractions of the coarse aggregates were immersed in water for 24 hours and towel-dried to SSD before batching.

Theoretical mixture proportions, using SSD coarse aggregate and oven-dry fine aggregate SPG values, are given in Tables 3.7 and 3.8 for salt-treated aggregate and half-immersion methods, respectively. AEA amounts varied as a result of switching to a new container of the same admixture over the course of batching. Batch designations were based on aggregate type and treatment method, using the first term to reference aggregate source and the second term for test method. The "STA" designation refers to salt-treating the aggregate before batching concrete, and "IS" refers to batches to be half-immersed in salt solution during ASTM C666 testing.

Table 3.6: Phase II Fresh Concrete Properties

Aggregate Source	Mix ID	Aggregate Salt Treatment	Slump (in.)	Air Content (%)
Penny's Aggregates	3143	Yes	1.25	6.5
	3144	No	1.25	6.5
Eastern Colorado Aggregates	3189	Yes	4	6.8
	3190	No	2.5	7.2
Jasper Stone	3199	Yes	4	7.4
	3201	No	2.25	6.3
Bayer Construction	3200	Yes	5.50	7.4
	3202	No	2.25	6.8
Hamm WB	3204	Yes	6.5	7.2
	3205	No	1.5	5.5
Mid-States Materials – Edgerton	3206	Yes	6.5	Not Provided
	3207	No	2.25	6.0
Mid-States Materials – Osage (Bed 3)	3220	Yes	1.25	5.3
	3221	No	1.25	5.0
Mid-States Materials – Osage (Bed 4)	3222	Yes	2.5	5.3
	3223	No	1.5	5.1
Florence Rock	3227	Yes	7.25	6.8
	3228	No	Not Provided	Not Provided
Midwest Minerals – Parsons	3234	Yes	2.25	5.8
	3235	No	1.75	5.8
Midwest Minerals – Ft. Scott	3236	Yes	4.75	5.9
	3237	No	1.75	4.8
Cornejo Stone	3238	Yes	3.75	6.8
	3239	No	1.25	5.5

Table 3.7: Salt-Treated Aggregate Mixture Proportions

Batch Designation	Cement (lbs/yd^3)	Water (lbs/yd^3)	Fine Aggregate (lbs/yd^3)	Coarse Aggregate (lbs/yd^3)	AEA (fl. oz./yd^3)
L2-STA	602	235	1,511	1,480	6.8
L3-STA	602	235	1,511	1,504	6.8
L4-STA	602	235	1,511	1,489	6.8
L5-STA	602	235	1,511	1,505	7.4
L6-STA	602	235	1,511	1,510	7.4
L7-STA	602	235	1,511	1,464	7.4

Table 3.8: Half-Immersion Mixture Proportions

Batch Designation	Cement (lbs/yd^3)	Water (lbs/yd^3)	Fine Aggregate (lbs/yd^3)	Coarse Aggregate (lbs/yd^3)	AEA (fl. oz./yd^3)
L2-IS	602	235	1,511	1,480	6.7
L3-IS	602	235	1,511	1,504	6.7
L4-IS	602	235	1,511	1,489	6.3
L5-IS	602	235	1,511	1,505	6.7
L6-IS	602	235	1,511	1,510	6.7
L7-IS	602	235	1,511	1,464	6.7

Mixture proportions for concrete prisms subjected to wet-dry cycling are given in Table 3.9. Prisms from these batches were individually labeled according to solution used in the wet-dry test.

Table 3.9: Wet-Dry Test Mixture Proportions

Coarse Aggregate Used	Cement (lbs/yd^3)	Water (lbs/yd^3)	Fine Aggregate (lbs/yd^3)	Coarse Aggregate (lbs/yd^3)	AEA (fl. oz./yd^3)
L3	602	235	1,511	1,504	6.5
L4	602	235	1,511	1,489	5.8

Mixture proportions for the Phase II concrete prisms are provided in Table 3.10.

Table 3.10: Phase II Mixture Proportions

Mix ID	Cement (lbs/yd^3)	Water (lbs/yd^3)	Fine Aggregate (lbs/yd^3)	Coarse Aggregate (lbs/yd^3)	AEA (mL/1.5 ft^3)
3143	602	240.8	1,498.8	1,498.8	11.6
3144	602	240.8	1,498.8	1,498.8	11.6
3189	602	240.8	1,501.4	1,501.4	3.8
3190	602	240.8	1,501.4	1,501.4	3.8
3199	602	240.8	1,516.1	1,516.1	7.6
3201	602	240.8	1,516.1	1,516.1	7.6
3200	602	240.8	1,507.5	1,507.5	7.6
3202	602	240.8	1,507.5	1,507.5	7.6
3204	602	240.8	1,458.7	1,458.7	7.6
3205	602	240.8	1,458.7	1,458.7	7.6
3206	602	240.8	1,506.3	1,506.3	7.6
3207	602	240.8	1,506.3	1,506.3	7.6
3220	602	240.8	1,516.7	1,516.7	7.6
3221	602	240.8	1,516.7	1,516.7	7.6
3222	602	240.8	1,509.5	1,509.5	7.6
3223	602	240.8	1,509.5	1,509.5	7.6
3227	602	240.8	1,405.7	1,405.7	7.6
3228	602	240.8	1,405.7	1,405.7	7.6
3234	602	240.8	1,513.5	1,513.5	7.6
3235	602	240.8	1,513.5	1,513.5	7.6
3236	602	240.8	1,497.1	1,497.1	7.6
3237	602	240.8	1,497.1	1,497.1	7.6
3238	602	240.8	1,489.3	1,489.3	7.6
3239	602	240.8	1,489.3	1,489.3	7.6

Chapter 4: Methods

Experiments were conducted on rock salt, limestone prisms saw-cut from boulders collected from quarries in Kansas, and concrete prisms made using aggregates typically used in Kansas. Methods used in this study are summarized in Figure 4.1.

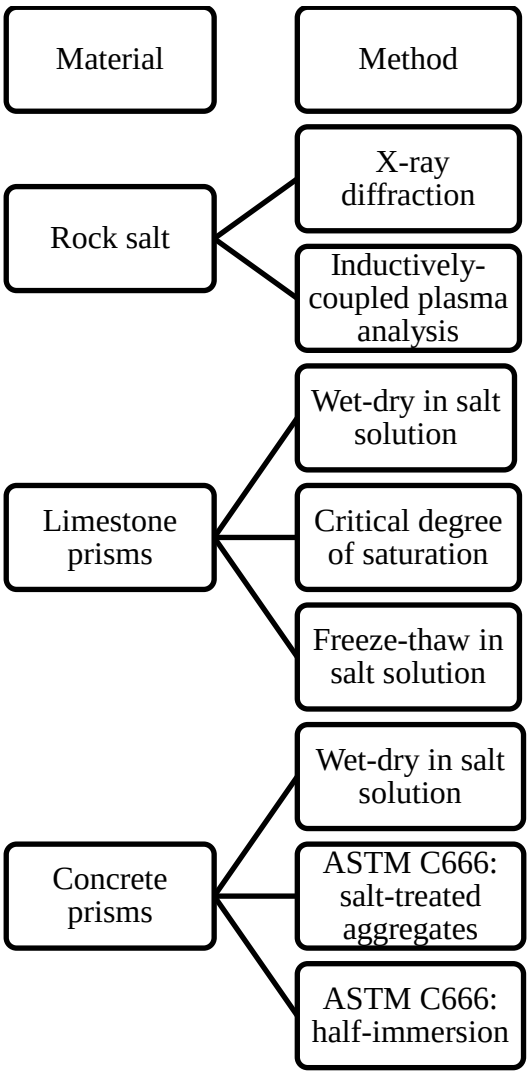

Figure 4.1: Test Method Flow Chart

4.1 Chemical Analysis of Rock Salt Samples

Rock salt samples received were analyzed using X-ray diffraction and ICP analysis. ICP analysis was conducted by KDOT.

4.1.1 X-Ray Diffraction of Rock Salt

For each rock salt sample, a small amount of rock salt was finely crushed using a mortar and pestle. The salt was then placed in a glass plate and placed in the X-ray machine.

Rock salt was analyzed in a Rigaku Miniflex II diffractometer. Samples passed through the diffractometer at 30mV 15mA with a scanning speed of 3.5 seconds per 0.02° two theta. Proprietary PDXL analysis software package controlling the diffractometer was used to analyze patterns for phases present. The software package automatically searches for compounds that may be present in a sample based on comparison of stored diffraction patterns. The software assigns a Figure-of-Merit (FOM) value for each phase, indicating quality of match. The lower the FOM value, the more likely it is that the phase is present in the sample. For sample analysis, the software was used to search for inorganic compounds potentially in the sample containing one or more of the following elements: sodium, calcium, magnesium, hydrogen, sulfur, oxygen, and chloride. This search generated a list of possible phases in each sample. Theoretical peak patterns of possible phases were then visually compared to the sample pattern to verify quality of the match.

Fifteen salt samples were analyzed. Thirteen samples were rock salt from various samples sent by KDOT. Another sample of USP grade NaCl was also crushed and analyzed. The last sample was made from leftover residue after making a trial brine batch. The brine was made using approximately an equal amount of salt from all salt samples, except for the Manhattan sample, which had not yet been delivered. A residue sample was taken and dried at 80 °C for several days. The sample was then ground and analyzed similarly to the other samples.

4.1.2 Inductively Coupled Plasma Analysis of Rock Salt

Twelve of the rock salt samples were subjected to ICP analysis by KDOT. The percentage amounts of sodium, chloride, magnesium, and calcium were determined. The

percentage amounts of sodium and chloride forming NaCl were also determined (Joshua Welge, KDOT Engineer of Tests, personal communication, December 22, 2011).

4.2 Rock Salt Brine Production

The process of making rock salt brine roughly simulated field production. The brine was made by filling a 5-gallon bucket with distilled water while leaving enough space so that stirring would not cause the brine to overflow. Rock salt was then added and stirred until most of the rock salt dissolved. Stirring continued until the concentration reached 23% based on the salt hydrometer reading. In all cases, the brine contained small amounts of insoluble material that could be temporarily brought into suspension but would settle out of solution. In suspension, the insoluble material caused the brine to take on a dark gray color.

For the salt-treated aggregate ASTM C666 test procedure, three individual batches of brine were made at a time. This quantity was sufficient to salt-treat three coarse aggregate samples. Approximately equal proportions of each brine batch were combined to make the brine used to treat one coarse aggregate sample. This procedure was done to reduce the influence of a single batch of brine in C666 testing.

4.3 Length Comparator Measurements

Length comparator measurements were taken for various tests. Before measurements were taken, the comparator was reset using an invar rod. Samples were then placed in the comparator and rotated slowly and the lowest value taken as the reading. Samples were placed in the comparator with a consistent orientation, with one sample end taken to be the “top” and one longitudinal face the “front.”

4.4 Wet-Dry Testing in Salt Solution

4.4.1 Concrete Prism Wet-Dry Test

Concrete prisms were subjected to isothermal cycles of wetting and drying in salt solutions. Prisms were 3×3×11 inches and made using concrete batch proportions from KTMR-22 (2006). Two sets of eight prisms each were made varying only the limestone coarse

aggregate. The first set was made with Zeandale quarry limestone (L3) and the second set was made with Severy quarry limestone (L4). Prisms were cured in molds for 24 hours, followed by 13 days wet curing in a fog room, and then dried in a shrinkage room maintained at 50% RH and 73 °F for 7 days before starting the wet/dry test.

Four prisms, two containing L3 and two containing L4 aggregate, were placed in each of four different solutions, using a separate container for each solution and each aggregate type for a total of eight containers. All solutions were prepared using distilled water. The following solutions were used: distilled water, 23% by weight USP-grade NaCl, 23% by weight USP-grade NaCl with 3% solute weight replaced with ACS grade gypsum, and rock salt brine. Respectively, the solutions were referred to as: water, NaCl, gypsum, and brine. The solutions were replaced every 10 cycles. The rock salt brine contained particles that settled out of solution, and the brine was stirred before returning samples to the brine. Upon removal from rock salt brine, the top of the samples retained some settled particles during the drying stage of the cycle.

The wet-dry test took place in a shrinkage room maintained at 50% RH and 73 °F. Prisms were immersed in solution for 96 hours and dried for 72 hours. Prisms were measured for length change, mass, and relative modulus within the last 2 hours of the drying period.

4.4.2 Limestone Prism Wet-Dry Test

Saw-cut limestone prisms were also subjected to isothermal cycles of wetting and drying in salt solutions. Gauge pins were inserted into the prism ends for length comparator measurements. To insert the pins, holes were drilled into the ends of the limestone. The interior of the holes were then roughened up with steel wool and cleaned with compressed air. Gauge pins were then placed into the holes using epoxy to secure them.

Prisms were oven-dried at 122 °F until constant mass and stored in an environmental chamber maintained at 73 °F and 50% RH for 9 days before starting the wet-dry test. Prisms were placed in the same four solutions as the concrete wet-dry test. Forty-eight prisms were subjected to the test with three different prisms from each of the four limestone sources for each solution. For the first 25 cycles, the wet-dry cycles consisted of 24-hour immersion followed by 24 hours of drying. The duration of the wetting and drying periods were respectively changed to

96 and 72 hours for the next 25 cycles, as the first 25 cycles produced negligible damage. The solution was replaced after the first 25 cycles were completed and then replaced after every 10 cycles. Similar to the concrete test, the rock salt brine contained particles that settled out of solution. The brine was stirred at the start of the wet stage of the cycle, causing particles to be retained on top of limestone prisms during the drying stage.

4.5 Limestone Prism Freeze-Thaw Tests

Two freeze-thaw test procedures were attempted using limestone prisms.

4.5.1 Limestone Prism Critical Degree of Saturation

Limestone prisms were vacuum-saturated, dried to varying degrees of saturation, and exposed to freeze-thaw cycles after the manner of Li et al. (2012). Prisms were oven-dried at 176 °F until constant mass and then stored at 73 °F and 50% RH for 24 hours. At this time, the prisms were measured for oven-dry mass and relative modulus. The prisms were then placed in a vacuum desiccator maintained at 0.6 psi for 3 hours to draw air out of the prisms. Distilled water was introduced into the desiccator while maintaining vacuum. When the prisms were completely immersed, the water flow into the desiccator was stopped. Vacuum pressure in the desiccator was maintained for an additional 24 hours before introducing air back into the desiccator.

After saturation, prisms were towel-dried to SSD and measured for mass. Based on this measurement, prisms were allowed to dry at 73 °F and 50% RH until the appropriate degree of saturation was reached. Prisms at the higher degrees of saturation (e.g. 95) dry rapidly so they were stored in a lab room containing a desiccator. When the appropriate degree of saturation was reached, the prisms were wrapped in plastic wrap and sealed in plastic tubing to prevent additional water loss. Prisms were then subjected to 10 freeze-thaw cycles in which the prisms were placed in a 0 °F freezer for 12 hours, followed by 12 hours in a shrinkage room maintained at 73 °F. At the end of the last freeze-thaw cycle, the prisms were removed from plastic and oven-dried at 176 °F. Prisms were then stored at 73 °F and 50% RH for 24 hours, after which time final mass and relative modulus readings were taken.

4.5.2 Limestone Prism Freeze-Thaw Test in Salt

The second freeze-thaw test procedure subjected prisms to freeze-thaw cycles while immersed in 1% by weight rock salt brine. Ten L4 limestone prisms were oven-dried at 176 °F then stored in a desiccator containing a silica desiccant packet at room temperature until the test was started. Prisms were placed on a plastic grid (cut from a plastic light diffuser) in a 5-gallon bucket and then enough salt solution to completely immerse the prisms was added to the bucket. The bucket was sealed and placed in the solution for 24 hours at 73 °F before starting freeze-thaw cycles. Prisms were subjected to five freeze-thaw cycles alternating between 48 hours at 0 °F and 48 hours at 73 °F.

4.6 Concrete Batching

Concrete was batched using a pan mixer with a capacity of 2 cubic feet. For consistency, fine aggregate was oven-dried and coarse aggregate towel-dried to a saturated-surface-dry condition before batching. The batch water amount was adjusted based on the aggregate moisture conditions. The batching procedure followed the steps of ASTM C192 (2007).

Except for the L4 wet-dry prisms which were consolidated by using a vibrator, concrete samples were consolidated by rodding. After samples were made, samples were left in place in prism molds for 24±4 hours by covering the prisms with a layer of damp burlap and a plastic sheet. Prisms were then de-molded and placed in a fog room for moist curing.

4.7 ASTM C666 Testing

4.7.1 Freeze-Thaw Machine

The freeze-thaw machine used to conduct freeze-thaw testing for Phase I of this study had a capacity of twenty 3×4×16-inch concrete prisms in either Method A or B of ASTM C666 (2008). The machines used for Phase II freeze-thaw testing could hold 80 concrete prisms. For both test methods, the chamber was free of water during the freeze stage of the cycle and flooded with water during the thaw stage. To run ASTM C666 Method A, concrete prisms were placed in plastic sample containers designed to surround 3×4×16-inch prisms with a water layer between $^{1}/_{32}$ and $^{1}/_{8}$ inches thick. The containers were open at the top so when the chamber is flooded with

water during the thaw stage, the thaw water mixes with water in the sample containers. No plastic containers were used for ASTM C666 Method B testing. Prisms were subjected to freezing in air and thawing in water when tested according to ASTM C666 Method B. For Phase II, all 12 aggregates were used to batch separate prisms for Method A and Method B testing. Concrete batching for prisms tested in Phase II was performed by KDOT.

In all of the chambers used, two slots contained samples with embedded thermocouple wire to control chamber operation. All slots were filled for either testing method. When half-immersed samples were placed in the chamber, all samples were half-immersed. If sufficient test samples were not available, old test specimens were inserted to maintain consistent chamber conditions.

4.7.2 Data Measurement

Freeze-thaw prisms were measured for mass, expansion, and transverse frequency to monitor deterioration. Expansion was measured by comparator measurements, using an invar reference bar. Transverse frequency was measured using a James E-Meter Mk II.

4.7.3 Data Calculations

Transverse frequency of freeze-thaw prisms was used to calculate the relative modulus and durability factor according to equations in ASTM C666 (2008). The relative dynamic modulus of elasticity (RDME) was calculated according to Equation 4.1:

$$Relative\ modulus\ (\%) = \frac{(n_x{}^2)}{(n_i{}^2)} * 100 \qquad \textbf{Equation 4.1}$$

Where:

n_x = Transverse frequency at freeze-thaw cycle x

n_i = Initial transverse frequency

Durability factor was calculated according to Equation 4.2:

$$Durability\ Factor = \frac{RM}{M} * N$$ **Equation 4.2**

Where:

RM = Relative modulus after the last freeze-thaw cycle

N = Total number of freeze-thaw cycles completed

M = Specified number of freeze-thaw cycles for the test

For Phase I testing, prisms were subjected to 300 freeze-thaw cycles, which was the value used for M. N was considered to be 300 cycles or the cycle at which the relative modulus dropped below 60%. Linear interpolation was used to calculate the relative modulus at exactly 300 cycles or the cycle at which the relative modulus was 60%.

Length change was calculated according to Equation 4.3 from ASTM C666 (2008):

$$Length\ Change\ (\%) = \frac{(l_x - l_0)}{(l_g)} * 100$$ **Equation 4.3**

Where:

l_x = Comparator reading at cycle x

l_0 = Initial comparator reading

l_g = Gauge length

Gauge length was 14 inches as the prisms were cast in 3×4×16-inch molds using recessed gauge pins.

4.7.4 Curing Procedure of Concrete Freeze-Thaw Specimens

Per KTMR-22 (2006), concrete prisms were cured for 90 days prior to the start of freeze-thaw cycling according to ASTM C666. Prisms were cured for 1 day in molds and then placed in the fog room until the prisms were 67 days old. Prisms were then placed in a shrinkage room maintained at 73 °F and 50% RH for 21 days, followed by full immersion in room-temperature water for 24 hours and an additional 24 hours in approximately 40 °F water. Initial prism measurements were taken and the prisms were subjected 300 and 660 freeze-thaw cycles for Phase I and Phase II testing, respectively.

4.7.5 Salt-Treated Aggregates

Coarse aggregates were subjected to five cycles of wetting and drying in salt solution before use in concrete prisms, similar to the method of Dubberke and Marks (1985). Cycles consisted of 24-hour immersion in salt solution, followed by 24 hours of drying in an oven at approximately 230 °F. Rather than using saturated NaCl solution, 23% rock salt brine was used to determine if impure salt had a noticeable influence on the ASTM C666 results. After the salt treatment, aggregates were placed in a wire basket through which water was run for 30 seconds. The wire basket was agitated while rinsing to ensure all aggregates were washed. Following rinsing, coarse aggregates were towel-dried to SSD.

Phase I concrete prisms for ASTM C666 Method B testing were then made using concrete made with the salt-treated aggregates and the mix proportions given in Table 3.7 (KTMR-22, 2006). Prisms were cured as described in Section 4.7.4, "Curing Procedure of Concrete Freeze-Thaw Specimens," and then subjected to freeze-thaw cycling according to ASTM C666 (2008) Method B for approximately 300 freeze-thaw cycles. The freeze-thaw machine was set to conduct one freeze-thaw cycle in 3 hours, lowering sample temperature from 40 °F to 0 °F in 110 minutes and raising the temperature back to 40 °F in 70 minutes. Phase II concrete prisms were made for ASTM C666 Methods A and B following the KTMR-22 (2006) mix design proportions presented in Table 3.10. These prisms were cured using the same procedure as described for Phase I and then subjected to freeze-thaw cycling for approximately 660 freeze-thaw cycles (ASTM C666, 2008). The freeze-thaw machine used for Phase II Method A testing was set to conduct one freeze-thaw cycle in 4.75 hours. For Method B, prisms were subjected to one freeze-thaw cycle in 3 hours.

4.7.6 Half-Immersion in Salt Solution

In the half-immersion method, concrete prisms were made and cured according to KTMR-22 (2006) procedure. These prisms were subjected to ASTM C666 freeze-thaw testing while half-immersed in 3% by weight salt solution. Time and temperature profile of the freeze-thaw chamber was determined according to ASTM C666 (2008) Method A requirements.

4.7.6.1 Salt Solution

The salt solution used in the test was made by diluting 23% by weight rock salt brine down to 3% concentration by weight. The 23% brine was made with distilled water according to the procedure previously described and its concentration was verified using a salt hydrometer. Distilled water and 23% brine were combined to form a 3% solution by weight, as determined by hydrometer measurements. The solution was stored in a sealed 5-gallon bucket and stored in a chest freezer maintained at 40 °F so solution replacement would not raise concrete prism temperature.

4.7.6.2 Prism Immersion

Prisms were placed in plastic sample containers used to perform ASTM C666 Method A. The containers were designed for the 3×4×16-inch prisms for use in ASTM C666 (2008) Method A. Prisms were placed in these containers and salt solution added to approximately mid-height on the prisms. The solution was replaced whenever the prisms were removed from the plastic containers for measurement.

4.7.6.3 Sample Sealing

The freeze-thaw machine used in the study flooded the chamber containing the concrete prisms with water during the thaw stage and then drained the water so that the chamber was dry during the freeze stage. To prevent dilution of the salt solution surrounding the prisms as well as prevent the salt solution from corroding elements of the freeze-thaw machine, samples were sealed with plastic for approximately the first 60 freeze-thaw cycles.

Plastic tubing was used to create a water-proof top on the container. The base of the tubing was attached to the container using tape. Two layers of tubing were used in case of leaks. This method proved cumbersome, particularly for thermocouple blocks, due to the added difficulty of creating a leak-proof seal around the thermocouple wire. This method was abandoned in favor of raising the top of the samples above the water level during thawing for the remaining cycles.

After consulting with David Berger (ScienTemp Production Engineer, personal communication, May 2013), it was determined that raising the samples would prevent the salt solution from mixing with thaw water without sealing the tops of sample containers. The metal frame holding the concrete samples was raised such that the water level during the thaw stage remained below the top of the plastic sample containers. This was accomplished by inserting small pieces of solid plastic beneath the metal frame corners. Raising the samples eliminated the need to seal containers with plastic.

Leaving the sample containers open allowed evaporation of salt solution. Evaporation was noticeable in the thermocouple blocks, since initially additional solution was not added to these samples every time the freeze-thaw chamber was opened for sample measurement. When solution evaporation from thermocouple samples was noted, additional solution was added. No obvious drop in solution level for the test specimens was observed, but this was not measured. The open container also allowed the top of the specimens to dry out, possibly reducing damage in the un-immersed portion of concrete samples.

4.7.6.4 Time and Temperature Profile

The time and temperature profile used in the half-immersed samples is given in Figure 4.2. Temperatures are the program set-points to which the machine is programmed in order to adjust the concrete sample temperature to reach throughout one freeze-thaw cycle. The machine was designed to freeze with the thaw water drained, so the machine was set to drain thaw water from the chamber during the last 15 minutes of the thaw cycle (David Berger, ScienTemp Production Engineer, personal communication, May 2013).

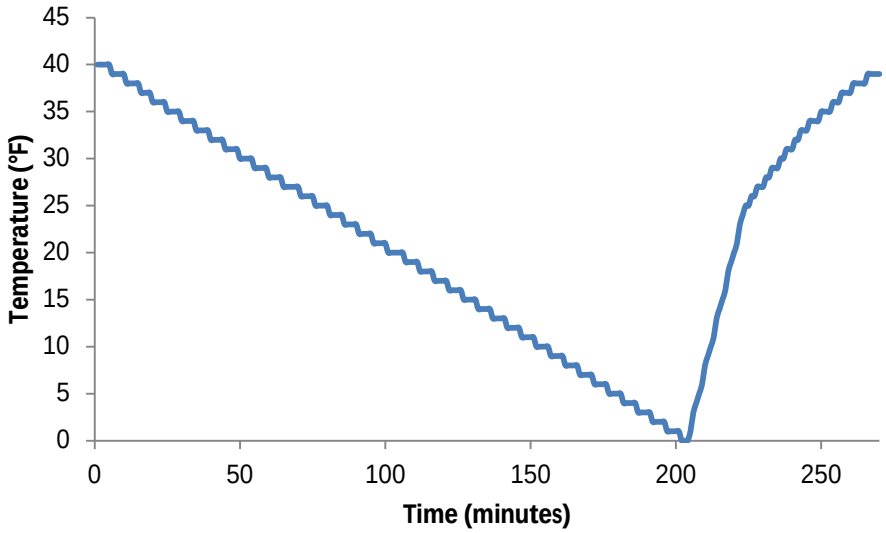

Figure 4.2: Time and Temperature Profile for ASTM C666 Method A

Chapter 5: Results

5.1 Rock Salt Analysis Results

5.1.1 Rock Salt X-Ray Diffraction Patterns

X-ray diffraction patterns of various samples are shown in Figure A.1 of Appendix A which shows the intensity in counts per second (cps) vs. 2θ angle. Patterns generally are similar to the USP grade NaCl sample, though variations in size and distribution of peaks indicate the presence of impurities. Of particular interest is the pattern labeled "Brine Residue." This pattern departs significantly from the USP grade sample and may indicate that impurities in the rock salt are more apt to stay in residue than to dissolve into brine.

Halite (NaCl) was present in all samples. A calcium sulfate phase was also indicated by the software as a possible phase in all samples except the Independence, Manhattan, Phillipsburg, Pratt, and ACS grade NaCl samples. Theoretical peak pattern for anhydrite ($CaSO_4$) indicated its principal peak is around 25.5 degrees two theta. A peak exists at that location for all rock salt samples tested, though its prominence varies. This particular peak is most prominent in the brine residue sample and least prominent in the Belleville sample.

Other phases such as hydrogen chloride or sodium chlorate (VII) were generated by the software as potential phases, typically with higher FOM values than NaCl or $CaSO_4$, indicating a less likely match. Phases other than NaCl or $CaSO_4$ were determined to not be present in detectable quantities as the principal peaks were either not present in the sample pattern or they lined up with peaks found in the NaCl or $CaSO_4$ pattern.

5.1.2 ICP Analysis Results

Results of KDOT's ICP analysis of rock salt samples are given in Table 5.1. These results show varying amounts of sulfur, calcium, and magnesium in the salt and the variation is less than 1% between all samples. The Independence sample contained almost 1% magnesium, though XRD analysis only identified NaCl in the sample pattern. In this case, XRD analysis software search for the Independence sample did not generate other potential phases.

Table 5.1: KDOT ICP Analysis Results

Source	Chloride (%)	Chloride as NaCl (%)	Sodium (%)	Sodium as NaCl (%)	Sulfur (%)	Calcium (%)	Magnesium (%)
Belleville	57.70	95.08	37.45	95.19	0.58	0.65	0.12
Dodge City	55.62	91.66	36.26	92.18	1.31	1.45	0.14
El Dorado	57.83	95.30	37.75	95.96	0.79	0.91	0.04
Garnett	56.33	92.83	36.64	93.15	1.11	1.25	0.10
Grainfield	56.98	93.90	37.28	94.76	0.76	0.87	0.11
Independence	57.41	94.64	37.12	94.36	1.00	0.99	0.99
Lamar	56.79	93.61	36.94	93.90	0.81	0.92	0.16
Marion	56.91	93.79	37.30	94.82	0.89	1.02	0.10
Phillipsburg	57.02	93.97	36.86	93.69	0.74	0.84	0.12
Pratt	56.83	93.65	37.24	94.66	0.86	0.97	0.14
Syracuse	54.72	90.18	35.87	91.18	1.20	1.32	0.26
Wamego	56.48	93.08	38.03	96.68	0.92	1.05	0.13

ICP results were theoretically compared to the sulfate exposure categories of the American Concrete Institute (ACI) Committee 318 (2008) based on the amount of sulfate in rock salt solutions of varying concentrations by weight. Sulfur concentrations, given in Table 5.1, were converted to sulfate by multiplying sulfur concentration by the molecular weight ratio of sulfate to sulfur. The sulfate concentration was then multiplied by the amount of solute theoretically in each salt solution, giving sulfate content in grams. Sulfate content in grams was then converted into parts per million (ppm) by dividing the sulfate mass by the total mass of solution and multiplying by 10^6. Results are given in Table 5.2. The assumption that all sulfur in each rock salt sample is present as the sulfate ion may be overly conservative but allows for comparison of rock salt from various locations in Kansas.

According to ACI Committee 318 (2008), moderate sulfate exposure occurs if the water soluble sulfate concentration is between 150 and 1,500 ppm and severe exposure occurs between 1,500 and 10,000 ppm. Table 5.2 shows that one-third of the rock salt samples contain enough sulfate content to generate a moderate sulfate exposure in a 0.5% by weight rock salt solution. At a 1% rock salt solution, all the samples generate a moderate sulfate exposure. At 23%, all rock salt samples generate a severe sulfate exposure.

Table 5.2: Theoretical Sulfate Content in Rock Salt Solutions of Varying Concentration

Source	Sulfate concentration (%)	Sulfate Content in 23% Solution (ppm)	Sulfate Content in 3% Solution (ppm)	Sulfate Content in 1% Solution (ppm)	Sulfate Content in 0.5% Solution (ppm)
Belleville	1.74	3996	521	174	87
Dodge City	3.92	9026	1177	392	196
El Dorado	2.37	5443	710	237	118
Garnett	3.33	7648	998	333	166
Grainfield	2.28	5236	683	228	114
Independence	3.00	6890	899	300	150
Lamar	2.43	5581	728	243	121
Marion	2.67	6132	800	267	133
Phillipsburg	2.22	5099	665	222	111
Pratt	2.58	5925	773	258	129
Syracuse	3.59	8268	1078	359	180
Wamego	2.76	6339	827	276	138

5.2 Wet-Dry Test Results

Wet-dry test results showed noticeable surface damage to specimens in salt, though internal damage to the specimens was not observed in length change measurements in concrete or limestone prisms. Relative modulus measurements of concrete prisms also did not indicate internal damage.

5.2.1 Concrete Wet-Dry Test

Concrete prisms made using L3 and L4 coarse aggregates were subjected to 40 wet-dry cycles in salt solutions. Photographs of the prisms before and after testing are shown in Appendix C. The average relative modulus, length change, and mass change of L3 concrete prisms during cycling are given in Figures C.1, C.2, and C.3, respectively. The average relative modulus, length change, and mass change of L4 concrete prisms are given in Figure C.4, C.5, and C.6, respectively. Each data point represents an average of two prisms, each measurement taken during the last 2 hours of the drying cycle. Length and mass change were negligible for

concrete prisms regardless of solution or coarse aggregate type. RDME values increased above 100% and then remained constant, reflecting continuing hydration of cement and very little internal damage from the wetting and drying cycles. Relative modulus values varied for L4 prisms in NaCl, but this was reflective of inconsistent readings from one specimen rather than damage. Aside from L4 prisms in NaCl, for each aggregate type RDME values were within 4% of each other throughout the test.

5.2.2 Limestone Prism Wet-Dry Test

Average length change and mass change for limestone prisms is given in Appendix B. Each data point represents the average of three prisms with four exceptions. Two exceptions are length change data for L1 and L2 prisms in water, which are the average of two prisms since one L1 prism broke during the oven-drying process and one L2 prism was too fractured to drill holes for gauge pins. The other two exceptions are length and mass change for L3 prisms in NaCl from Cycles 46 to 50 because one prism was dropped and broke at the start of the 46^{th} cycle. Photographs of the prisms before and after testing are given in Appendix D.

Length change data only starts from Cycle 11 because the method of length measurement was changed at that point. Initially, prisms were measured by placing the sample in the comparator and taking a reading without rotating the sample, relying on consistent prism placement for accuracy. Beginning in Cycle 11, samples were placed in the comparator, rotated 360 degrees, and the lowest comparator reading was taken as the measurement. For both measurement methods, the comparator was set to zero using an invar rod that was rotated 360 degrees, and the lowest comparator reading set as the zero measurement.

Variation in average length change is minimal with variations possibly due to the method of measuring expansion rather than damage from salt weathering. Gauge pins used to measure expansion were set in holes with epoxy and the holes were drilled into the limestone so the pins were not perfectly aligned, causing alignment of the longitudinal axis of the limestone prism to vary as the prism was rotated in the comparator. This factor alone is likely insufficient to explain the variation, but the comparator used was adjustable to accommodate prisms of different lengths, and the comparator was adjusted during wet-dry testing to measure both concrete and

limestone prisms which were different lengths. Because of adjusting the comparator, exact alignment of the limestone prism could change depending on adjustment of the comparator, possibly affecting the measurement. Prism flaws and comparator adjustment would be sufficient to cause the observed length change, particularly as values were entirely within ±0.02%. Also, length change measurements for all four limestone prism types show peaks at roughly Cycles 27 and 38, suggesting variation from the measurement procedure rather than damage from salt solution.

One L1 prism in brine contracted 0.07% at Cycle 24, causing noticeable contraction in average length change for L1 prisms in brine at Cycle 24, as shown in Figure B.1. Subsequent measurements of this prism remained within ±0.02% of this amount, suggesting change came from mishandling of the specimen (though it is unclear what may have caused the change) rather than salt weathering. Contraction of this specimen accounts for the apparent contraction of L1 prisms in brine, as seen in Figure B.1.

Mass change data shows slight loss in mass, particularly after Cycle 25 when cycle duration was increased. The noticeable drop in mass change after the 25^{th} cycle is due to increased cycle length which allowed the samples to lose more water during drying. The drop in mass change for L1 prisms in brine at Cycle 31 is due to the loss of a fragment from one of the three samples during handling. The sharp drop at Cycle 46 for L3 prisms in NaCl is due to breaking of one of the samples, as mentioned previously.

Overall scaling was observed in only the salt solutions. During wet-dry testing, two large fragments detached from two L1 prisms: one during the first immersion cycle from a sample in NaCl and another prism lost a fragment during Cycle 31. The outline of the second fragment in question appeared during the first few cycles, as indicated by crack formation even though the fragment did not break off entirely at that point. Loss of these fragments appeared to be caused by swelling of a clay seam within the limestone prism.

5.3 Limestone Prism Critical Degree of Saturation Test

Visually, no apparent damage in the form of scaling or pop-outs was evident. Figure 5.1 shows results of this test procedure for L4 limestone prisms, using the relative modulus as

calculated according to Equation 4.1. The wide gap in relative modulus for samples from the same limestone quarry and the same degree of saturation indicate that prisms vary too much for the test to yield meaningful results. However, three prisms were cut from one block and showed a trend of decreasing relative modulus with increasing saturation level, as shown in Figure 5.1. Since the other prisms were cut from different blocks and their results do not match, a quality difference based on the block a prism is cut from is indicated. All the prisms from one limestone source would not be expected to respond the same under the same freeze-thaw conditions so a uniform critical degree of saturation for this particular limestone source could not be determined with this test. This testing further underscores the variability seen in aggregates based on the bed and location in the bed.

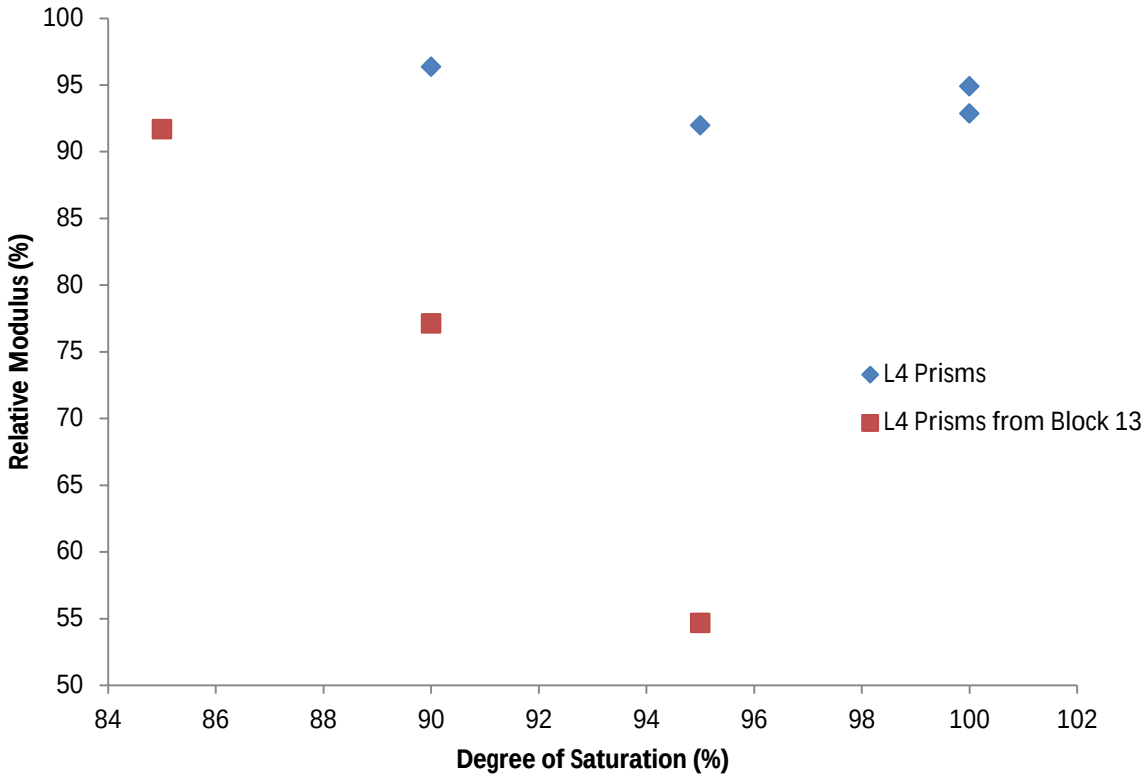

Figure 5.1: L4 Limestone Prism Critical Degree of Saturation Results

5.4 Limestone Prism Freeze-Thaw Test in Salt Solution

This test produced inconsistent results due to variations in limestone prisms. Ten prisms showed widely varying results, ranging from negligible damage to complete disintegration, even though the source was the same. Cracks in the prisms were exploited by frost action as well as laminations in the limestone. Figures D.1 through D.7 of Appendix D show L4 prisms after test exposure. In the photographs containing eight faces, the four on the left are from before the test and the four faces on the right are corresponding sides after freezing and thawing. Only seven of the 10 prisms are shown as the other three completely disintegrated. Figure D.1 shows one prism that lost its surface during the test and could not be positively identified as three other prisms disintegrated. Therefore, process of elimination could not be used.

5.5 Salt-Treated Aggregate Results

Six coarse aggregate types, L2, L3, L4, L5, L6, and L7 (as described in Table 3.1), were treated in salt solution before casting concrete prisms subjected to freeze-thaw testing. Results of the salt-treated aggregate method are shown in Figures E.1 through E.4 of Appendix E and contain an average of three prisms per aggregate type. Length change data for L7-STA prisms contains the average of two prisms, as a gauge pin of one prism fell out during casting. Designations and batch designs for concrete prisms correspond to those given in Table 3.7.

The drop in relative modulus was negligible. Length change values showed some variation, but in light of consistent RDME values, the length change values do not indicate damage to prisms from freeze-thaw action. Mass change, based on comparison to sample mass right before freeze-thaw cycling, was negligible. This test procedure failed to cause significant damage to any concrete prisms, indicating that all coarse aggregates were durable or that the test method failed to degrade frost-susceptible aggregate. The latter is more plausible since at least L2 aggregates were considered frost-susceptible. It is possible that washing the aggregates in water after soaking them salt solution washed away enough of the salt to reduce any salt-induced damage.

5.6 Half-Immersed Results

The same six coarse aggregate types used in the salt-treatment method were also used in concrete subjected to freeze-thaw testing half-immersed in salt solution. L2, L3, L4, L5, L6, and L7 coarse aggregates, as described in Table 3.1, were used. Designations and batch designs for concrete prisms correspond to those given in Table 3.8. Coarse aggregates were not salt-treated before casting concrete. Results of the half-immersion method are shown in Figures F.1 through F.4 of Appendix F and are the average of two prisms per aggregate type.

Relative modulus values for half-immersed samples are slightly lower than those of the salt-treated aggregate samples but still show negligible quantifiable differences between the aggregates tested. Significant scaling occurred on immersed portions of the prisms. Several exposed aggregates showed visible deterioration, from salt scaling or frost damage when directly exposed to salt solution. Scaling influenced the mass change data, shown by decline for all samples even though the aggregate type does not appear to have a significant influence on mass change. Expansion results show considerable variation but relative modulus values did not significantly decline. The expansion variation could be an effect of the half-immersion. Scaling occurred around the gauge pins, which could have influenced results.

The test failed to quantifiably differentiate between aggregates. Because much of the damage was manifested as scaling, it is probable that this test method caused damage to the paste or very locally to the aggregates in the case of popouts. Qualitatively, the exposed aggregate did deteriorate, although measured results were not influenced. For example, L2 concrete prisms contained numerous aggregates that showed signs of scaling or caused pop-outs. In one L2 prism an aggregate disintegrated, as shown in Figure F.5, which shows an L2 prism after completion of the freeze-thaw test and 3 days drying. L4 concrete prisms also contained numerous aggregates that either scaled or caused pop-outs. L3 concrete prisms also showed aggregates that caused pop-outs or scaled, but to a lesser extent compared to L4 and particularly L2 concrete prisms. A prism made with L3 aggregate is shown in Figure F.6 after the test and a drying period of 3 days. Severe scaling and aggregate damage, including surface flaking, are apparent. These effects indicate that some aggregate tested was not frost durable.

5.7 Phase II Results

The 12 limestone aggregates listed in Table 3.3 were used to batch concrete prisms that were subject to ASTM C666 freeze-thaw testing. Each of the 12 aggregates was used to batch 12 prisms, yielding 144 total samples. Different combinations of testing conditions for each aggregate are summarized in Table 5.3.

Table 5.3: Phase II Testing Conditions for Each Aggregate Set

Number of Concrete Prisms	ASTM C666 Test Method	Aggregate Condition
3	A	No Salt Treatment
3	A	Salt Treated
3	B	No Salt Treatment
3	B	Salt Treated

Mass, expansion, and RDME were measured for each sample. Averages of these three properties were calculated for each of the four testing conditions. Average values were plotted through 660 cycles unless one of the following conditions existed:

- Readings could not be obtained for all three prisms due to excessive deterioration.
    - Exception: Salt-treated Florence aggregate samples subject to Method B only had one sample with expansion readings. This data was still plotted.
- Samples had to be removed from the chamber early
    - This applies to the non-salt-treated Hamm aggregate samples subject to Method A testing.

A summary of mass change, expansion, and RDME results for all samples is provided in Appendix G.

5.7.1 Summary of ASTM C666 Results

None of the prisms that were subject to ASTM C666 Method A testing met the KTMR-22 (2006) expansion and RDME requirements.

An analysis was conducted to correlate the results of Method A and Method B testing for the aggregates without salt treatment. For each aggregate set, the final cycle during which all three Method B relative modulus readings could be obtained was identified. The average modulus at this cycle was calculated and recorded. The cycle at which the equivalent average Method A relative modulus occurred was then identified. This cycle was calculated through linear interpolation between the two Method A relative modulus values which were larger and smaller than the final Method B relative modulus. The difference between the final Method B cycle and the equivalent Method A cycle was then calculated. The results of this analysis are displayed in Table 5.4. A comparison was made between the RDME under Method A at 300 cycles and the RDME under Method B at 660 cycles, as shown in Figure 5.2. The same comparison was made using the RDME at 450 cycles instead of 300 cycles, as shown in Figure 5.3. An acceptance RDME value of 95 gave the same results using Method A at 300 cycles and Method B at 660 cycles except for the aggregates from Quarry 1-046-04-LS, giving promise to the use of fewer freeze-thaw cycles using Method A for aggregate qualification.

The same procedure used for non-salt-treated aggregates to calculate the number of freeze-thaw cycles needed with Method A to reach an equivalent RDME with Method B at 660 cycles was used to calculate the equivalent Method A cycles for salt-treated aggregate sets. These results are summarized in Table 5.5. While there were no direct correlations seen between the freeze-thaw results of salt-treated aggregates and non-salt-treated aggregates, the results could be used in the future for comparison to field performance of these aggregates in pavements that would certainly be exposed to deicer salts. A comparison of the freeze-thaw results of concrete made with salt-treated aggregates showed that in all cases concrete prisms tested using Method A showed lower RDME values and failed in fewer cycles than using Method B. This is most likely because the concrete prisms in Method A stay immersed in water longer, allowing the samples to become more saturated. The salt in the aggregates is hygroscopic and encourages water to enter the concrete, increasing the concrete degree of saturation.

Table 5.4: Equivalent Cycle Determination for Non-Salt-Treated Aggregates

Aggregate Set Name	Quarry	Bed	Method B Average RDME at Final Cycle	Method B Final Cycle	Method A Cycle with Equivalent Average RDME	Difference between Final and Equivalent Cycles
Mid-States – Edgerton	1-046-04-LS	9	95.3	660	253	407
Mid-States – Plummer's Creek	1-070-11-LS	3	59.8	660	511	149
Mid-States – Plummer's Creek	1-070-11-LS	4	34.3	327	236	91
Hamm WB	2-021-16-LS	2,3	86.3	660	395	265
Bayer	2-031-04-LS	1,2	98.6	660	28	632
Florence	2-057-05-LS	1,2	98.7	660	11	649
Midwest Minerals – Ft. Scott	4-006-03-LS	6,7,8	88.4	660	389	271
Cornejo Stone	4-025-03-LS	1,2,3	89.6	660	418	242
Penny's Aggregates	4-030-05-LS	8,9,10,11	82.8	660	*	*
Midwest Minerals – Parsons	4-050-06-LS	1,2	98.0	660	55	605
Eastern Colorado Aggregates	CO-001-SG	Pit	97.0	660	*	*
Jasper Stone	MO-043-LS	1	93.0	660	122	538

* Method A RDME was not recorded long enough to drop below final Method B RDME

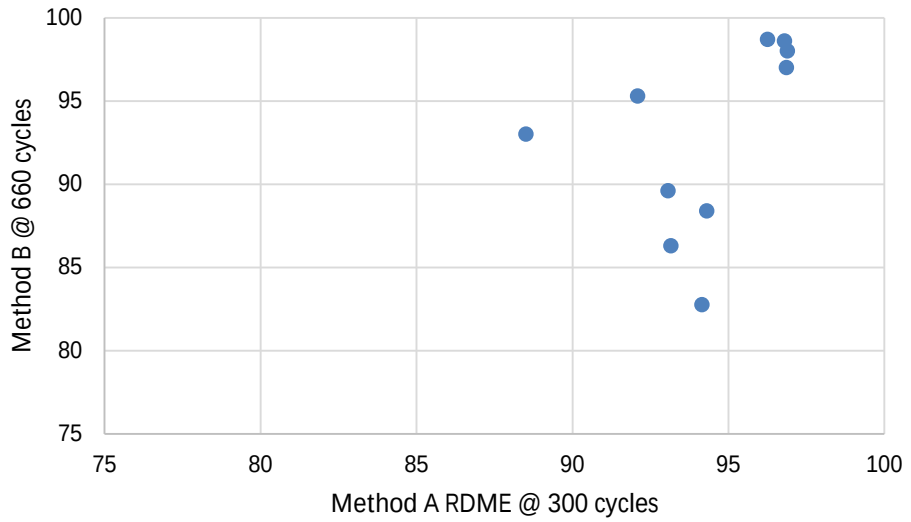

Figure 5.2: Comparison of Method B RDME Results at 660 Cycles to Method A RDME Results at 300 Cycles

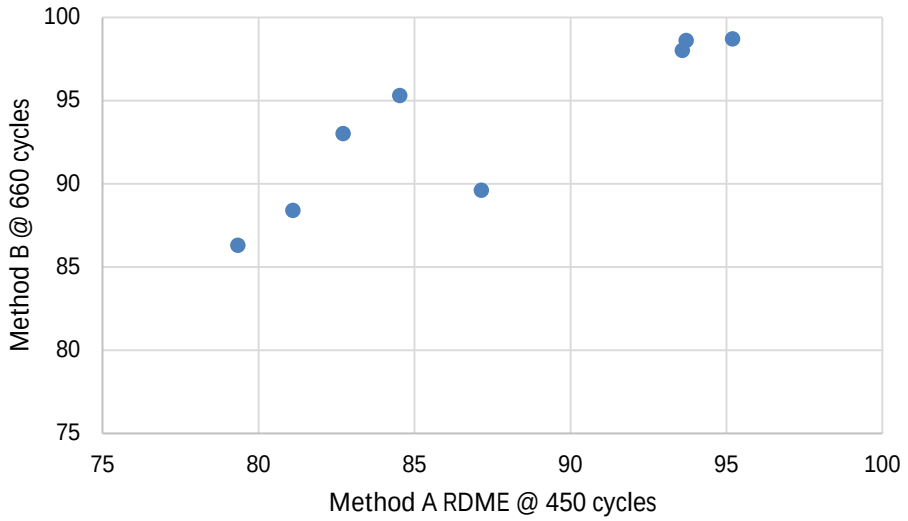

Figure 5.3: Comparison of Method B RDME Results at 660 Cycles to Method A RDME Results at 450 Cycles

Table 5.5: Equivalent Cycle Determination for Salt-Treated Aggregates

Aggregate Set	Quarry	Bed	Method B Average RDME at Final Cycle	Method B Final Cycle	Method A Cycle with Equivalent Average RDME	Difference between Final and Equivalent Cycles
Bayer	2-031-04-LS	1,2	86.3	656	20	636
Cornejo Stone	4-025-03-LS	1,2,3	71.7	104	16	88
Eastern Colorado Aggregates	CO-001-SG	Pit	86.3	660	153	507
Florence	2-057-05-LS	1,2	86	48	6	42
Hamm WB	2-021-16-LS	2,3	95	496	6	490
Jasper Stone	MO-043-LS	1	66	260	81	179
Mid-States – Edgerton	1-046-04-LS	9	79	104	25	79
Mid-States – Plummer's Creek	1-070-11-LS	3	31.3	327	217	110
Mid-States – Plummer's Creek	1-070-11-LS	4	48	272	159	113
Midwest Minerals – Ft. Scott	4-006-03-LS	6,7,8	69.3	111	25	86
Midwest Minerals – Parsons	4-050-06-LS	1,2	69.7	493	235	258
Penny's Aggregates	4-030-05-LS	8,9,10,11	45.4	660	*	*

* Method A RDME was not recorded long enough to drop below final Method B RDME

5.7.2 Saw-Cut Sample Damage

A visual inspection of saw-cut prisms was also conducted to obtain more information on the damage mechanisms occurring. The concrete prisms selected were from the Florence aggregate set due to its extremes in performance. With non-salt-treated aggregate, it finished with the highest average relative modulus compared to the other 11 aggregates. However, it performed poorly compared to the other aggregate sets when its aggregate was treated with salt. Figures 5.4 through 5.7 show images of these saw-cut samples. The salt-treated samples showed mass loss at the sample edges. Some internal aggregate cracking was seen in aggregates near the sample edge; however, much of the damage appears to be in removed paste.

Figure 5.4: Non-Salt-Treated Florence Sample Subject to Method A Testing

Figure 5.5: Salt-Treated Florence Sample Subject to Method A Testing

Figure 5.6: Non-Salt-Treated Florence Sample Subject to Method B Testing

Figure 5.7: Salt-Treated Florence Sample Subject to Method B Testing

Chapter 6: Discussion

6.1 Rock Salt Analysis

Chemical analysis shows trace compounds present in the salt. X-ray diffraction (XRD) analysis generally identified only $CaSO_4$ as a trace compound in the sample. This finding does not rule out the presence of other compounds, but may indicate that insufficient amounts of trace compound phases were present for detection by XRD without Rietveld analysis. In particular, ICP analysis showed that magnesium was present, though magnesium-bearing phases were not positively identified in XRD patterns, suggesting that $CaSO_4$ is the most common sulfur-bearing phase in rock salt and could possibly govern the chemical interaction between sulfur in rock salt and hydrated cement paste in concrete pavement. The presence of other sulfur compounds is not ruled out by this analysis and their presence could also have an influence on concrete durability.

A simple calculation, the results of which are given in Table 5.2, based on the ICP results shows that there is enough sulfate content in the rock salt to generate a moderate or even severe sulfate exposure condition depending on the rock salt concentration. The ICP analysis was conducted on rock salt solution, so the sulfur content was water soluble even if it was not all present as sulfate ions. The appreciable sulfate content showed that examining the effect of rock salt on concrete durability by using NaCl with low sulfate content, such as USP grade NaCl, may underestimate the severity of exposure to rock salt solution.

Impurities in the rock salt may be relatively insoluble and therefore not completely dissolved during the brine production process. Insolubility of rock salt impurities is demonstrated by the difference between the XRD pattern of rock salt brine residue and the XRD pattern of the other rock salt samples. The brine residue pattern had a more prominent $CaSO_4$ peak (at roughly 25.5° 2θ) and peaks not present in other sample patterns. This would indicate the rock salt brine residue sample contained more material other than NaCl relative to the other samples, which could mean brine may have a higher NaCl content than rock salt, thereby reducing the influence of rock salt impurities on concrete durability. However, if dry rock salt is applied to roads, then whatever impurities are present would have an influence on concrete pavement performance.

6.2 Concrete Wet-Dry Test

Scaling was the principal damaging effect for this test. Lack of internal damage, indicated by lack of excessive length change or decline in relative modulus, showed the test was insufficiently severe. This may be due to the drying period, which was conducted at 73 °F and 50% RH. Darwin et al. (2007) noticed some decline in relative modulus to concrete prisms in NaCl solution. Their drying conditions were at a higher temperature and therefore more severe. That they saw a decline in relative modulus in NaCl solution and this testing did not indicates that to further study the interaction of the impure salts on concrete requires more severe drying conditions for a wet-dry test. Alkali-aggregate reaction may also be a factor in this type of testing as salt solutions contained sodium, but negligible expansion indicates that the reaction did not occur to a deleterious degree.

A freeze-thaw test in varying salt solution and concentrations would show more clearly the influence of impure salts on concrete frost durability than a wetting and drying test.

6.3 Limestone Wet-Dry Test

Each prism tested was unique to the extent that a comparison of limestone performance in the wet-dry test based on salt solution is inconclusive. Damage principally occurred from scaling, and each prism showed a non-uniform response to exposure conditions. The extent of scaling varied even on the same prism face. Therefore, individual characteristics of a limestone prism influenced the test more than the salt solution to which the prism was exposed. This shows the inhomogeneity found in aggregates and how crushed aggregate samples taken from large mixed piles are more likely to be representative of actual freeze-thaw durability.

Damage to prisms occurred principally through scaling. Negligible length change and lack of cracking indicate this test did not produce conditions similar to those which would cause D-cracking in a coarse aggregate, particularly as some of the samples contained cracks before the test which could have been exploited to cause internal sample damage. Expansive clay in L1 prisms caused fragmentation in the limestone, but crushed aggregate from this source was not tested. Without testing crushed aggregate, the importance of this effect in concrete aggregate performance cannot be determined from the limestone prism test results alone.

Limestone samples generally did not crack during wet-dry exposure but they did crack when subjected to freeze-thaw cycles in salt solution. This result indicates that a more severe test method would be to subject limestone to freeze-thaw cycles in varying salt solutions. The same solutions used in the wet-dry test would be suitable, although varying the concentration as well would be useful in determining the interaction of impure salts with limestone. Given the inconsistent nature of limestone prisms, crushed aggregate samples are more suitable for consistent results. Visual inspection of the prisms highlighted the role clays play in the aggregate freeze-thaw durability. Changed crushing operations that can remove more clay seams and pockets could remove more of the non-durable material from the aggregate.

6.4 Limestone Prism Freeze-Thaw Tests

For both limestone prism freeze-thaw tests, prism performance varied considerably even though only one limestone type was used. Results indicate neither of these test methods is suitable for determining aggregate performance, particularly given the wide range of performance in the freeze-thaw test in salt solution. However, non-durable characteristics of prisms may be identified in this test. The presence of cracks prior to testing was detrimental, as shown in Figure D.7. The portion of a stone near the exterior may be of lower quality, as shown in Figure D.2. The lamellar nature of limestone may also provide a weak plane susceptible to damage as shown in Figure D.5 and possibly Figure D.2.

Samples were saw-cut limestone prisms rather than crushed aggregate. The difference between the two may be enough that saw-cut prisms are not suitable for determination of aggregate durability.

6.5 ASTM C666 with Salt-Treated Aggregates

Damage in this test was negligible, which did not agree with predicted aggregate performance. In particular, L2 prisms were expected to deteriorate but did not and performed approximately the same as prisms containing other aggregate. The salt-treatment removed material from coarse aggregates because scaled aggregate particles were left in salt containers following the salt-treatment.

Insufficient salt may have been present in the aggregate to cause damage during freeze-thaw testing. Dubberke and Marks (1985) used saturated NaCl solution. The rock salt brine was also adjusted to 23±1% by weight by the addition of distilled water after each removal of aggregates from salt solution. Another factor reducing test severity may be that the rinsing procedure could have removed too much salt from the aggregate and reduced its effect in freeze-thaw testing. Since Dubberke and Marks used more saturated solutions, this may not have influenced their results.

Another factor reducing severity could be the curing procedure. Concrete samples were dried for 21 days during the curing period. Verbeck and Landgren (1960) observed that a drying period before samples were placed in the freeze-thaw chamber reduced the saturation level of concrete samples and delayed frost damage. The drying period may be a factor as Dubberke and Marks (1985) do not explicitly mention a drying period during the curing of their samples. Another factor reducing severity could be salt leaching during moist curing, although Dubberke and Marks moist-cured their samples for 90 days and still observed a significant increase in damage during freeze-thaw cycling. However, since they used more concentrated salt solution, the leaching effect could have been less of a factor in their testing.

6.6 ASTM C666 with Half-Immersed Samples

Measured data shows negligible differences between various aggregates, which does not agree with predicted aggregate durability. For example, L2 samples were expected to degrade in the test but had a durability factor approximately the same as L3 samples, which were expected to show little damage. Based on expected aggregate performance, this test is unsuitable for differentiating aggregate performance. Significant scaling did occur but is not necessarily a satisfactory indicator of aggregate performance, since internal concrete deterioration is the symptom most related to D-cracking susceptibility of an aggregate. Since the relative modulus of these samples did not appreciably decline during the test, internal damage to the specimens was negligible.

Qualitatively, aggregate performance differed in the deterioration of exposed aggregate by sample scaling as well as formation of pop-outs. One exposed aggregate particle from an L2

prism disintegrated, so frost susceptible aggregate was present in the concrete. The less durable aggregate, particularly L2 and L4 aggregate samples, tended to have more pop-outs as well as aggregate deterioration. Whether aggregate deterioration resulted from scaling, internal frost damage of the individual aggregate particle, or a combination of scaling and internal frost damage is unclear from this testing.

Results of this test method indicate little internal deterioration in the concrete, as the relative modulus did not appreciably decline. Similar to the salt-treated aggregate test method, samples for the half-immersion method were dried for 21 days during the curing period, which could have reduced test severity. The un-immersed half of all specimens appeared dry when measured. In that case, the top half of the specimen would dry and not contain sufficient solution for freeze-thaw damage. Solution evaporated from the samples, which could also have reduced test severity.

6.7 Phase II

A comparison of the Method B average RDME at its final measured cycle and the difference between the Method A final cycle number and equivalent cycle number showed a clear trend, as shown in Figure 6.1. The equivalent cycle number in Method A decreased as the performance increased in method. This is mainly because Method A accelerates damage in comparison to Method B, and a small difference in RDME in good aggregates can cause a very large difference in equivalent cycle number above an RDME of 95.

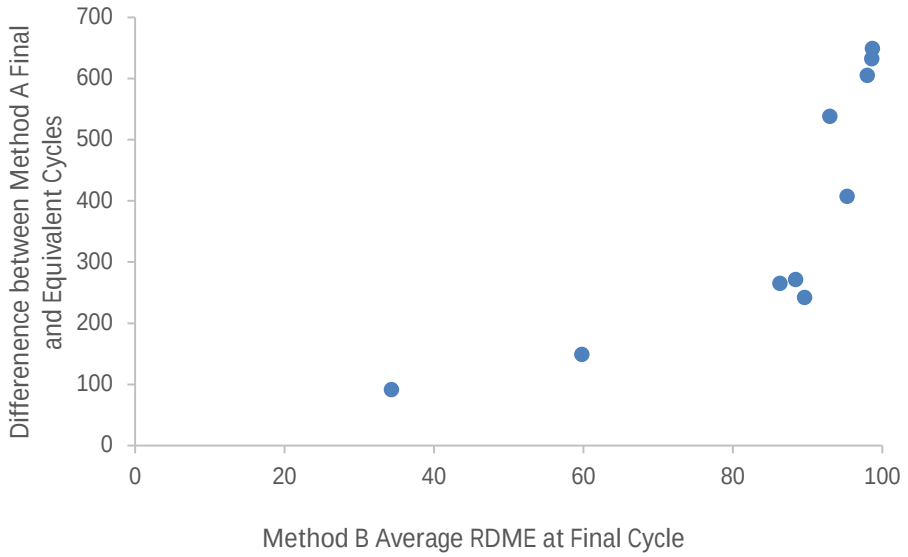

Figure 6.1: Comparison of Method B RDME Results at 660 Cycles to Method A RDME Results at 450 Cycles

A similar trend was observed for the salt-treated aggregate sets. In general, as the final cycle decreases, the difference between the final and equivalent cycles decreases as well. This further suggests that Method A and Method B testing yield comparable durability results for aggregates with poor Method B performance. The ability of the Method A test to produce similar acceptance classifications as Method B in all but one aggregate at 300 cycles gives hope that this test method could be used to decrease the time needed for KDOT to perform aggregate acceptance tests.

The saw-cut sample images presented in Figures 5.2 through 5.5 do not show significant damage in the coarse aggregate. Some D-cracking occurs in the Method A salt-treated aggregate samples, but not enough to lower the average relative modulus to 21 after just 35 cycles (See Figure G.4i). However, the deformed edges of this sample illustrate the severe surface scaling that occurred. This suggests that deterioration is primarily found in the exterior cement paste, rather than in the coarse aggregate. This test could be used to replicate and accelerate conditions seen in concrete pavement joints under distress to help determine material vulnerability to joint rot and find mitigation methods. The disparate performance of aggregates in the salt-treated test method could help explain differences in performance of concrete pavement joints in concrete pavements made with different aggregates.

Chapter 7: Conclusions

Concrete and saw-cut limestone prisms were subjected to both wet-dry and freeze-thaw testing. The testing provided little quantitative difference in limestone or concrete performance in NaCl solutions containing varying amounts of impurities.

Chemical analysis shows that impurities are present in rock salt and impurities are less soluble than NaCl. However, impurities such as sulfur are still present in rock salt brine and may contain enough sulfate that its effects would need to be considered in concrete performance.

Limestone prism wet-dry testing in varying salt solutions did not indicate a quantitative difference in performance based on the amount of impurities in the solution. However, significant damage occurred in limestone prisms subjected to freeze-thaw cycling in salt solution. Freeze-thaw testing in varying salt solutions and concentrations would more accurately show the influence of rock salt impurities. The inconsistency between limestone prisms from the same source indicates that crushed coarse aggregate would be more consistent material to test.

Concrete prism wet-dry testing did not indicate a quantitative performance difference based on salt solution. Increasing severity of the drying period or conducting freeze-thaw testing in salt solution would likely be more indicative of a difference based on salt composition.

Neither salt-treated aggregate nor half-immersion freeze-thaw test procedures in Phase I discriminated between limestone aggregate performance, indicating both test methods are insufficiently severe rather than all aggregates were durable. Eliminating the drying period during sample curing would increase test severity in both test methods. Increasing salt concentration and reducing or eliminating aggregate rinsing would likely increase test severity in the salt-treated aggregate method. Sealing samples in plastic to eliminate drying would likely increase severity in the half-immersion test method. Full immersion in salt solution may also increase severity, however it may only yield salt scaling deterioration and popout forms of damage, not internal deterioration associated with D-cracking.

It cannot be stated whether or not trace compounds in rock salt influence limestone aggregate durability based on test data shown. Testing procedures did not quantifiably produce a difference in sample performance based on salt composition, and more severe testing would be

required to show if there is such a difference. From the testing conducted, however, the impurities did not appear to be in large enough quantities to cause damage in freeze-thaw or wet-dry cycles alone.

Both salt-treated and non-salt-treated aggregates produced similar trends in freeze-thaw performance when comparing ASTM C666 Method A and Method B test results. It was generally observed that if an aggregate set performed well when subject to Method B testing, then it would perform poorly under Method A. However, a poor-to-moderate performance under Method B testing yielded comparable durability when subject to Method A at 300 cycles. Salt treatment of aggregates for Phase II testing did not appear to differentiate well from poor performing aggregates as compared to Method B results at 660 freeze-thaw cycles. Visual inspection of saw-cut samples suggests that the salt actually accelerates surface cement paste damage more than D-cracking of the coarse aggregate. It could however indicate a difference in performance of aggregates when exposed to salts in freeze-thaw conditions. It could also serve as a test to judge the quality of the paste portion of concrete under freezing and thawing conditions.

7.1 Recommendations

Use of saw-cut limestone prisms for testing the freeze-thaw durability of concrete aggregates is not recommended as crushing limestone may change its properties, prisms from the same source have variable quality, and prisms are labor-intensive to make. Further testing should be conducted to validate the potential use of ASTM C666 Method A as a method to achieve similar freeze-thaw acceptance results as Method B in fewer freeze-thaw cycles. Freeze-thaw tests of concrete made with aggregates presoaked in salt brine could provide a good method to test the effects of salt exposure on internal freeze-thaw distress on the paste portion of the concrete. However, salt treatment may not be an effective method to use for coarse aggregate qualification.

References

American Concrete Institute (ACI) Committee 318. (2008). Exposure categories and classes. In *Building code requirements for structural concrete and commentary* (ACI 318-08, Section 4.2). Farmington Hills, MI: American Concrete Institute.

ASTM C192 / C192M-07. (2007). *Standard practice for making and curing concrete test specimens in the laboratory*. West Conshohocken, PA: ASTM International. DOI: 10.1520/C0192_C0192M-07, www.astm.org

ASTM C666 / C666M-03. (2008). *Standard test method for resistance of concrete to rapid freezing and thawing*. West Conshohocken, PA: ASTM International. DOI: 10.1520/C0666_C0666M-03R08, www.astm.org

Benavente, D., Garcia del Cura, M.A., Garcia-Guinea, J., Sanchez-Moral, S., & Ordonez, S. (2004). Role of pore structure in salt crystallisation in unsaturated porous stone. *Journal of Crystal Growth, 260*(3-4), 532-544.

Buj, O., Gisbert, J., McKinley, J.M., & Smith, B. (2011). Spatial characterization of salt accumulation in early stage limestone weathering using probe permeametry. *Earth Surface Processes and Landforms, 36*(3), 383-394.

Cardell, C., Benavente, D., & Rodríguez-Gordillo, J. (2008). Weathering of limestone building material by mixed sulfate solutions. Characterization of stone microstructure, reaction products and decay forms. *Materials Characterization, 59*(10), 1371-1385.

Chappelow, C.C., McElroy, A.D., Blackburn, R.R., Darwin, D., de Noyelles, F.G., & Locke, C.E. (1992). *Handbook of test methods for evaluating chemical deicers* (SHRP-H-332). Washington, DC: Strategic Highway Research Program, National Research Council.

Chen, T.C., Yeung, M.R., & Mori, N. (2004). Effect of water saturation on deterioration of welded tuff due to freeze-thaw action. *Cold Regions Science and Technology, 38*(2-3), 127-136.

Collins, R.J. (1988). Microstructural studies of Jurassic limestone aggregates with reference to durability in concrete. *Magazine of Concrete Research, 40*(142), 35-42.

Crumpton, C.F., Smith, B.J., & Jayaprakash, G.P. (1989). Salt weathering of limestone aggregate and concrete without freeze-thaw. *Transportation Research Record, 1250*, 8-16.

Darwin, D., Browning, J., Gong, L., & Hughes, S.R. (2007). *Effects of deicers on concrete deterioration* (SL Report 07-3). Lawrence, KS: University of Kansas Center for Research, Inc.

Darwin, D., Browning, J., Gong, L., & Hughes, S.R. (2008). Effects of deicers on concrete deterioration. *ACI Materials Journal, 105*(6), 622-627.

Detwiler, R.J., & Powers-Couche, L.J. (1999). Effect of sulfates in concrete on their resistance to freezing and thawing. In B. Erlin (Ed.), *Ettringite—The sometimes host of destruction* (ACI Special Publication 177, pp. 219-248). Farmington Hills, MI: American Concrete Institute.

Dubberke, W., & Marks, V.J. (1985). The effect of deicing salt on aggregate durability. *Transportation Research Record, 1031*, 27-34.

Dunn, J.R., & Hudec, P.P. (1966). Water, clay and rock soundness. *The Ohio Journal of Science, 66*(2), 153-168.

Gillott, J.E. (1978). Effect of deicing agents and sulphate solutions on concrete aggregate. *The Quarterly Journal of Engineering Geology, 11*(2), 177-192.

Gillott, J.E. (1980). Effect of microstructure and composition of limestone, marble, basalt, and quartzite aggregate on concrete durability in presence of solutions of calcium chloride and magnesium sulfate. In P.J. Sereda & G.G. Litvan (Eds.), *Durability of Building Materials and Components* (ASTM Special Technical Publication 691, pp. 605-615). West Conshohocken, PA: ASTM International.

Gonçalves, T.D., Pel, L., & Rodrigues, J.D. (2007). Drying of salt-contaminated masonry: MRI laboratory monitoring. *Environmental Geology, 52*(2), 293-302.

Haynes, H., O'Neill, R., Neff, M., & Mehta, P.K. (2008). Salt weathering distress on concrete exposed to sodium sulfate environment. *ACI Materials Journal, 105*(1), 35-43.

Haynes, H., O'Neill, R., Neff, M., & Mehta, P.K. (2010). Salt weathering of concrete by sodium carbonate and sodium chloride. *ACI Materials Journal, 107*(3), 258-266.

Hudec, P.P. (1980). Effect of deicing salts on deterioration and dimensional changes of carbonate rocks. In P.J. Sereda & G.G. Litvan (Eds.), *Durability of building materials and components* (ASTM Special Technical Publication 691, pp. 629-640). West Conshohocken, PA: ASTM International.

Hudec, P.P. (1987). Deterioration of aggregates—The underlying cause. In *Concrete durability: Proceedings of Katharine and Bryant Mather International Symposium* (ACI Special Publication 100, pp. 1325-1342). Farmington Hills, MI: American Concrete Institute.

Koubaa, A., & Snyder, M.B. (1996). Evaluation of frost resistance tests for carbonate aggregates. *Transportation Research Record, 1547*, 35-45.

Koubaa, A., Snyder, M.B., & Janssen, D.J. (2002). Development and evaluation of D-cracking mitigation techniques. In D.J. Janssen, M.J. Setzer, & M.B. Snyder (Eds.), *PRO 25: International RILEM Workshop on frost damage in concrete* (pp. 265-288.). Bagneux, France: RILEM Publications S.A.R.L.

Koubaa, A., Snyder, M.B., & Peterson, K.R. (1997). *Mitigating concrete aggregate problems in Minnesota* (Report No. MN/RC 2004-46). St. Paul, MN: Minnesota Department of Transportation.

KT-6 Kansas Test Method. (2007). Specific gravity and absorption of aggregate. *Kansas Department of Transportation construction manual, Part V*. Topeka, KS: Kansas Department of Transportation.

KTMR-22 Kansas Test Method. (2006). *Resistance of concrete to rapid freezing and thawing*. Topeka, KS: Kansas Department of Transportation.

Li, W., Pour-Ghaz, M., Castro, J., & Weiss, J. (2012). Water absorption and critical degree of saturation relating to freeze-thaw damage in concrete pavement joints. *Journal of Materials in Civil Engineering, 24*(3), 299-307.

Litvan, G.G. (1976). Frost action in cement in the presence of de-icers. *Cement and Concrete Research, 6*(3), 351-356.

McCabe, S., McKinley, J.M., Gomez-Heras, M., & Smith, B.J. (2011). Dynamical instability in surface permeability characteristics of building sandstones in response to salt accumulation over time. *Geomorphology, 130*(1-2), 65-75.

McGreevy, J.P. (1982). 'Frost and salt' weathering: Further experimental results. *Earth Surface Processes and Landforms, 7*(5), 475-488.

Newlon, H.H., Jr. (1978). *Modification of ASTM C666 for testing resistance of concrete to freezing and thawing in sodium chloride solution*. Charlottesville, VA: Virginia Highway & Transportation Research Council.

Pigeon, M., & Pleau, R. (1995). *Durability of concrete in cold climates*. London, England: Taylor & Francis.

Pitt, J.M., Schluter, M.C., Lee, D.Y., & Dubberke, W. (1987). *Effects of deicing salt trace compounds on deterioration of portland cement concrete.* Ames: IA: Iowa Department of Transportation.

Rodriguez-Navarro, C., & Doehne, E. (1999). Salt weathering: Influence of evaporation rate, supersaturation and crystallization pattern. *Earth Surface Processes and Landforms, 24*(3), 191-209.

Ruiz-Agudo, E., Mees, F., Jacobs, P., & Rodriguez-Navarro, C. (2007). The role of saline solution properties on porous limestone salt weathering by magnesium and sodium sulfates. *Environmental Geology, 52*(2), 269-281.

Scherer, G.W. (2004). Stress from crystallization of salt. *Cement and Concrete Research, 34*(9), 1613-1624.

Scherer, G.W., & Valenza, J.J., II. (2005). Mechanisms of frost damage. In J. Skalny & F. Young (Eds.), *Materials science of concrete* (Vol. VII, pp. 209-246). Westerville, OH: American Ceramic Society.

Shi, X., Fay, L., Peterson, M.M., & Yang, Z. (2010). Freeze-thaw damage and chemical change of a portland cement concrete in the presence of diluted deicers. *Materials and Structures, 43*(7), 933-946.

Spragg, R.P., Castro, J., Li, W., Pour-Ghaz, M., Huang, P.T., & Weiss, J. (2011). Wetting and drying of concrete using aqueous solutions containing deicing salts. *Cement and Concrete Composites, 33*(5), 535-542.

Sun, Z. (2010). *Mechanism of frost damage to concrete* (Doctoral dissertation). Princeton University, Princeton, NJ.

Sutter, L., Peterson, K., Julio-Betancourt, G., Hooton, D., Van Dam, T., & Smith, K. (2008). *The deleterious chemical effects of concentrated deicing solutions on portland cement concrete* (Report No. SD2002-01-F). Pierre, SD: South Dakota Department of Transportation.

Verbeck, G., & Landgren, R. (1960). Influence of physical characteristics of aggregates on frost resistance of concrete. *Proceedings of the American Society for Testing Materials, 60*, 1063-1079.

Wang, K., Nelsen, D.E., & Nixon, W.A. (2006). Damaging effects of deicing chemicals on concrete materials. *Cement and Concrete Composites, 28*(2), 173-188.

Wessman, L.M. (1996). Deterioration of natural stone by freezing and thawing in salt solutions. In C. Sjostrom (Ed.), *Durability of building materials and components 7: Proceedings of the Seventh International Conference on Durability of Building Materials and Components* (pp. 342-351). London, England: E & FN Spon.

W.R. Grace & Co. (2007). *Daravair® 1000 Air-entraining admixture*. Retrieved from https://gcpat.com/construction/en-us/Documents/AIR-7G.pdf

Appendix A: Rock Salt Analysis

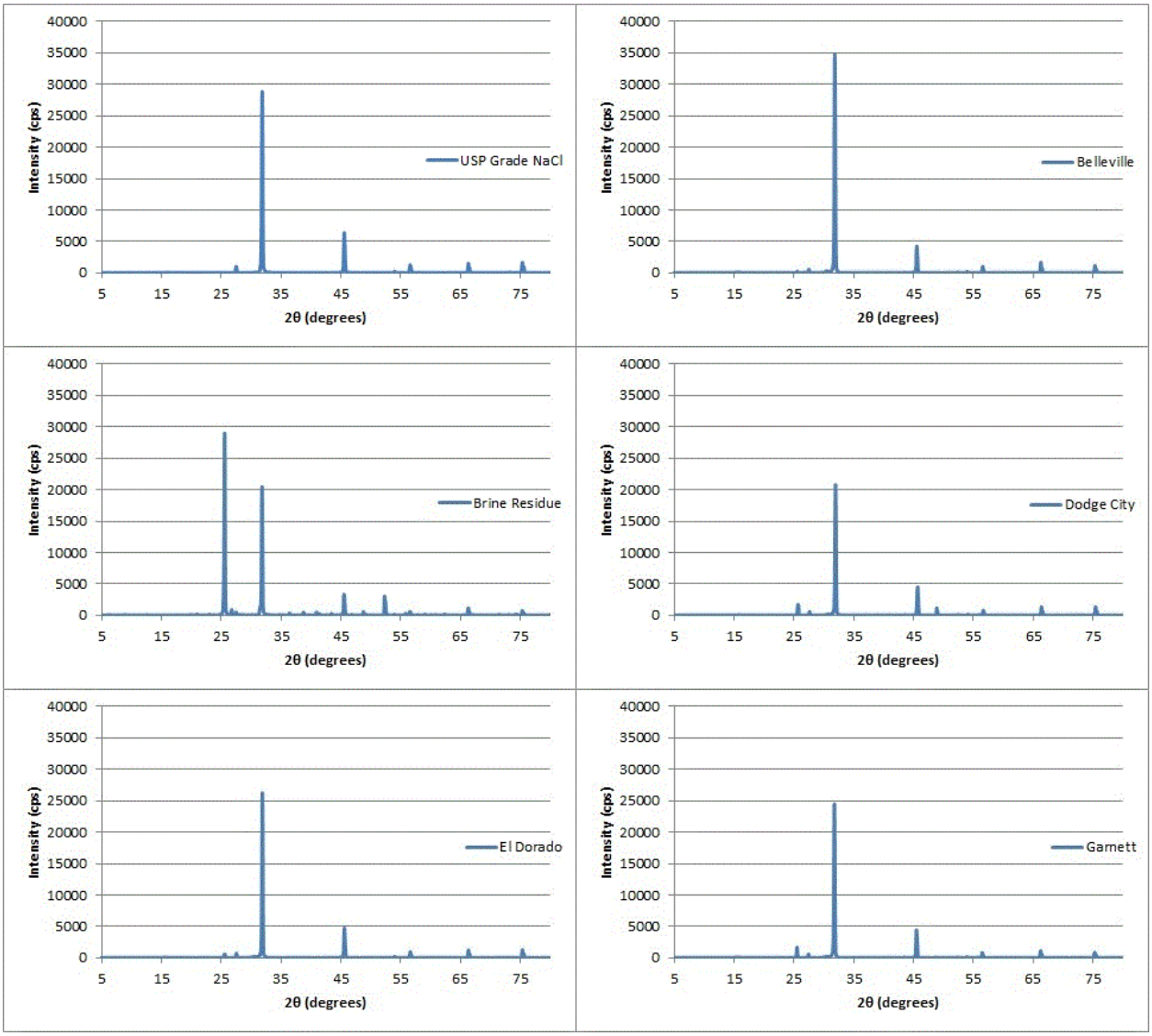

Figure A.1a: First Six Rock Salt Diffraction Patterns

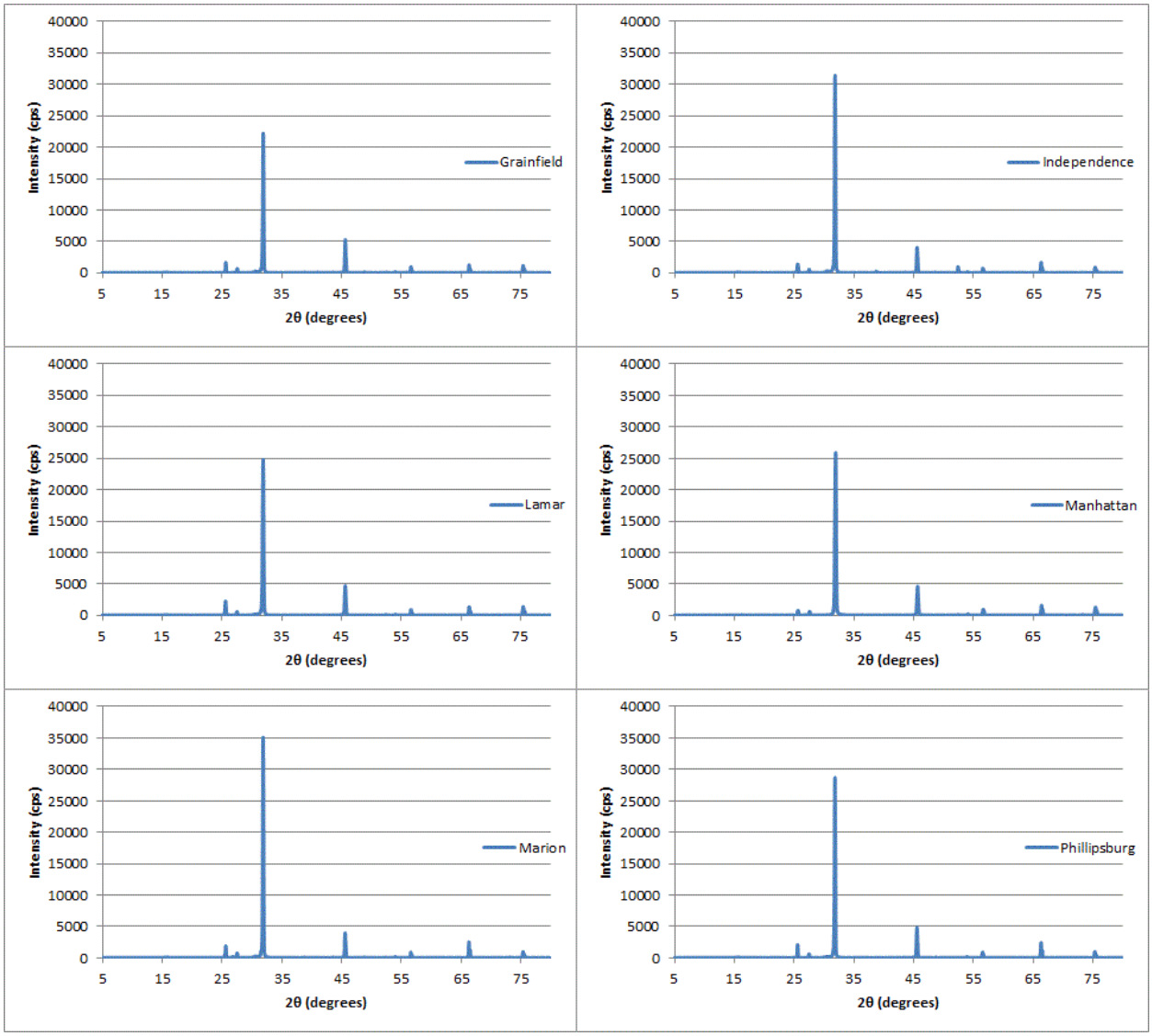

Figure A.1b: Second Six Rock Salt Diffraction Patterns

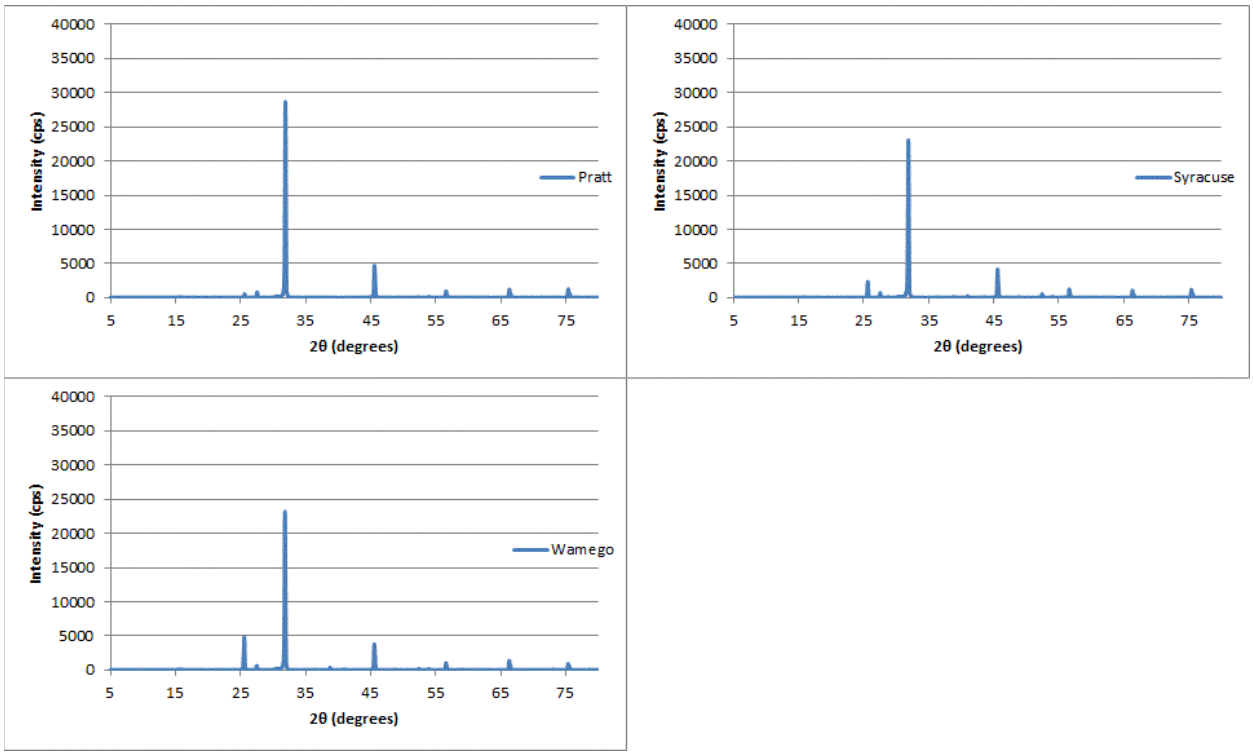

Figure A.1c: Last Three Rock Salt Diffraction Patterns

Appendix B: Limestone Prism Wet-Dry Samples

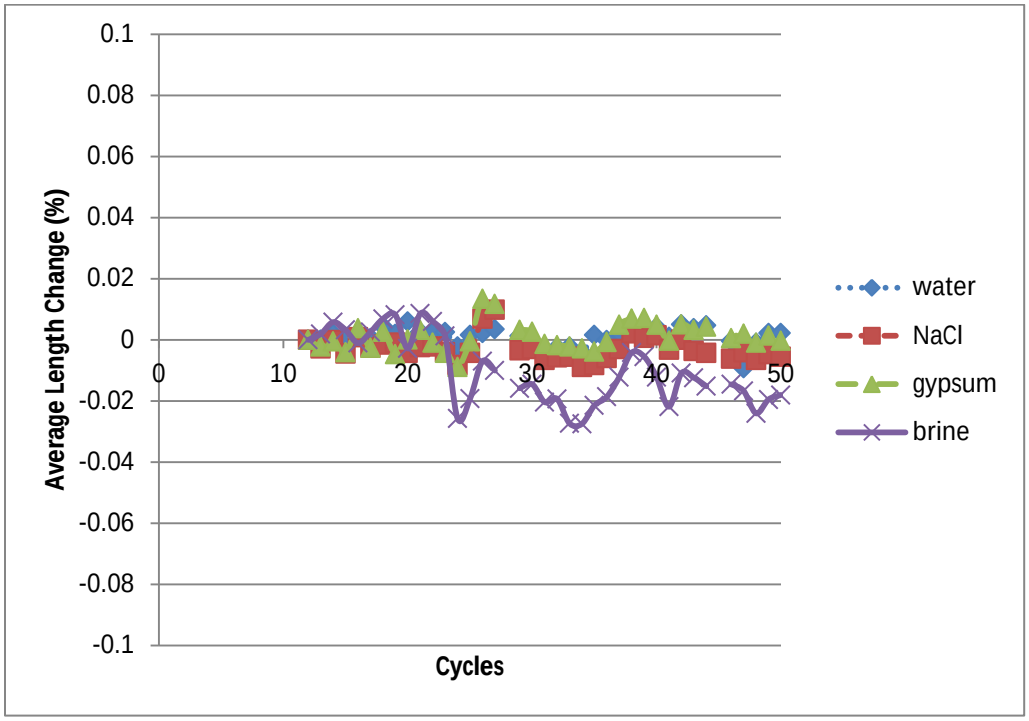

Figure B.1: L1 Average Length Change

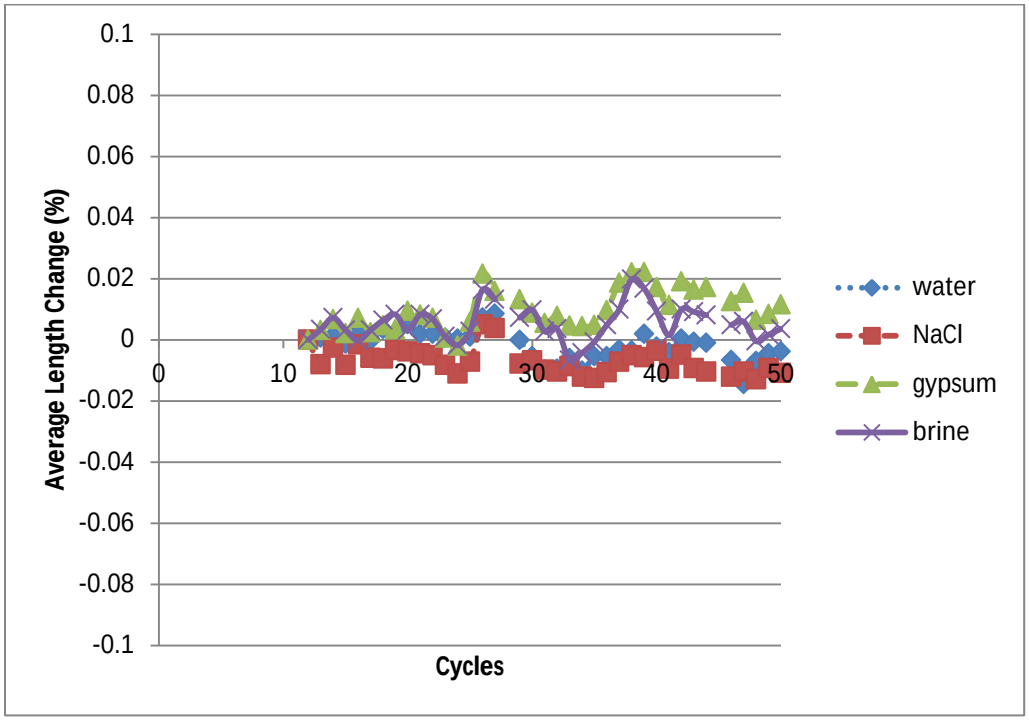

Figure B.2: L2 Average Length Change

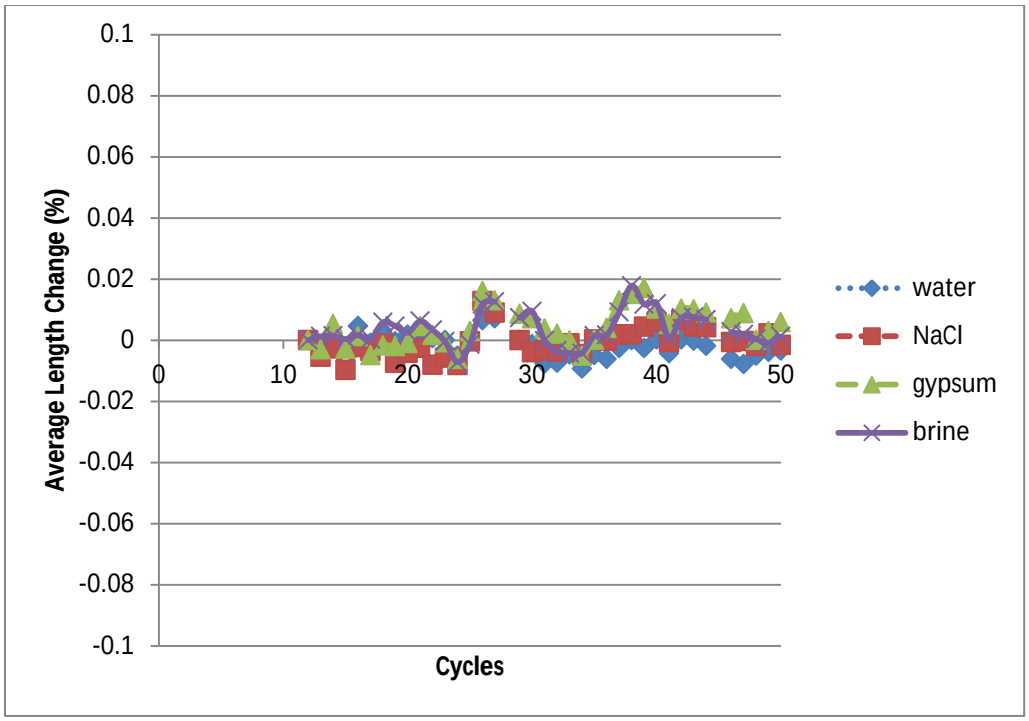

Figure B.3: L3 Average Length Change

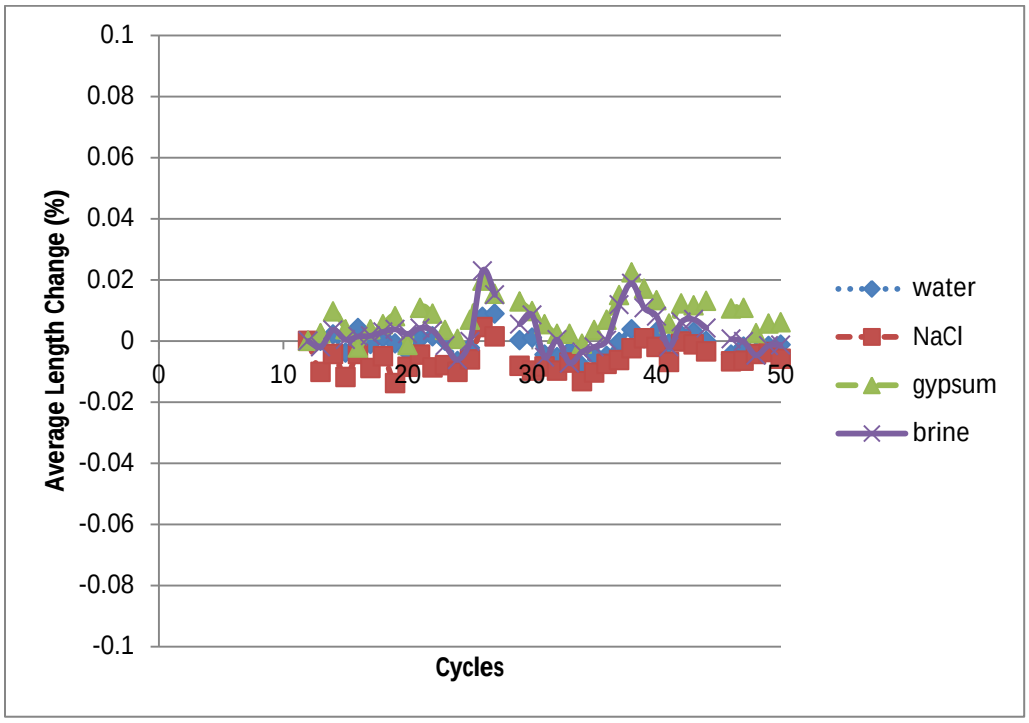

Figure B.4: L4 Average Length Change

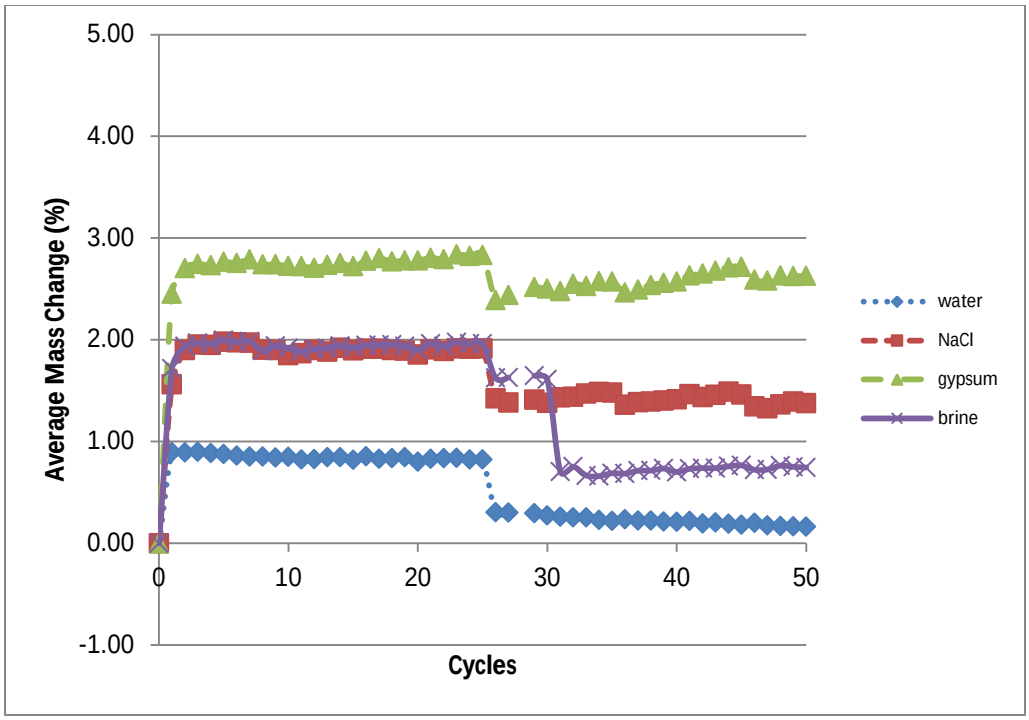

Figure B.5: L1 Average Mass Change

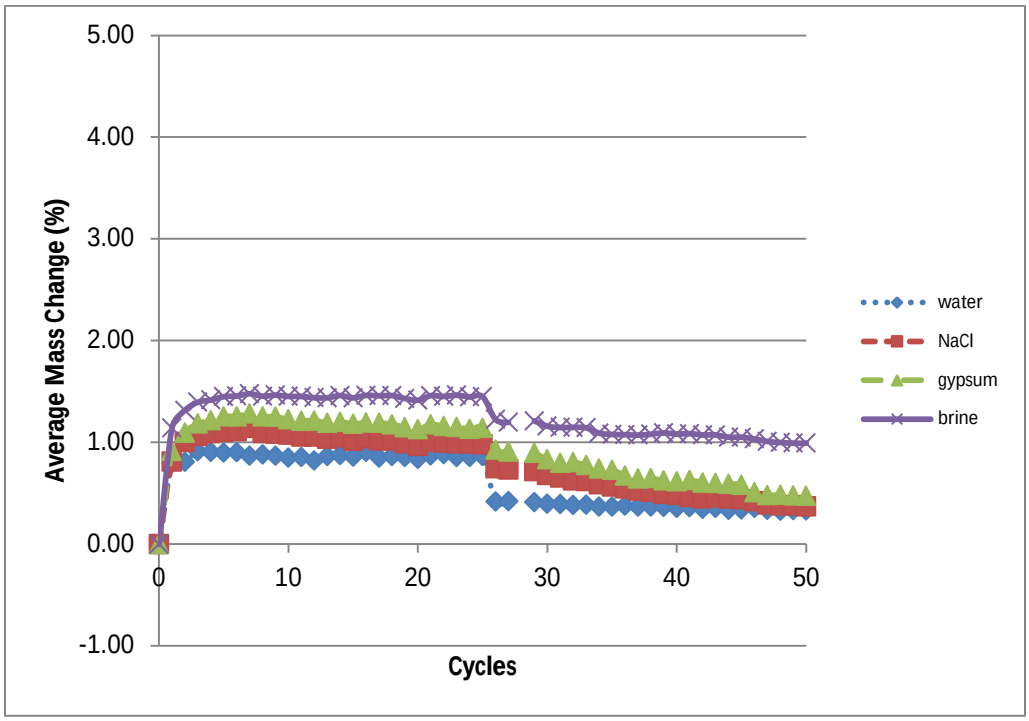

Figure B.6: L2 Average Mass Change

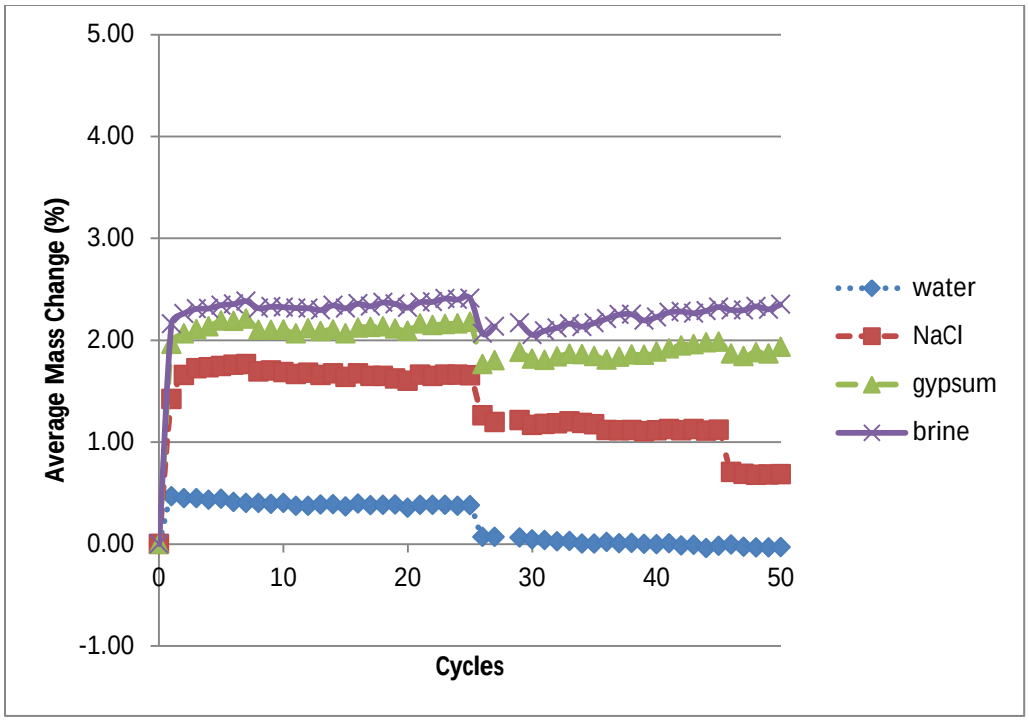

Figure B.7: L3 Average Mass Change

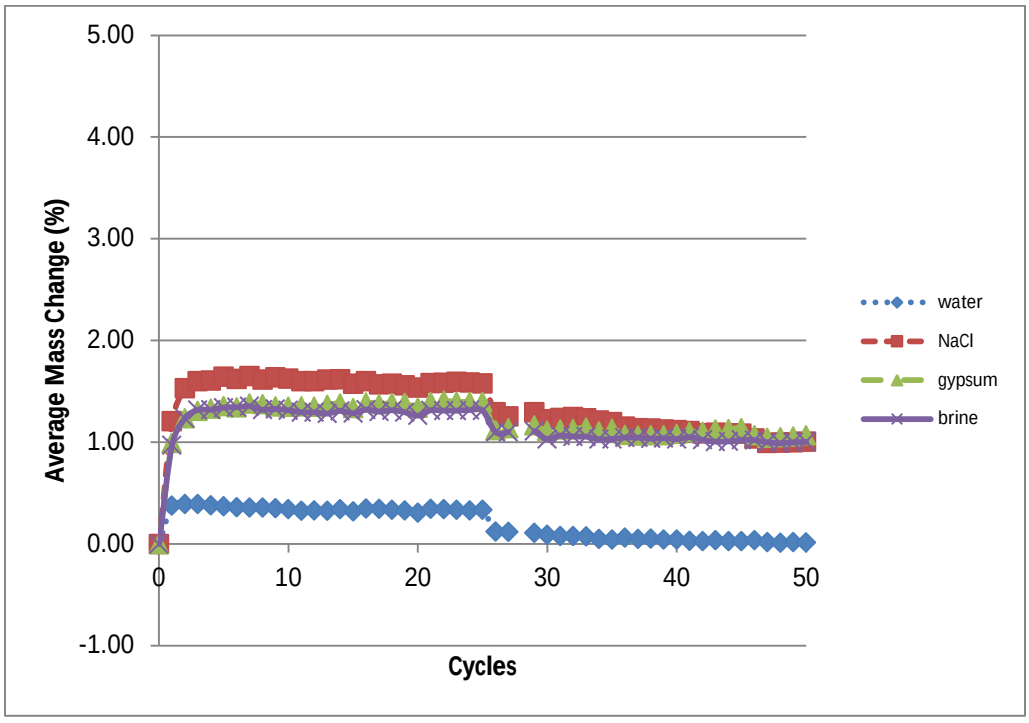

Figure B.8: L4 Average Mass Change

Limestone prisms were photographed before and after completion of the wet-dry test. The after pictures of the prisms in water were taken after the end of the last wet-dry cycle. The prisms were first rinsed in distilled water and wiped with a paper towel to remove excess surface water. Next prisms were immersed in distilled water for two days, dried for two days, and then photographed. Each figure is a compilation of photos taken of the four longitudinal faces of a prism before and after the test. The left column shows prism faces before the test and the right column the corresponding prism faces after the test and the rinsing procedure.

There was no scaling on the samples in water. Qualitatively the amount of scaling was greatest in NaCl followed by gypsum then brine. Some samples subjected to brine when rinsed seemed to have no scaling over a large portion of the prism surface area.

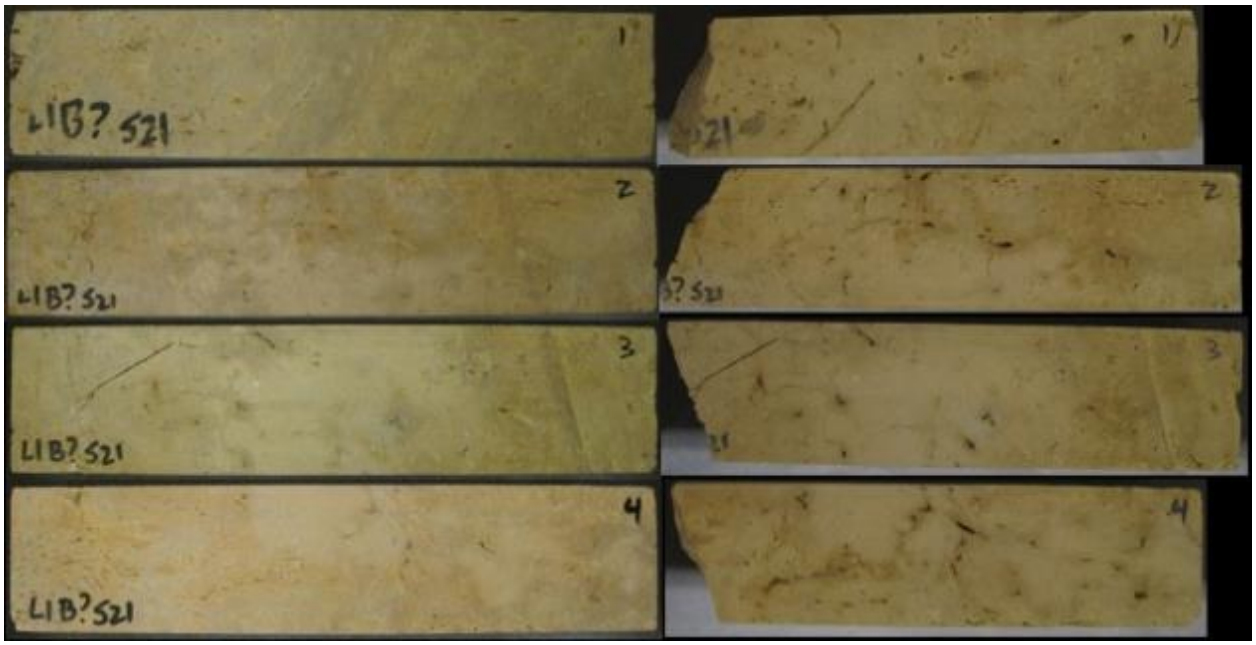

Figure B.9: L1 Sample 21 in Water

L1 sample 21 split during the oven-drying stage. Otherwise, damage was negligible.

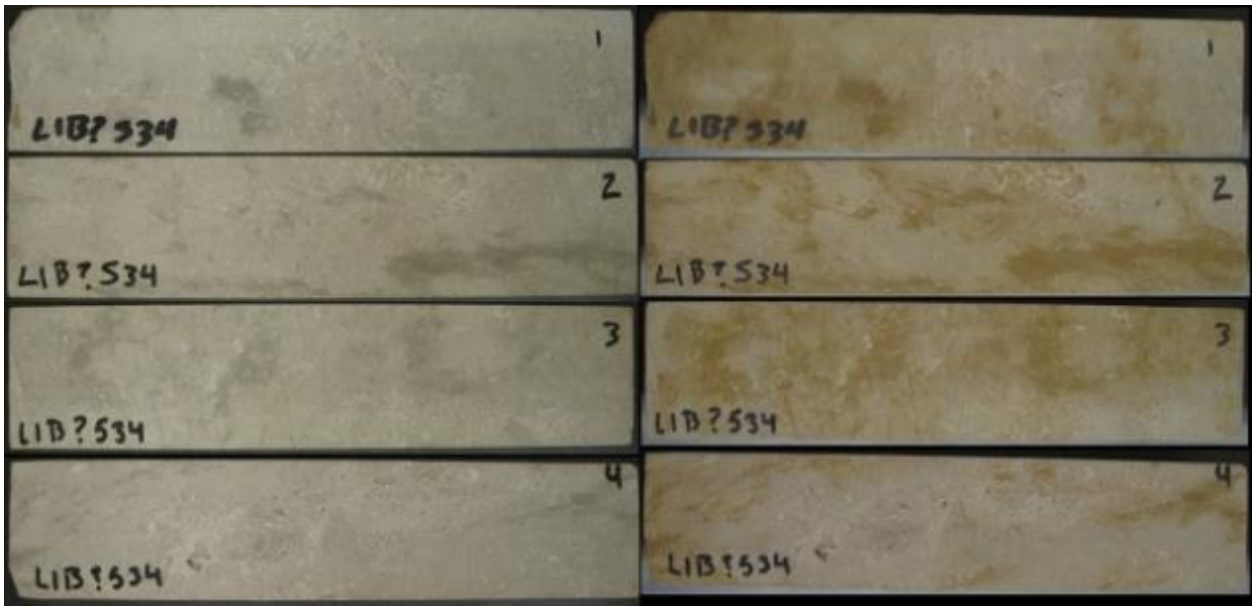

Figure B.10: L1 Sample 34 in Water

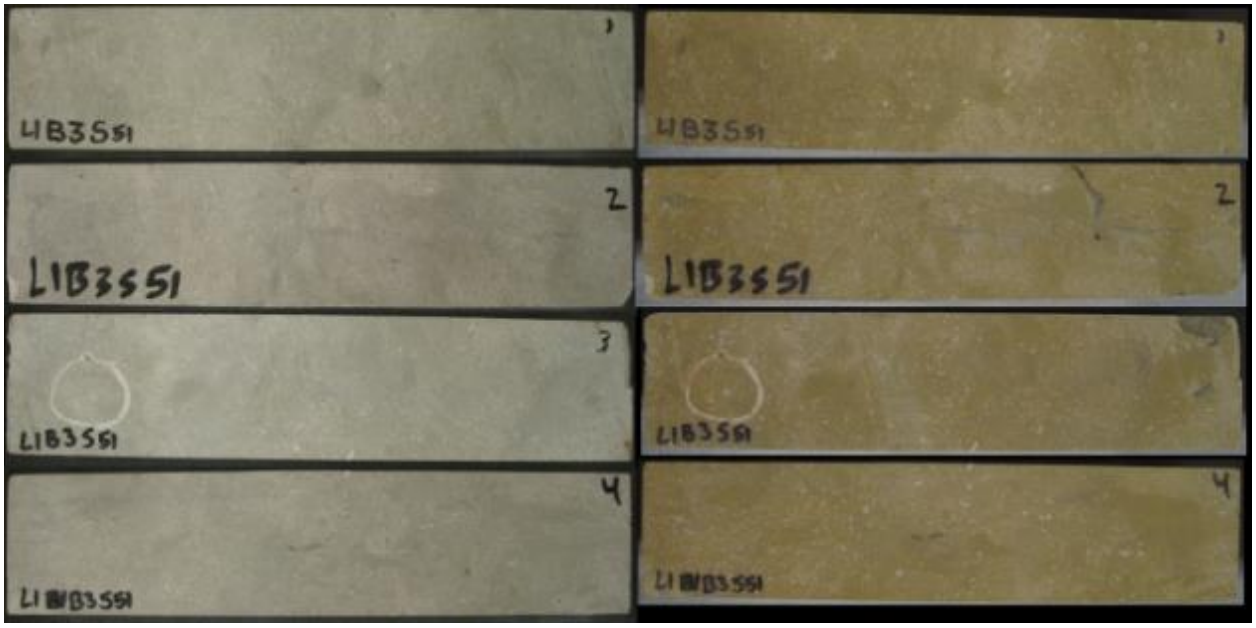

Figure B.11: L1 Sample 51 in Water

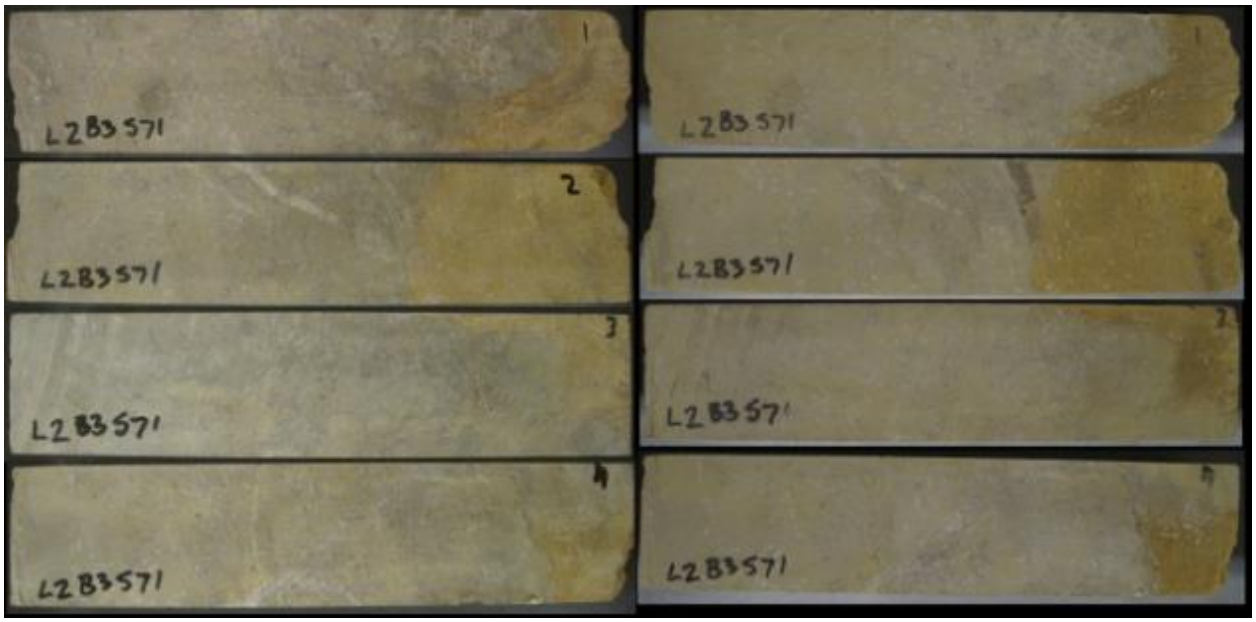

Figure B.12: L2 Sample 71 in Water

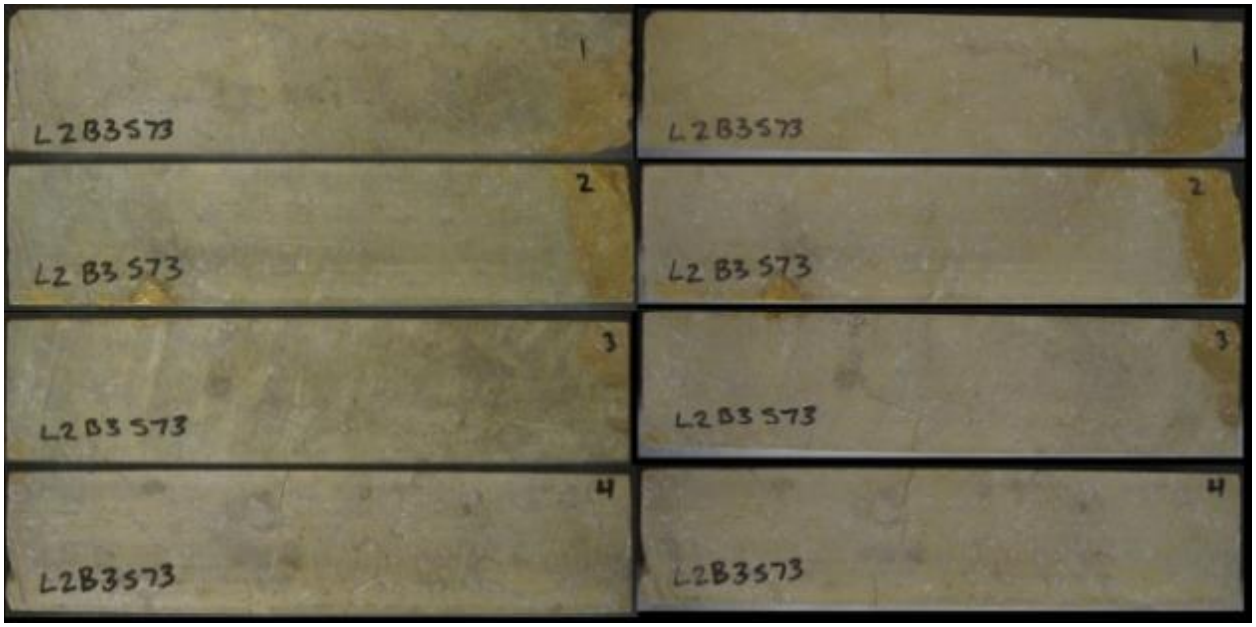

Figure B.13: L2 Sample 73 in Water

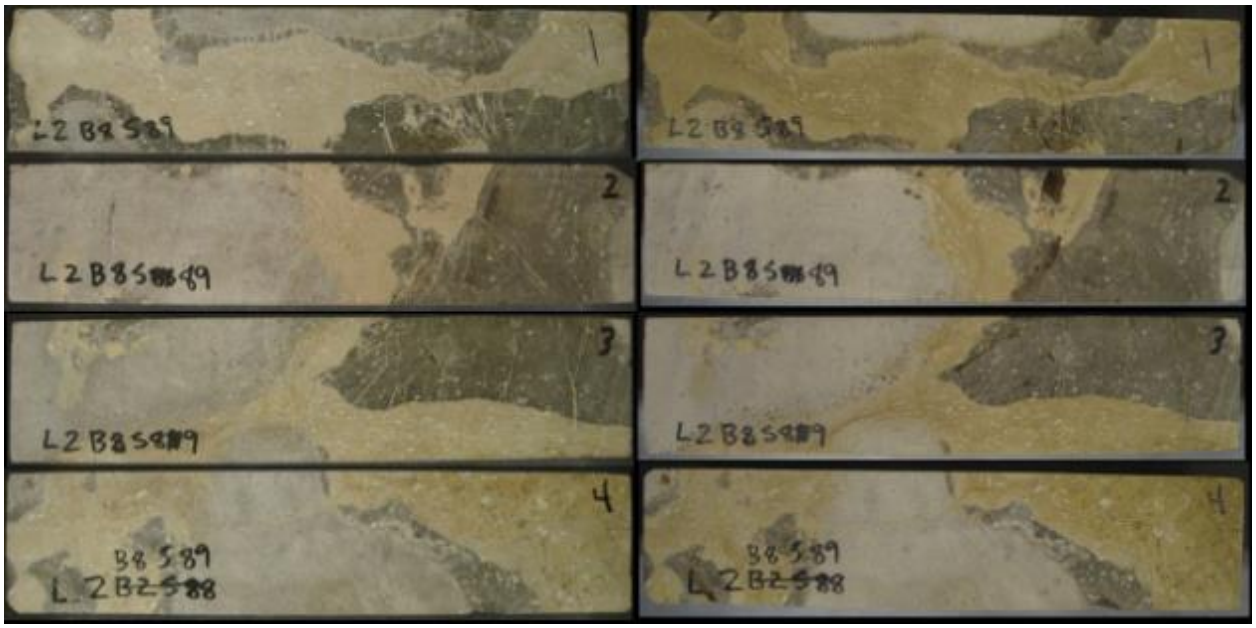

Figure B.14: L2 Sample 89 in Water

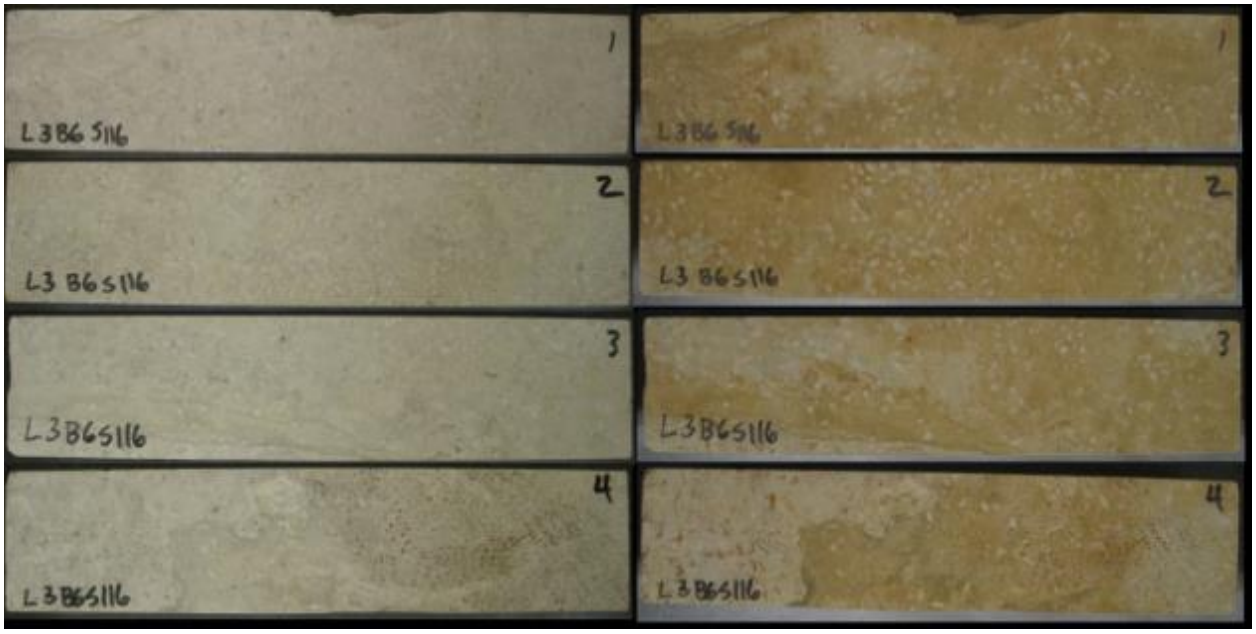

Figure B.15: L3 Sample 116 in Water

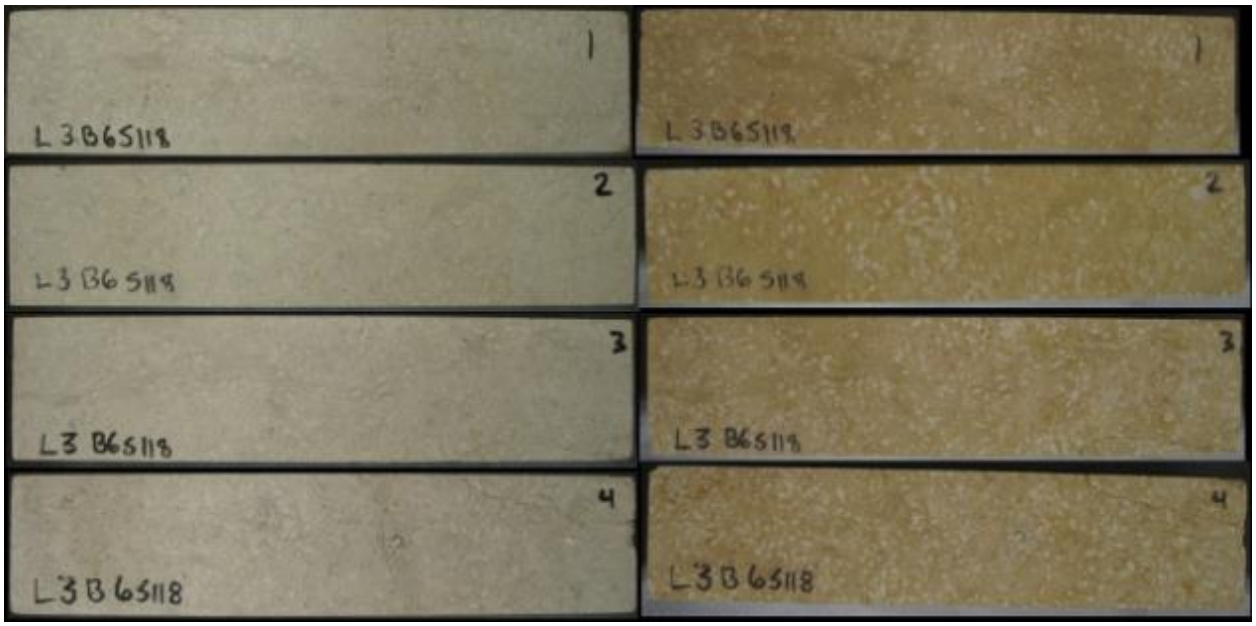

Figure B.16: L3 Sample 118 in Water

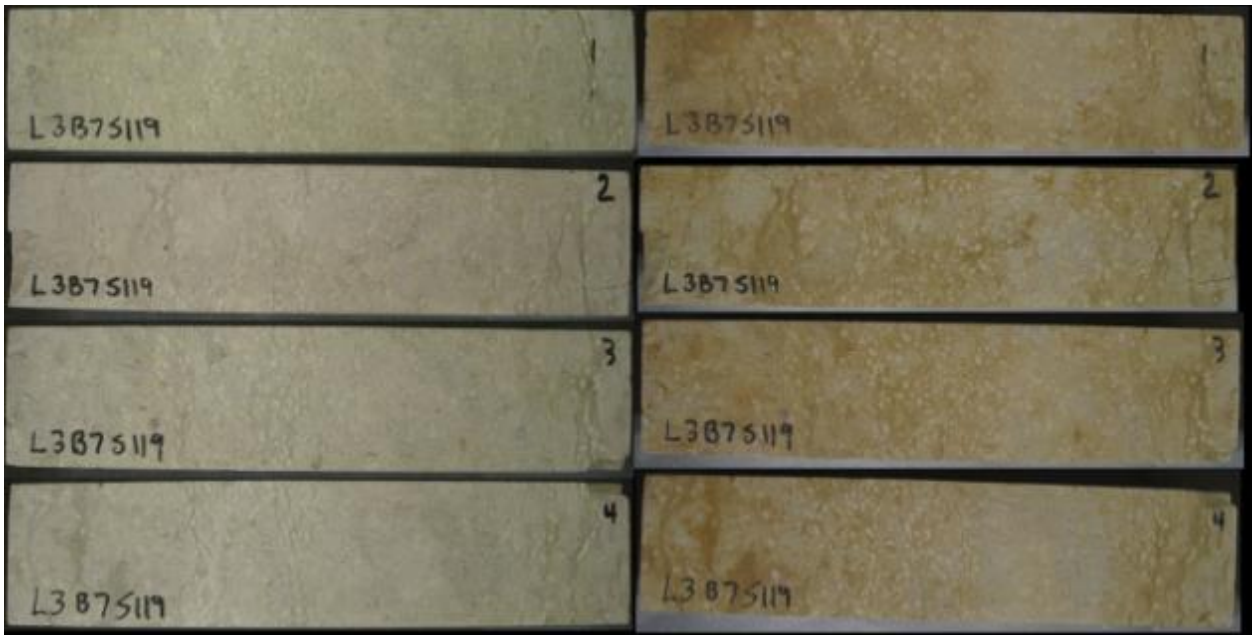

Figure B.17: L3 Sample 119 in Water

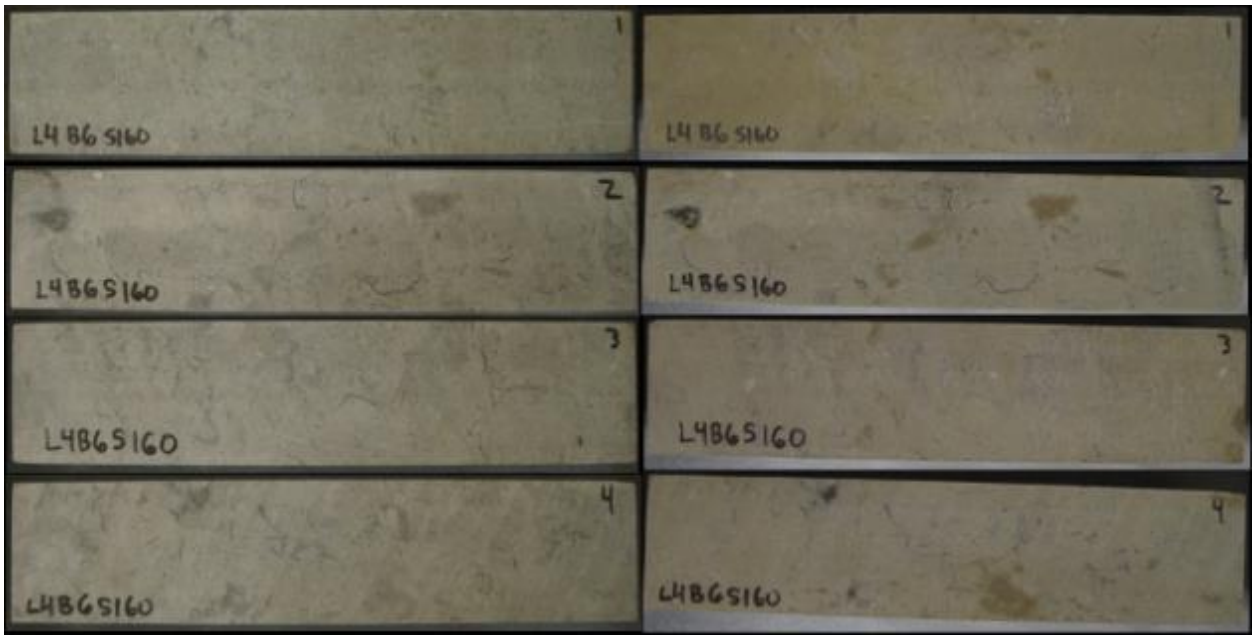

Figure B.18: L4 Sample 160 in Water

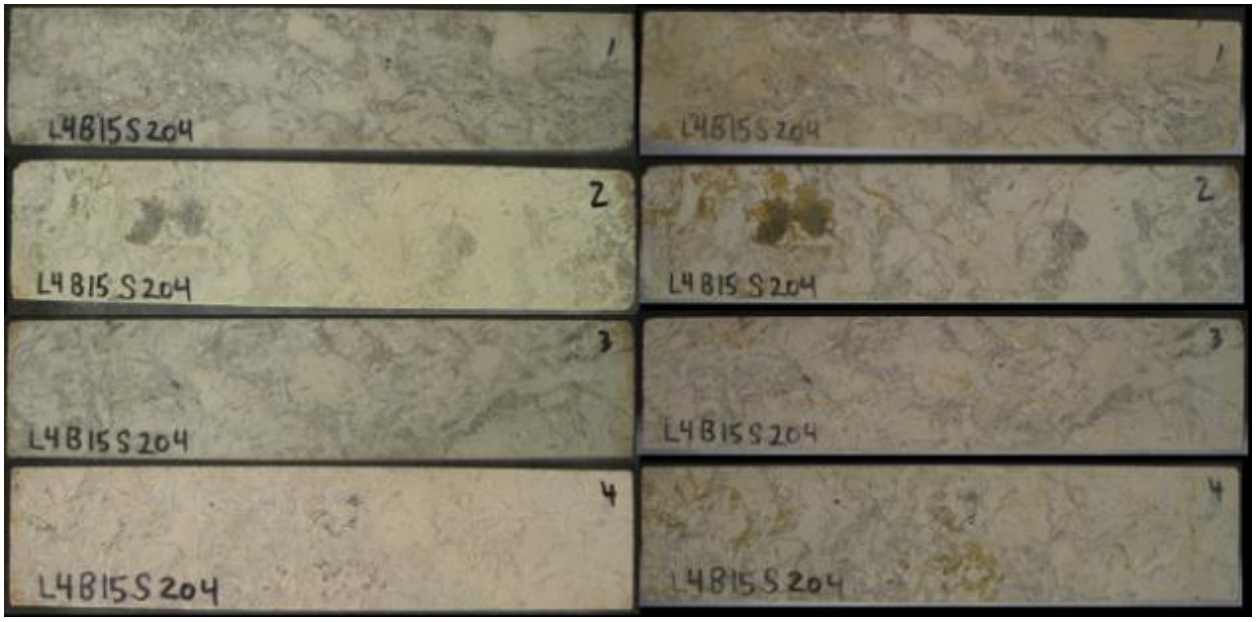

Figure B.19: L4 Sample 204 in Water

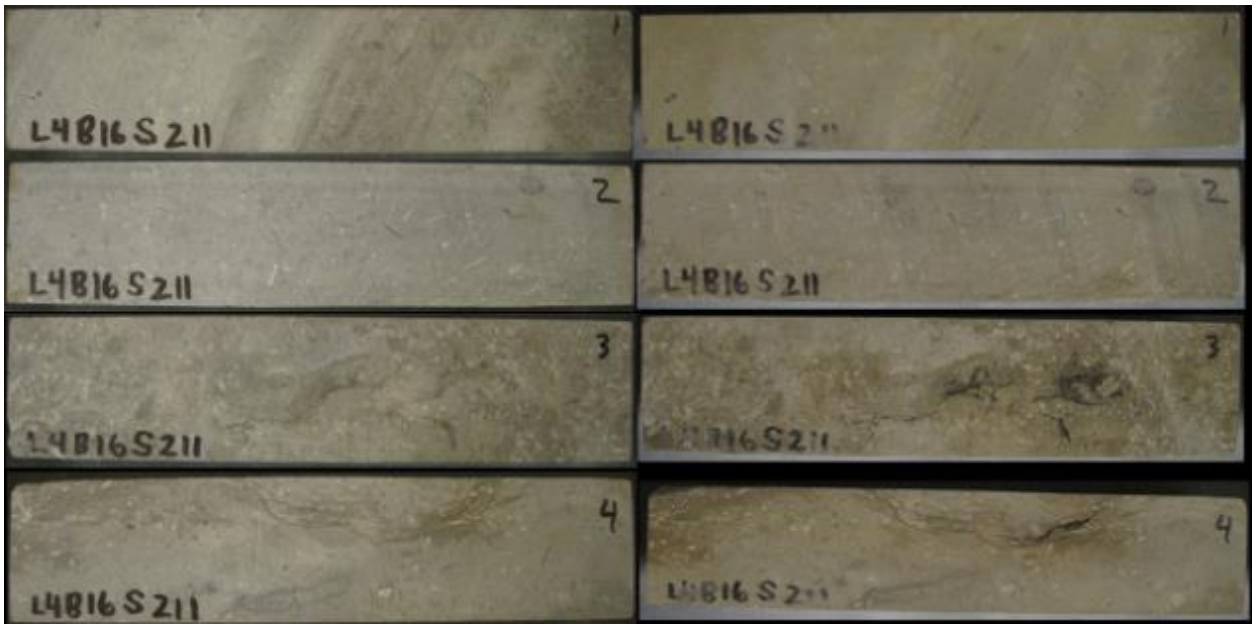

Figure B.20: L4 Sample 211 in Water

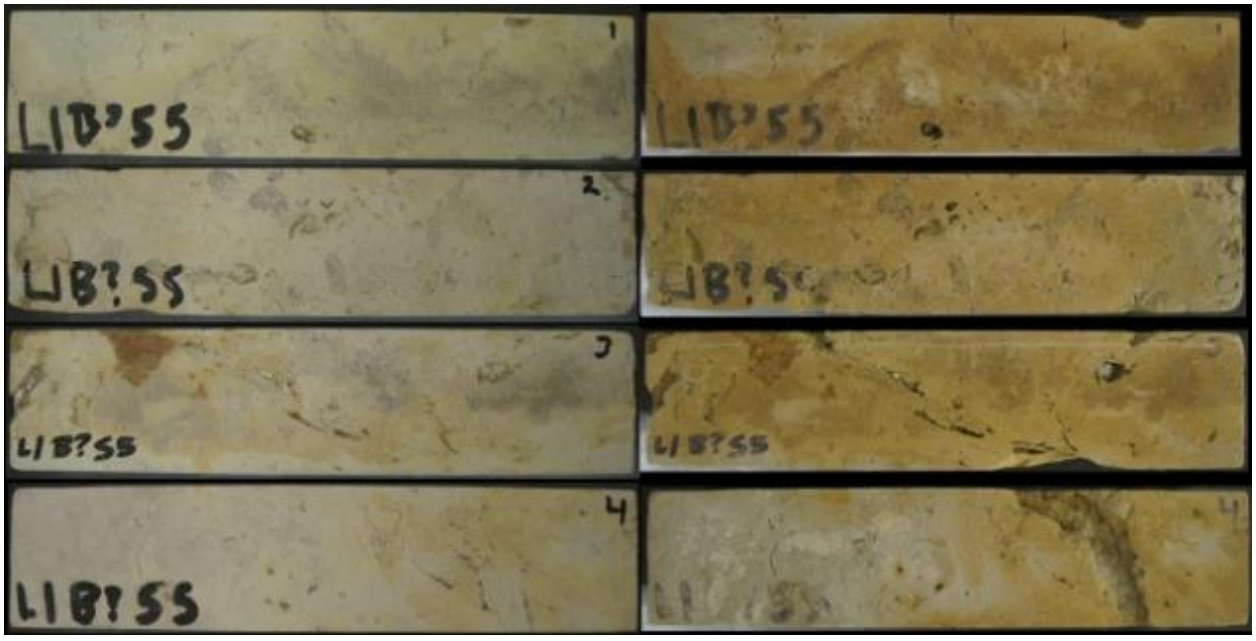

Figure B.21: L1 Sample 5 in NaCl

L1 sample 5 lost a fragment during the first wetting cycle. When the prism was removed from NaCl solution the first time, the section loss apparent on the face labeled "4" was noticed. Clay swelling underneath a weak layer of limestone during immersion appeared to be the cause.

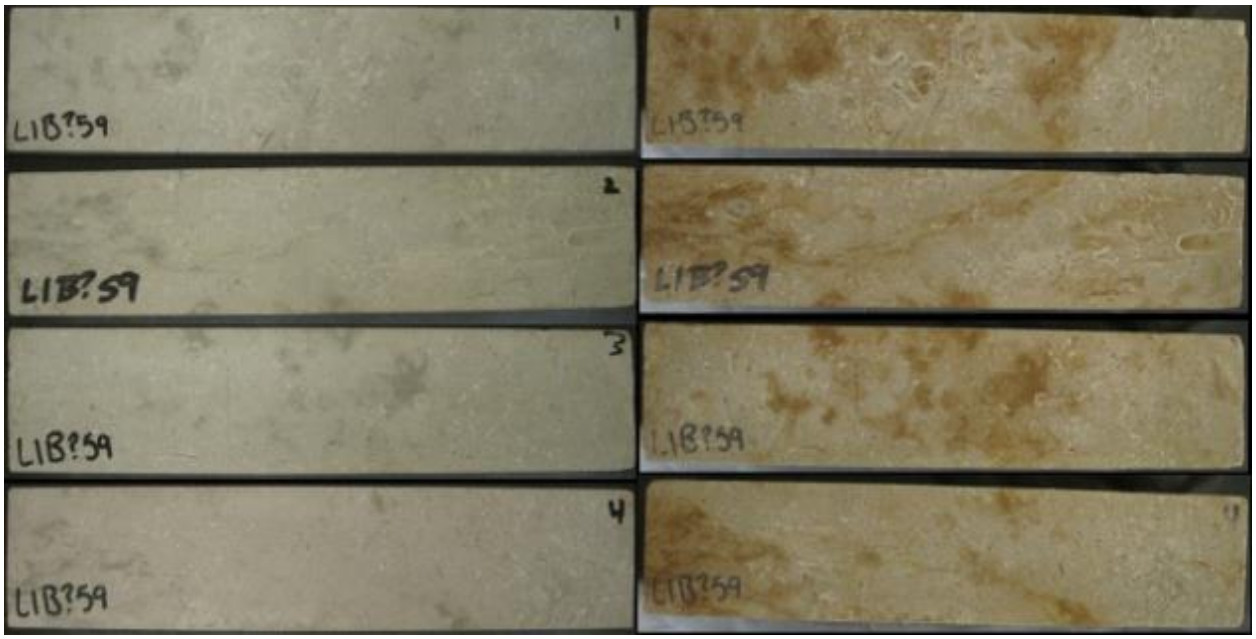

Figure B.22: L1 Sample 9 in NaCl

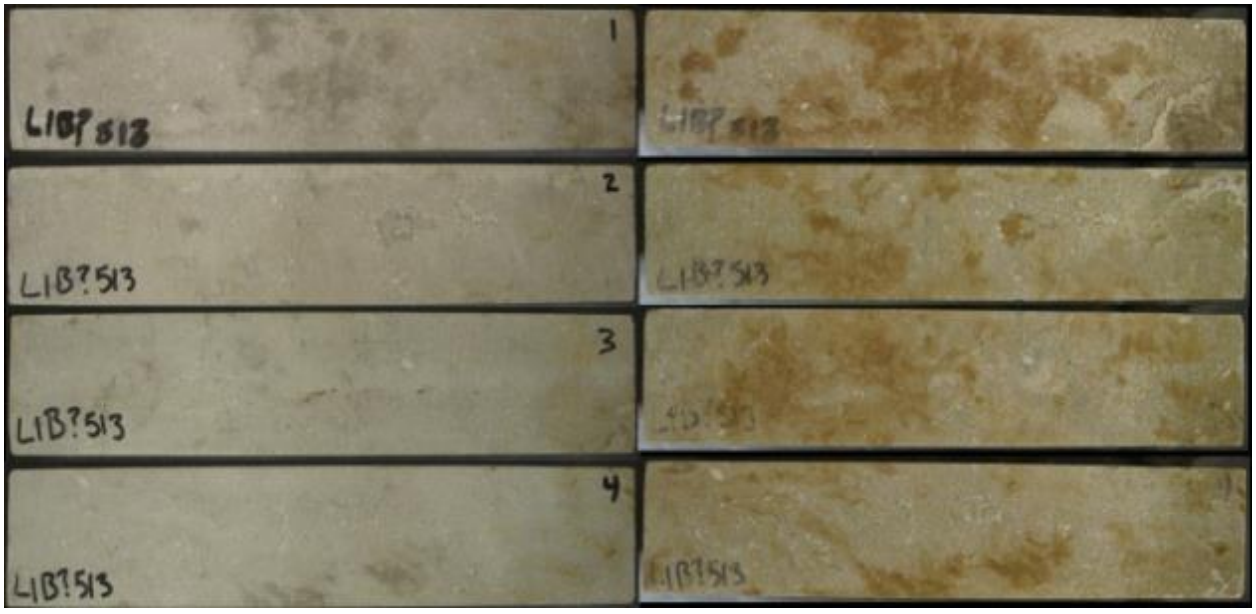

Figure B.23: L1 Sample 13 in NaCl

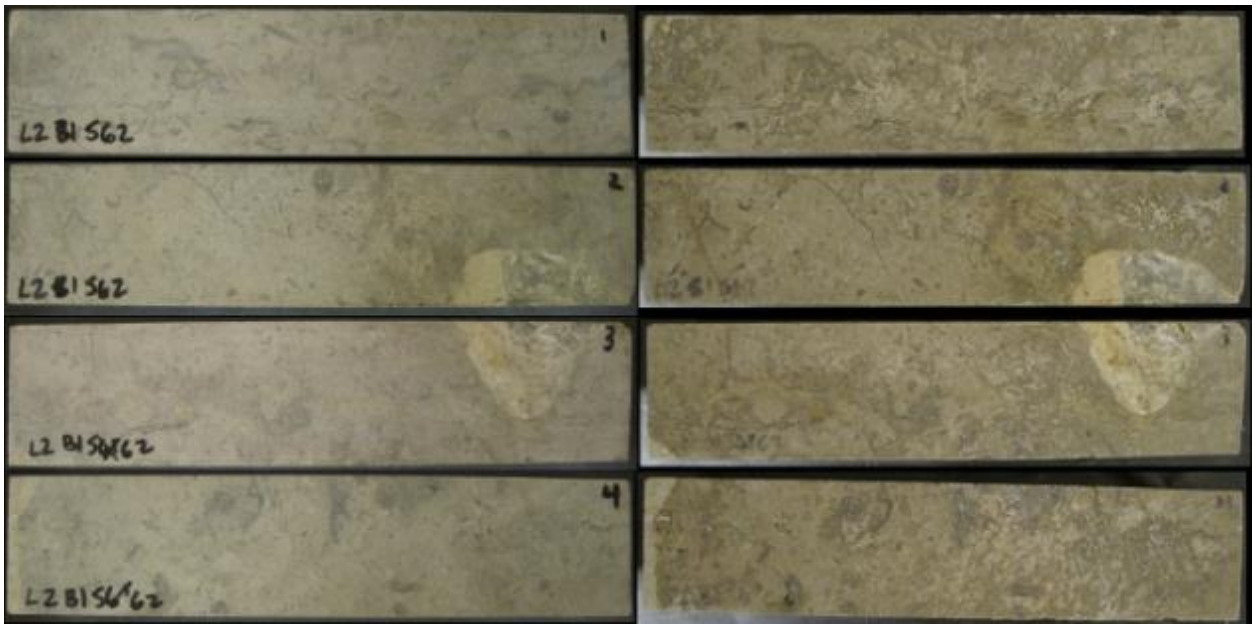

Figure B.24: L2 Sample 62 in NaCl

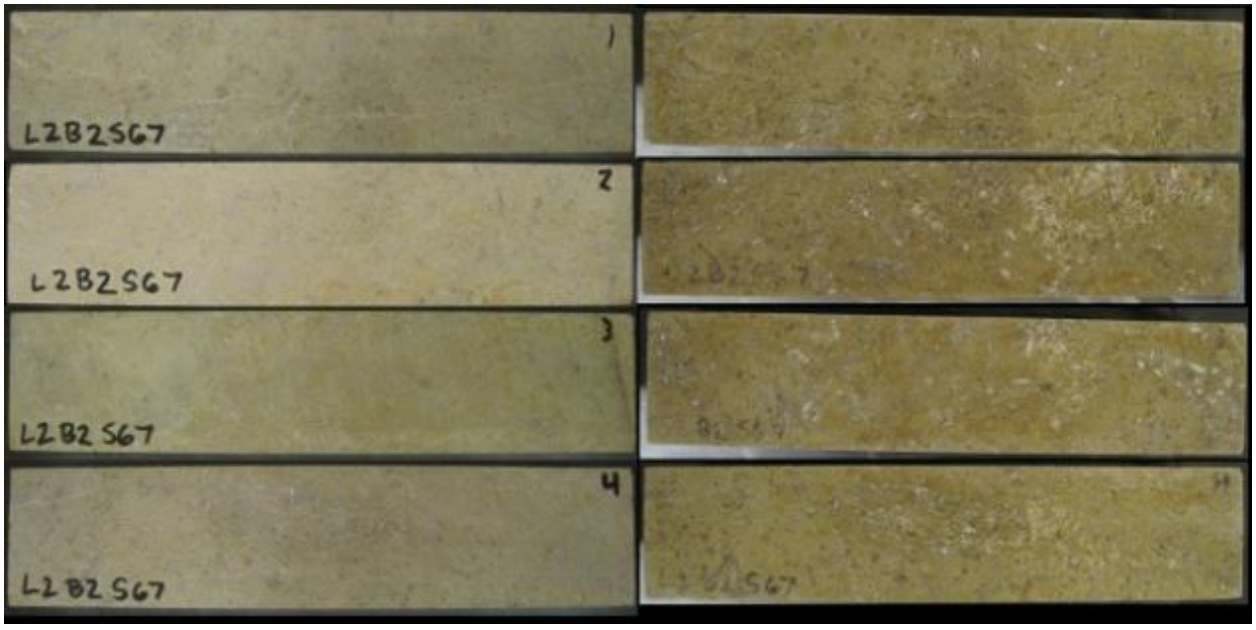

Figure B.25: L2 Sample 67 in NaCl

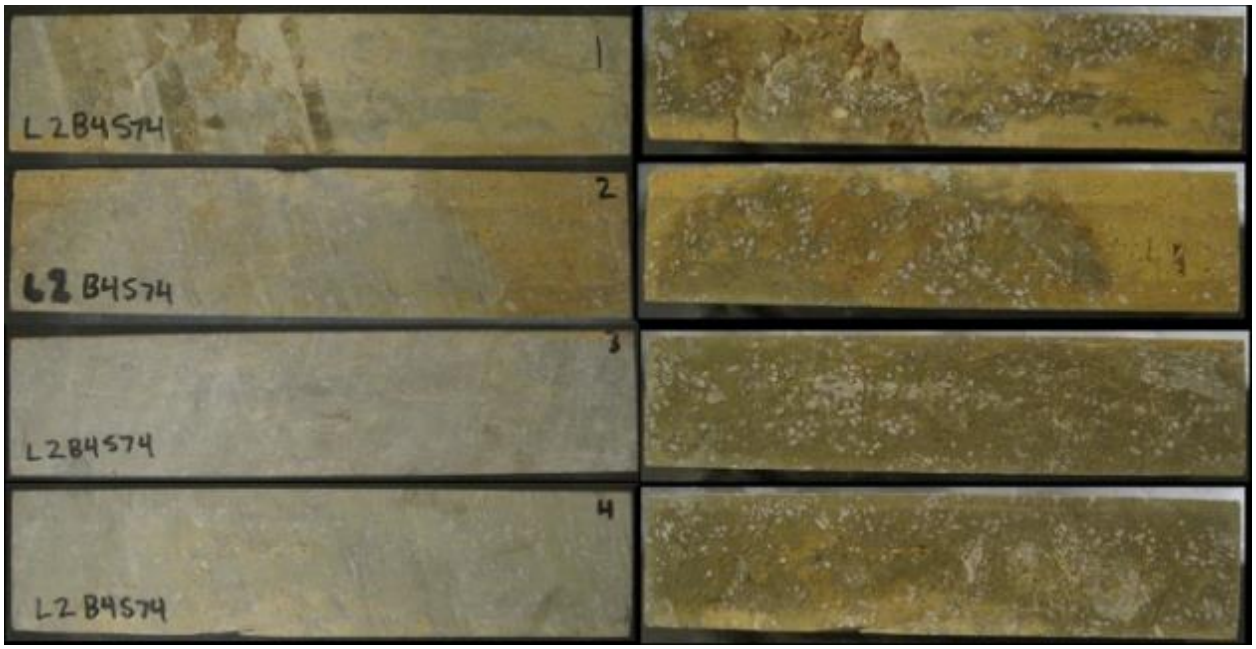

Figure B.26: L2 Sample 74 in NaCl

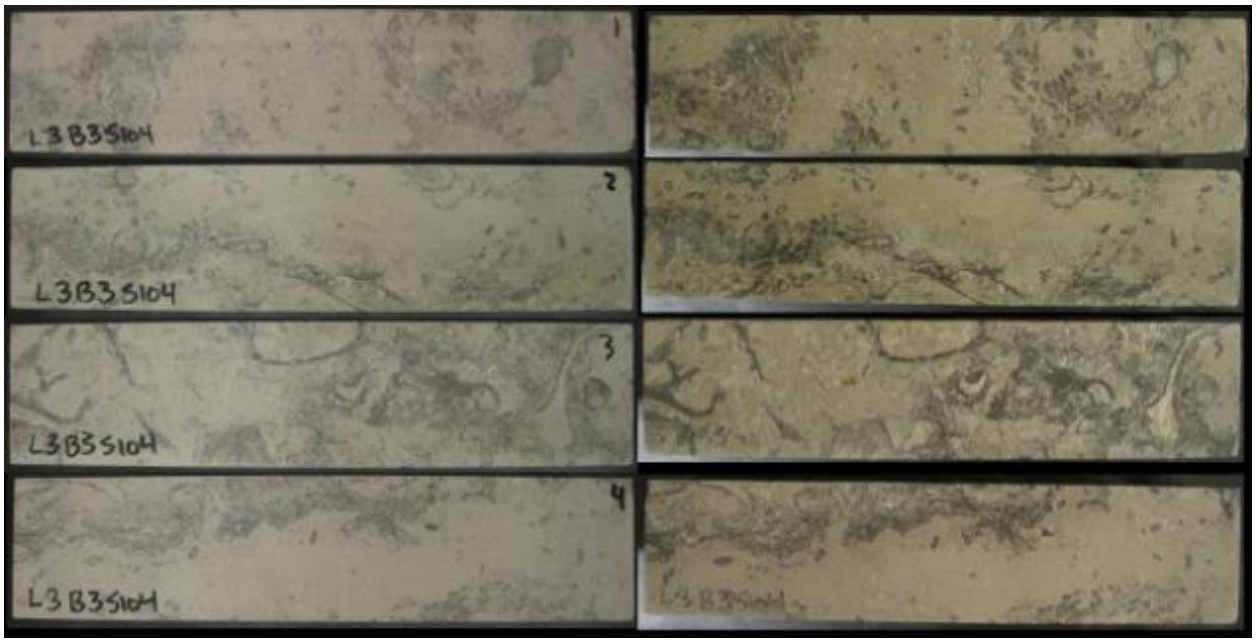

Figure B.27: L3 Sample 104 in NaCl

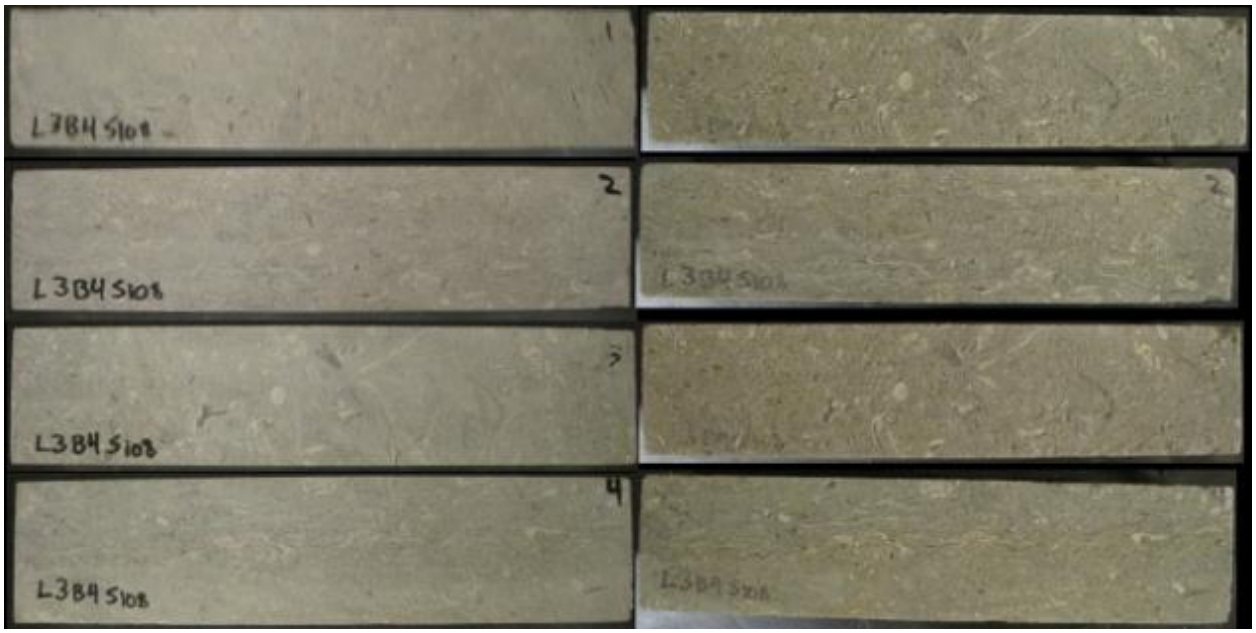

Figure B.28: L3 Sample 108 in NaCl

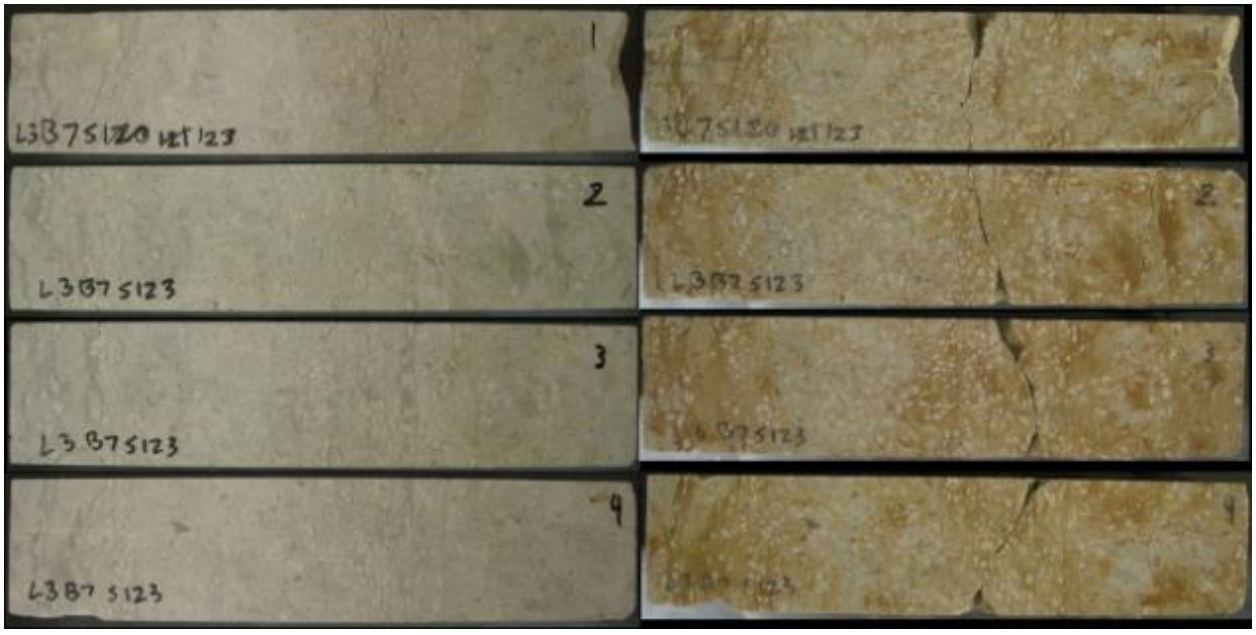

Figure B.29: L3 Sample 123 in NaCl

L3 sample 123 was dropped just before placement in solution for the start of the 46th wet-dry cycle, which is where the crack originated. Prior to that the sample showed minor scaling and behaved similarly to other L3 prisms. This particular sample was not measured for

mass or length after being dropped but was continued in the test to see if any visual changes occurred.

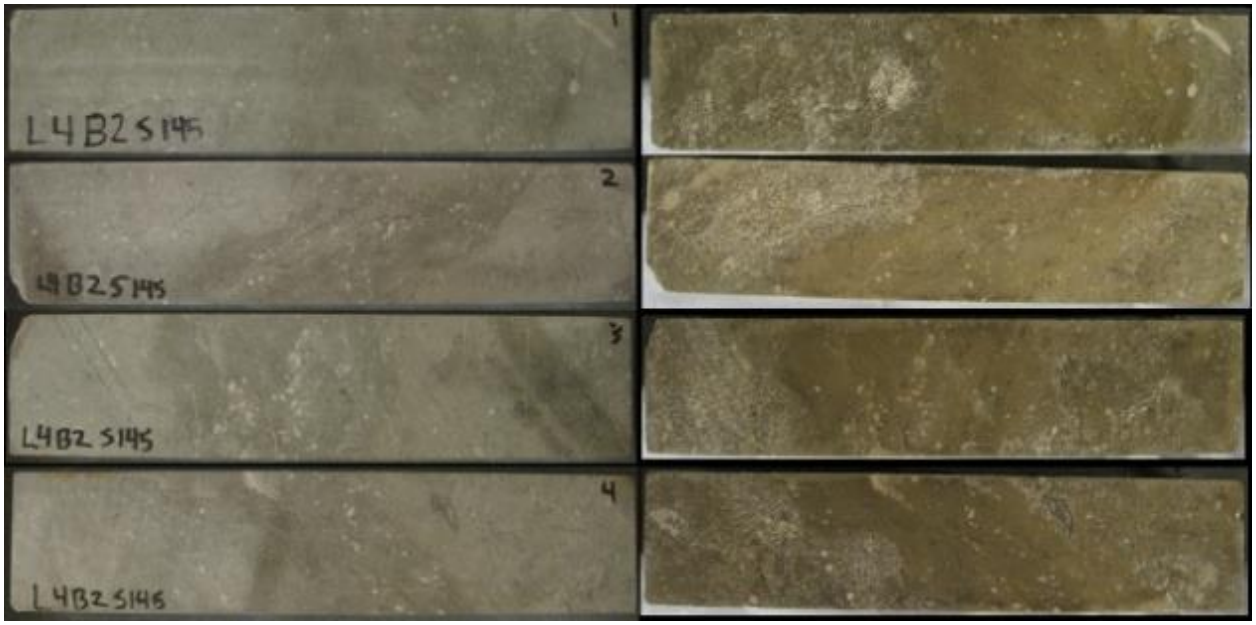

Figure B.30: L4 Sample 145 in NaCl

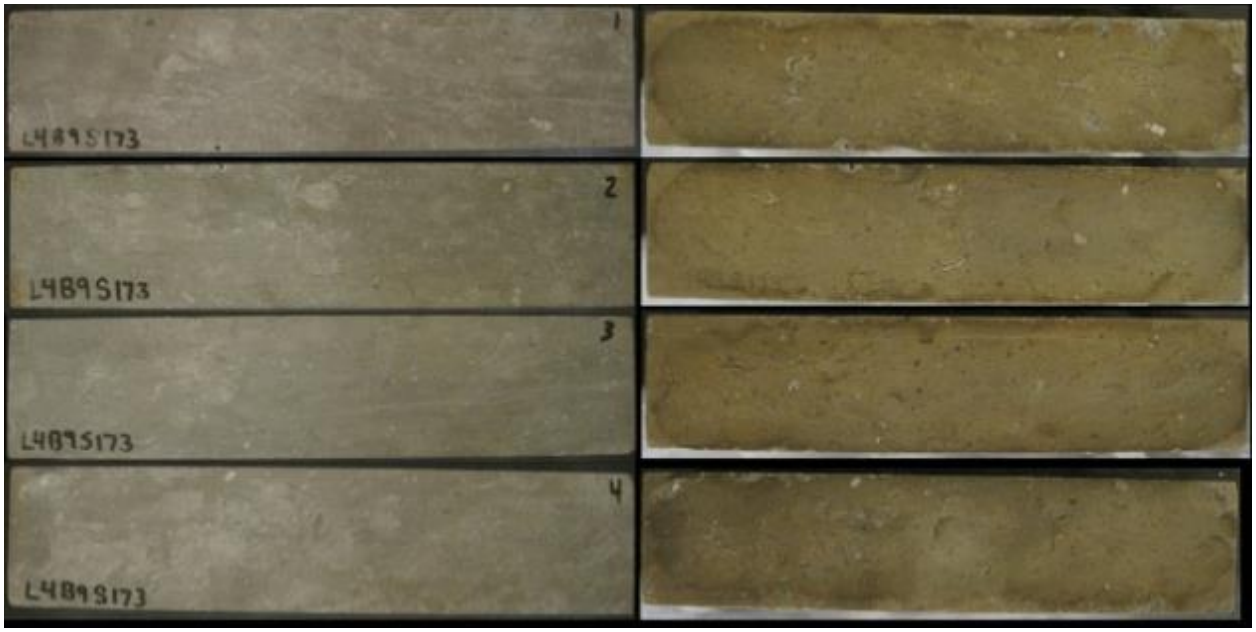

Figure B.31: L4 Sample 173 in NaCl

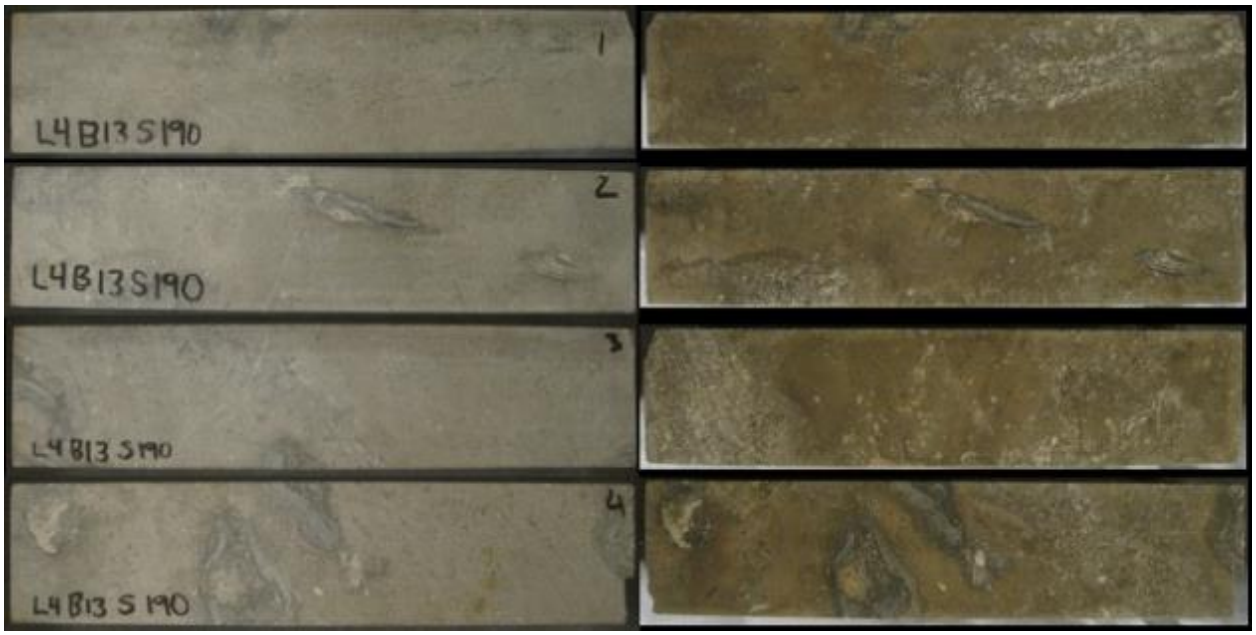

Figure B.32: L4 Sample 190 in NaCl

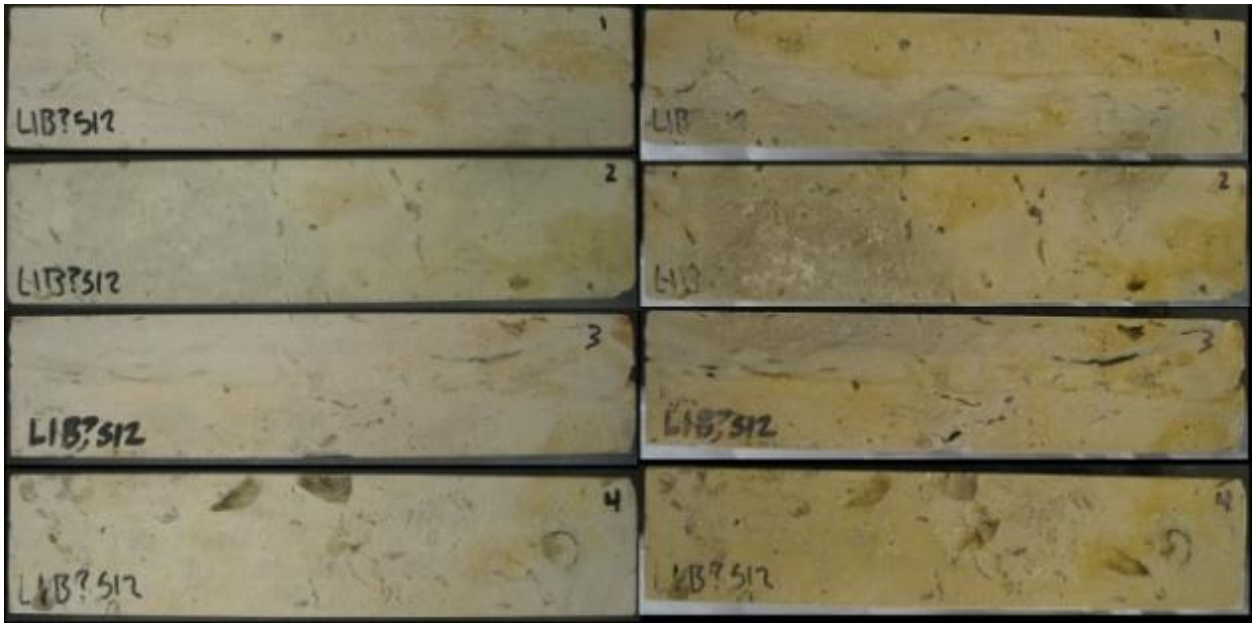

Figure B.33: L1 Sample 12 in Gypsum

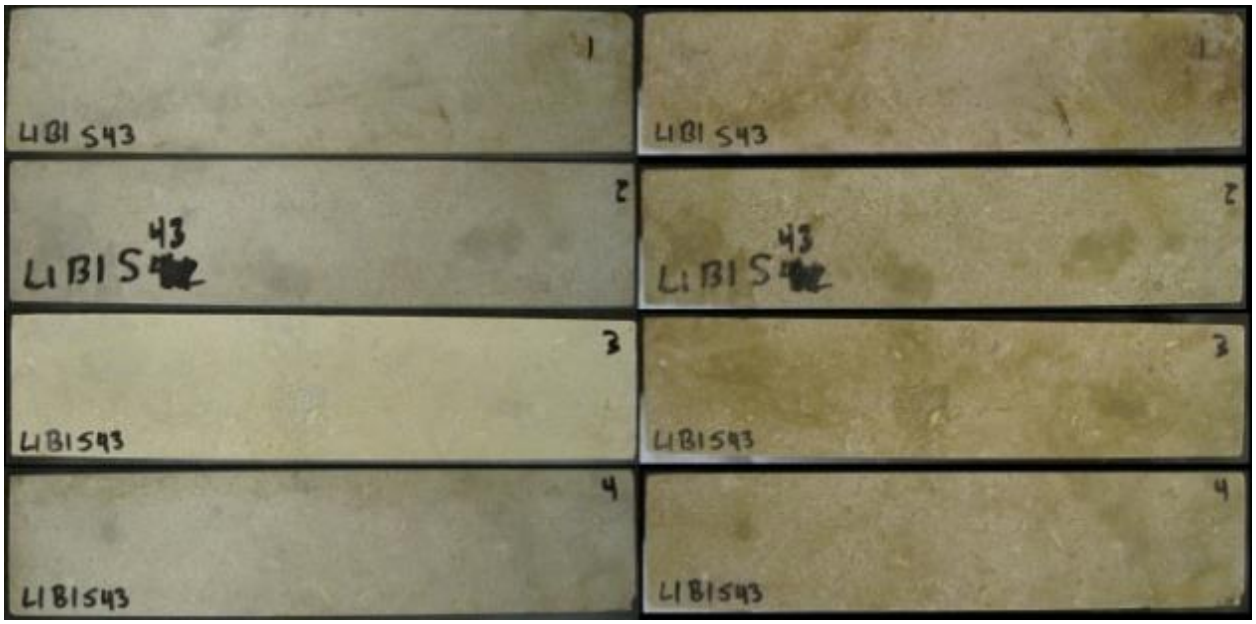

Figure B.34: L1 Sample 43 in Gypsum

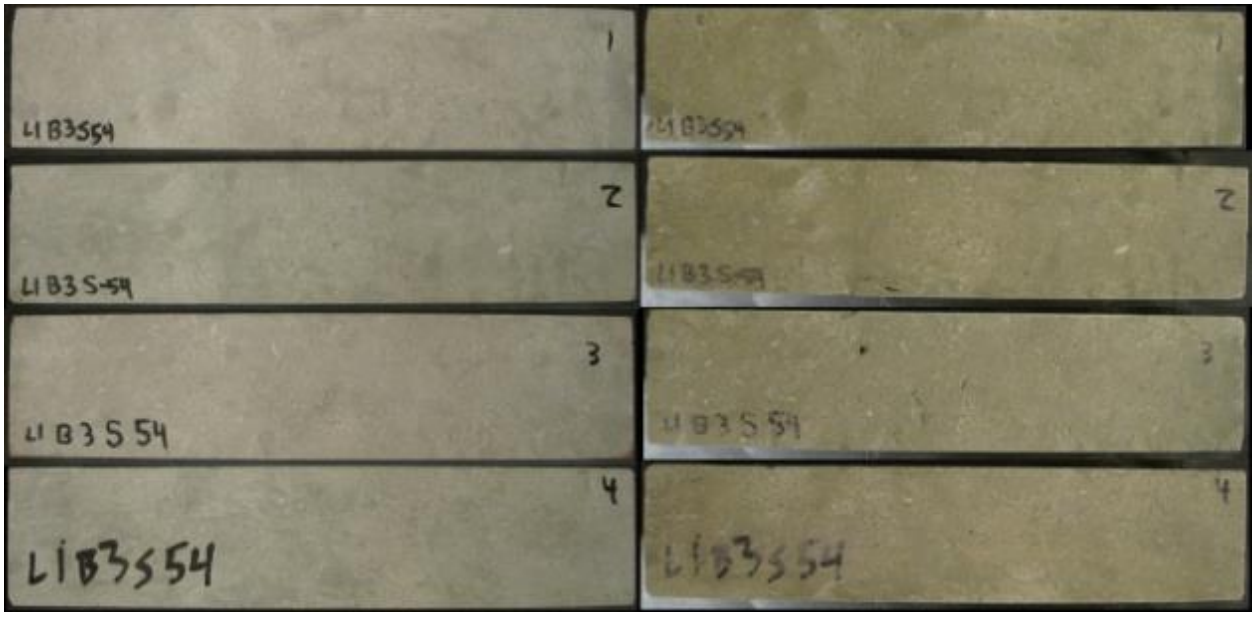

Figure B.35: L1 Sample 54 in Gypsum

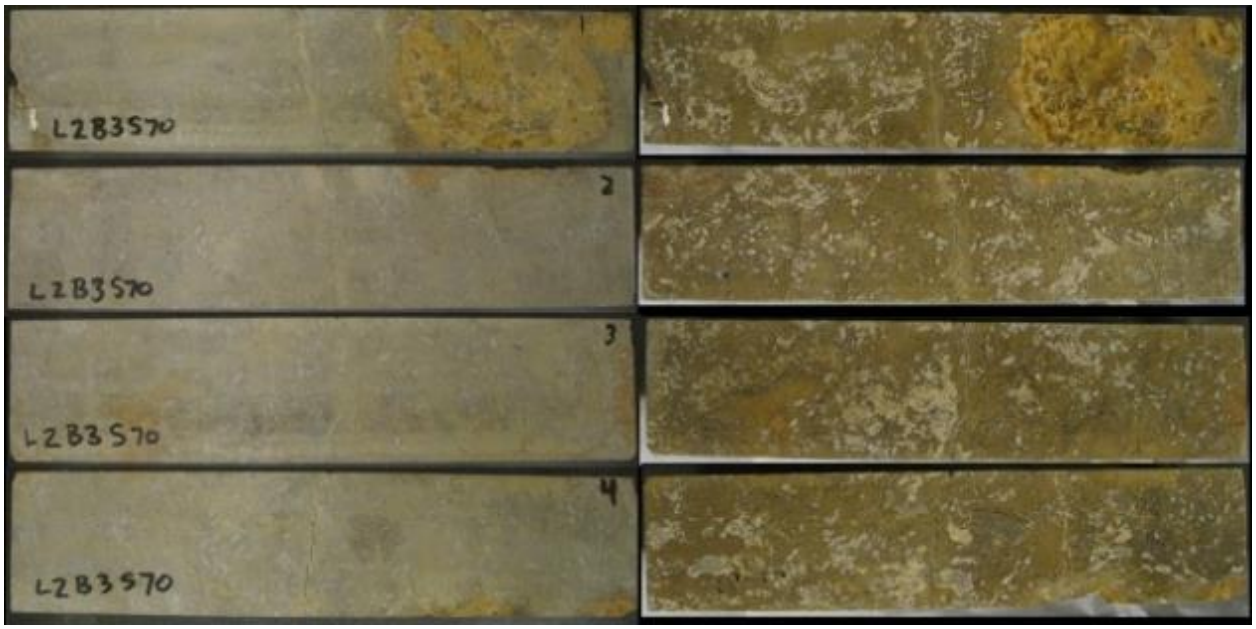

Figure B.36: L2 Sample 70 in Gypsum

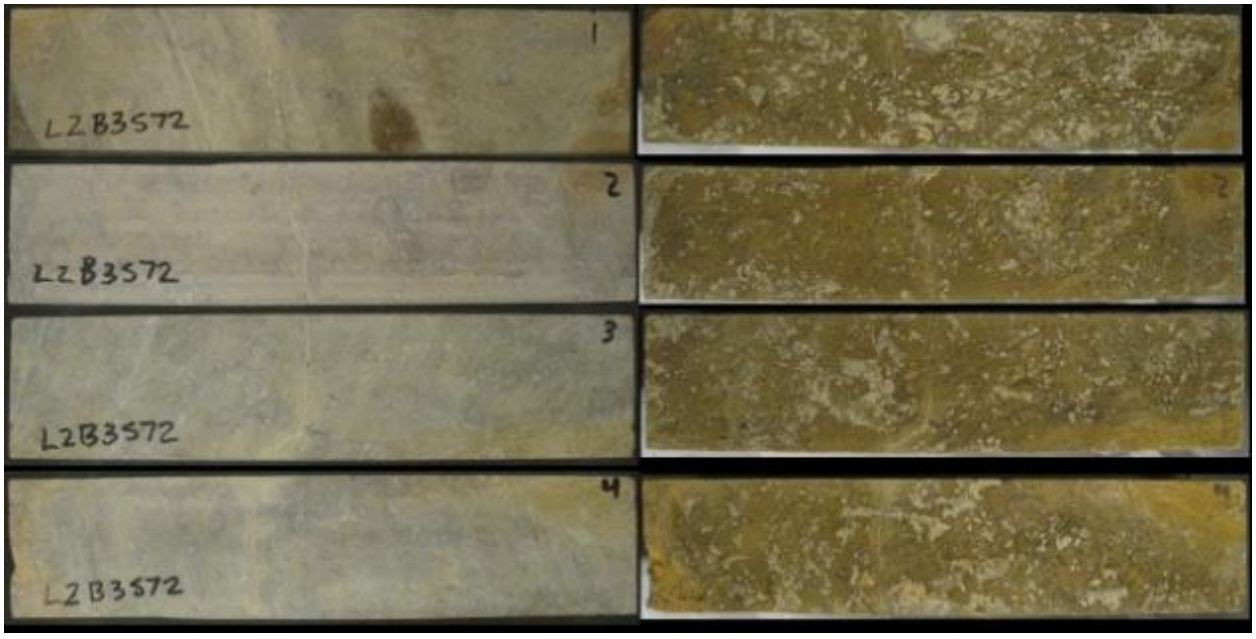

Figure B.37: L2 Sample 72 in Gypsum

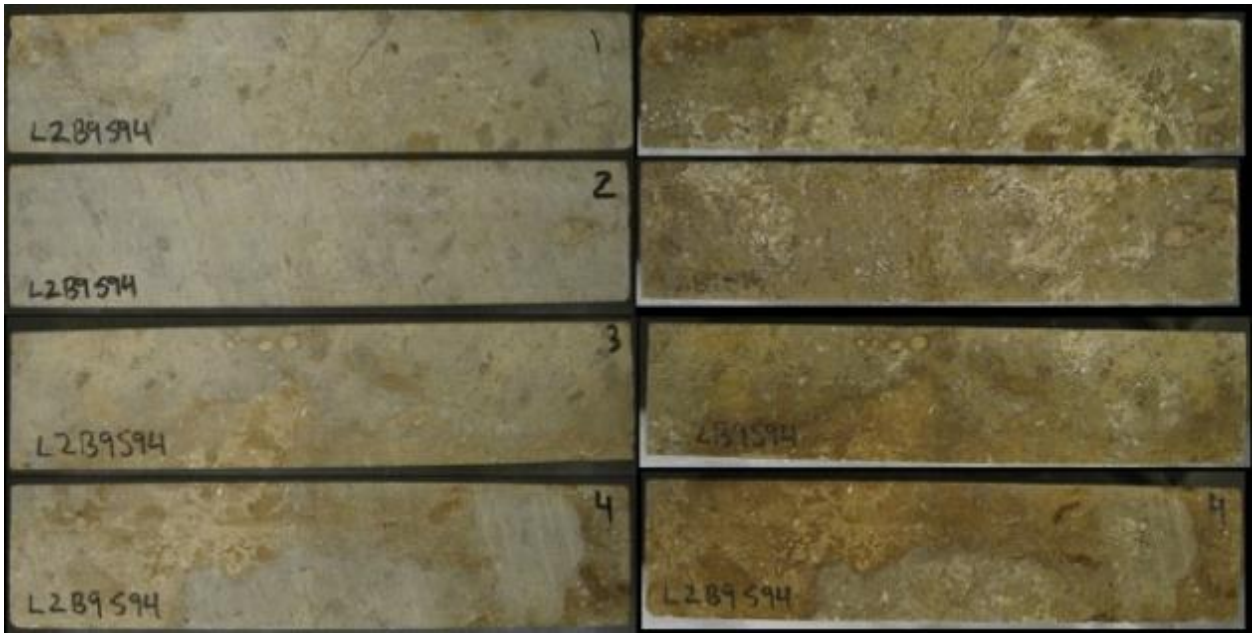

Figure B.38: L2 Sample 94 in gypsum

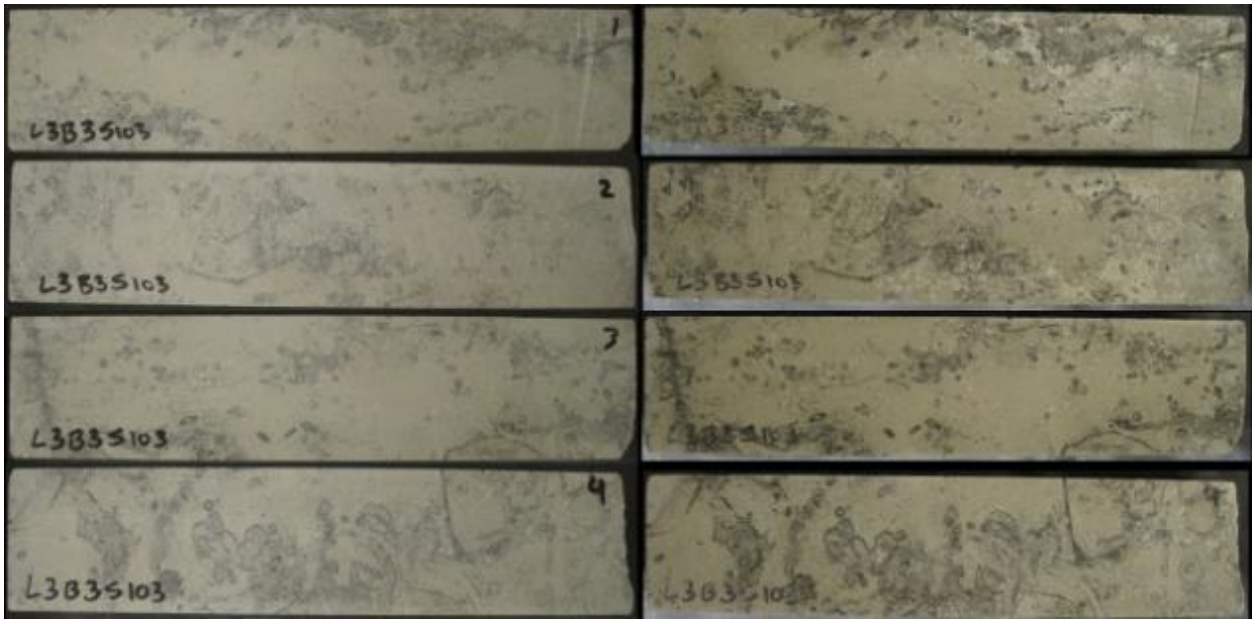

Figure B.39: L3 Sample 103 in Gypsum

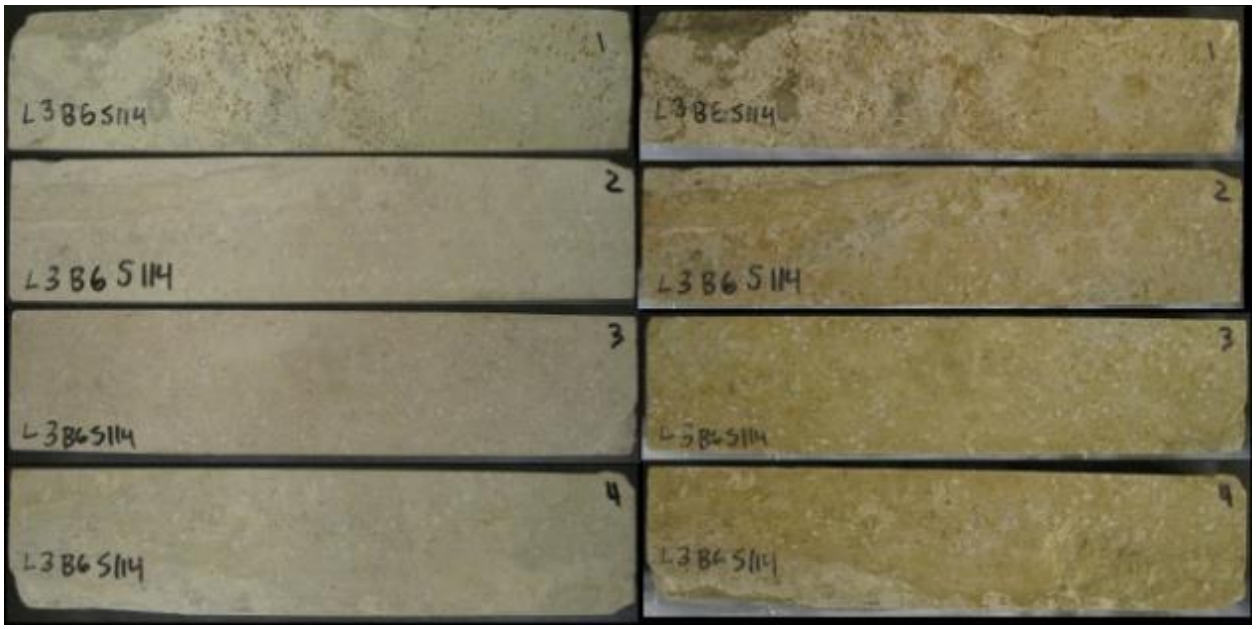

Figure B.40: L3 Sample 114 in Gypsum

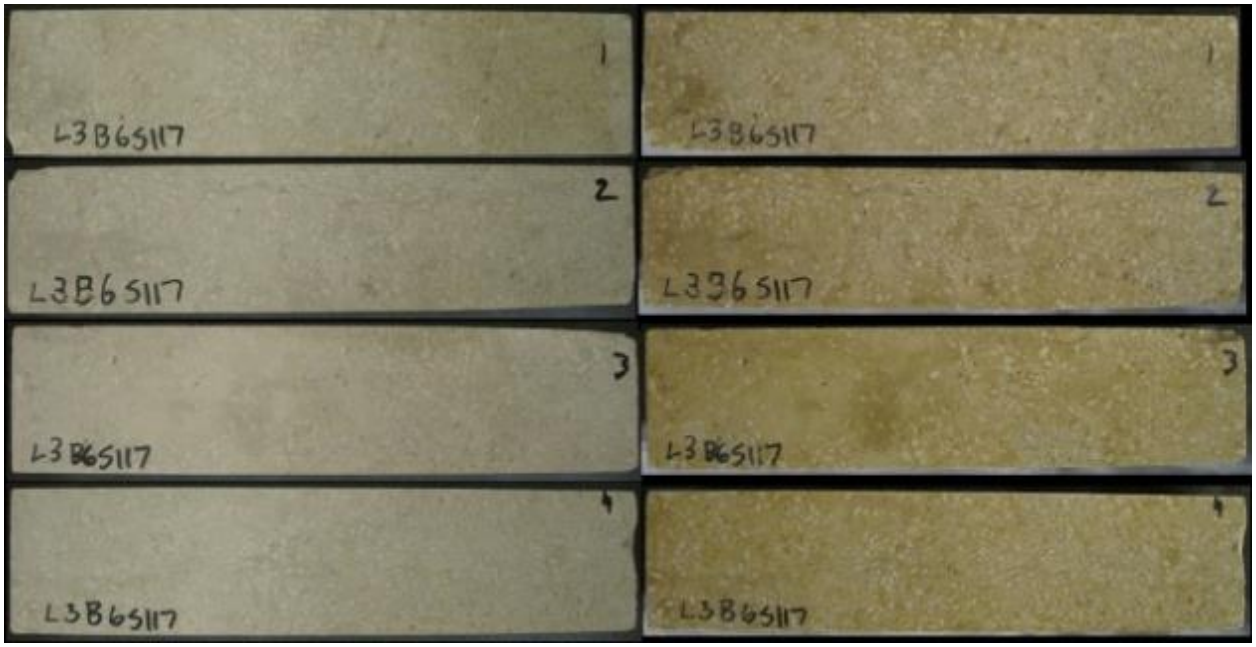

Figure B.41: L3 Sample 117 in Gypsum

Figure B.42: L4 Sample 168 in Gypsum

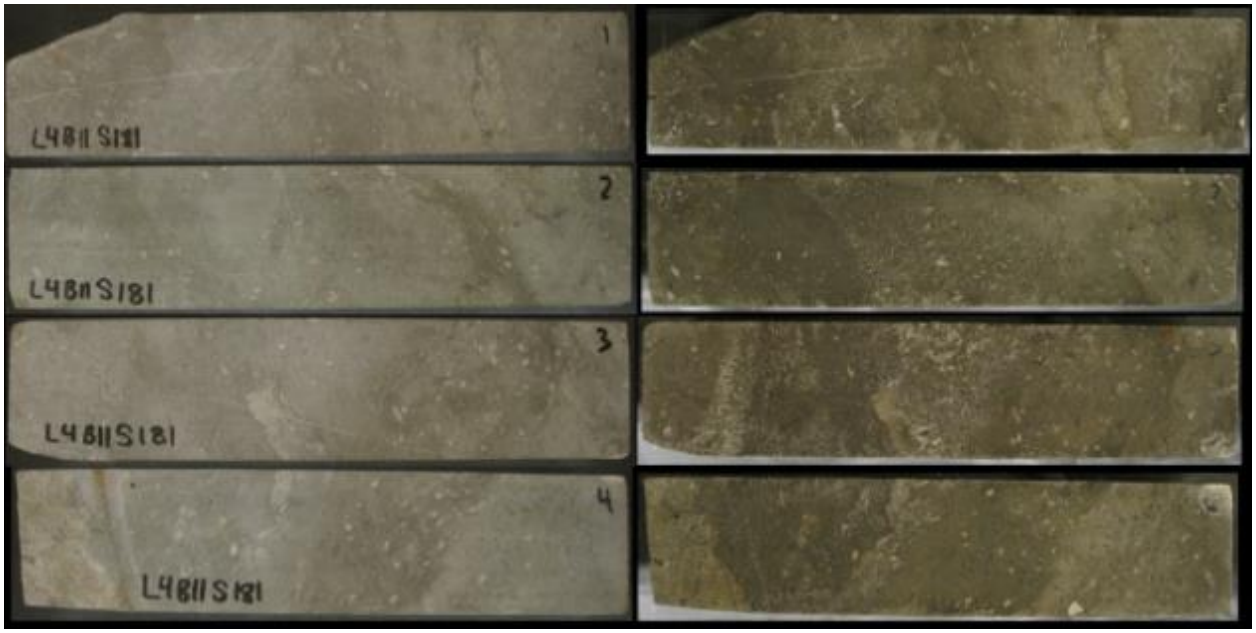

Figure B.43: L4 Sample 181 in Gypsum

Figure B.44: L4 Sample 210 in gypsum

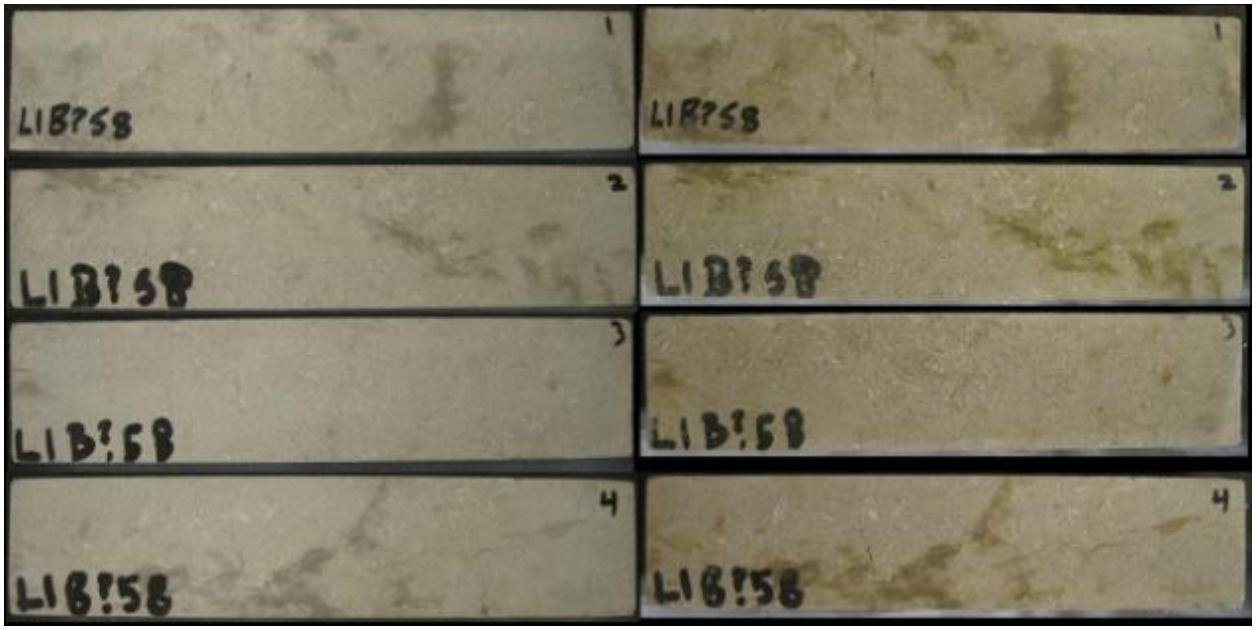

Figure B.45: L1 Sample 8 in Rock Salt Brine

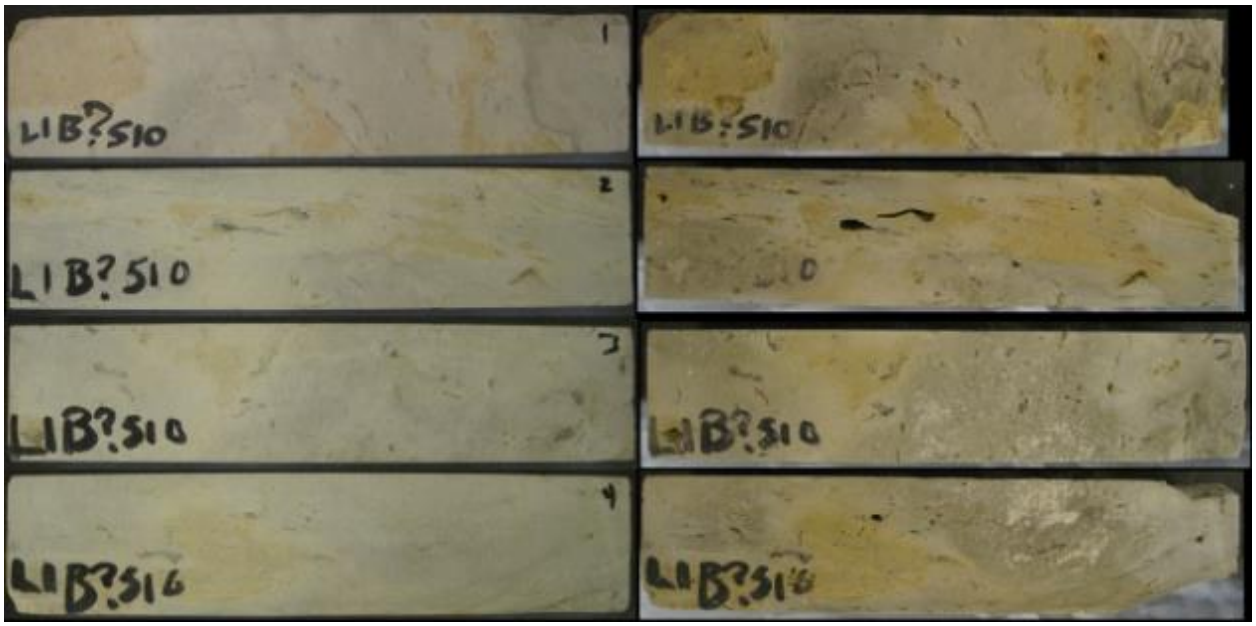

Figure B.46: L1 Sample 10 in Rock Salt Brine

L1 sample 10 contained, similarly to L1 sample 5, clay pockets causing section loss when clay swelled in the presence of brine. The corner that fragmented off visibly cracked early on in the testing, though the corner did not fall off until about the 30th wet-dry cycle.

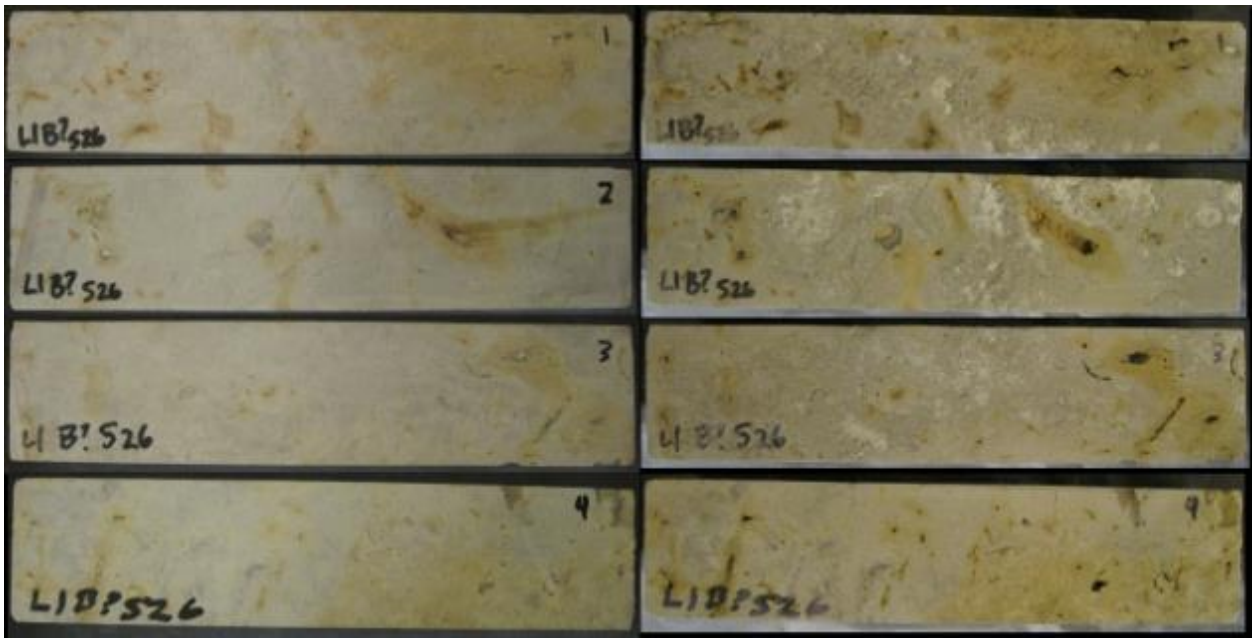

Figure B.47: L1 Sample 26 in Rock Salt Brine

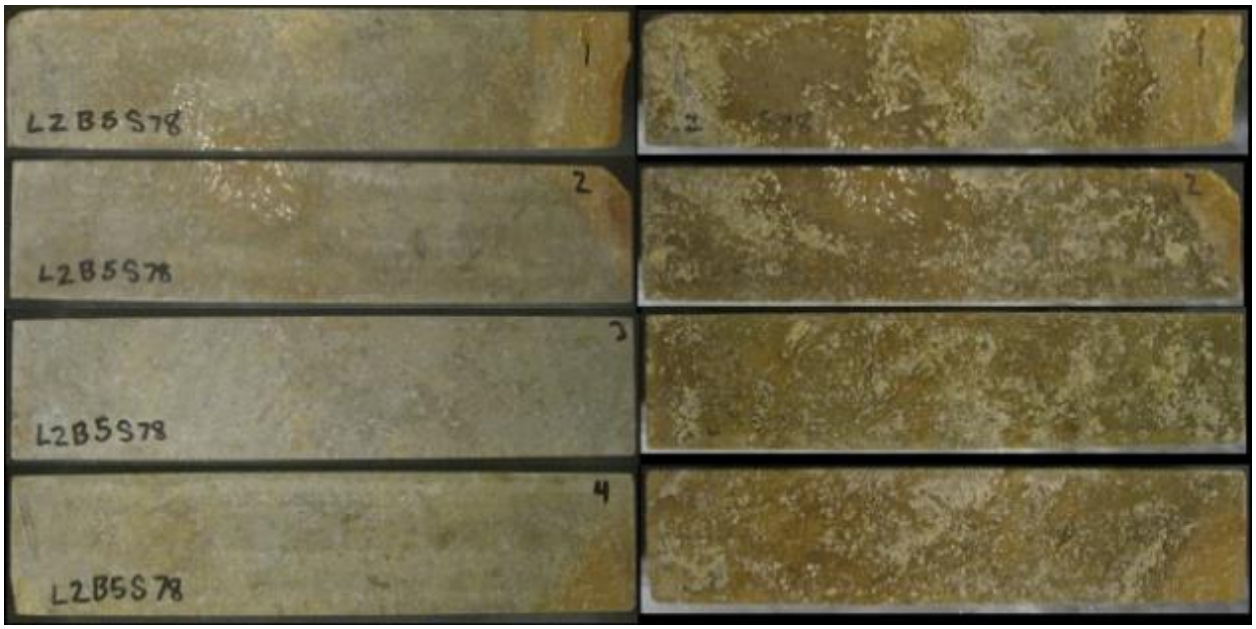

Figure B.48: L2 Sample 78 in Rock Salt Brine

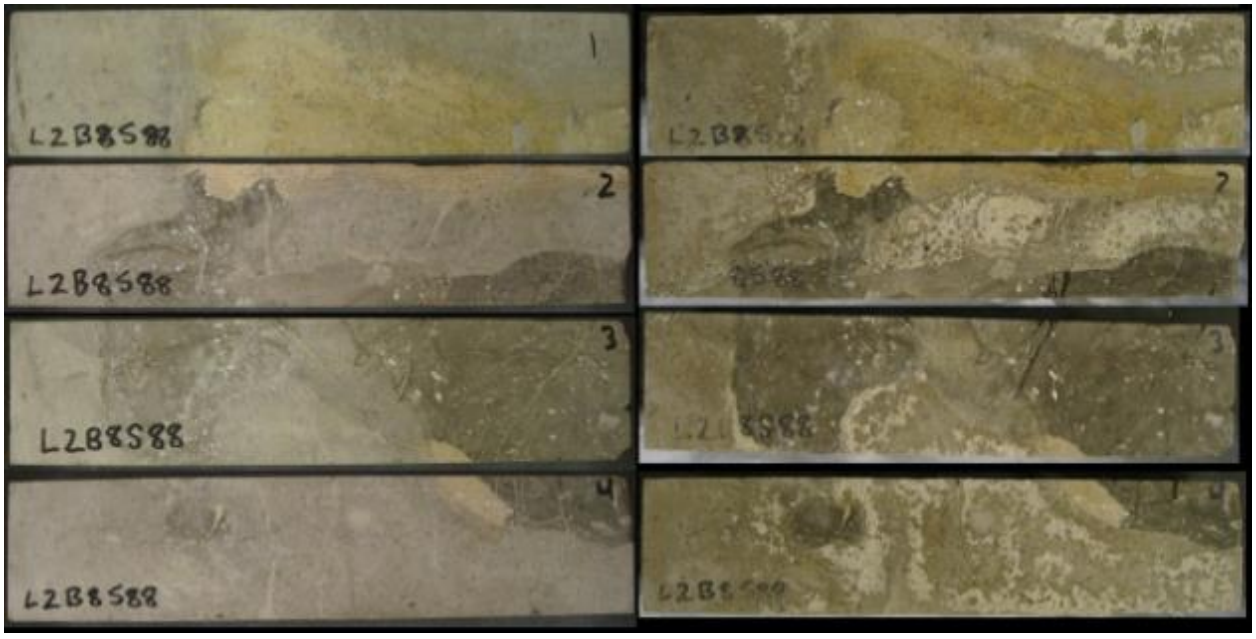

Figure B.49: L2 Sample 88 in Rock Salt Brine

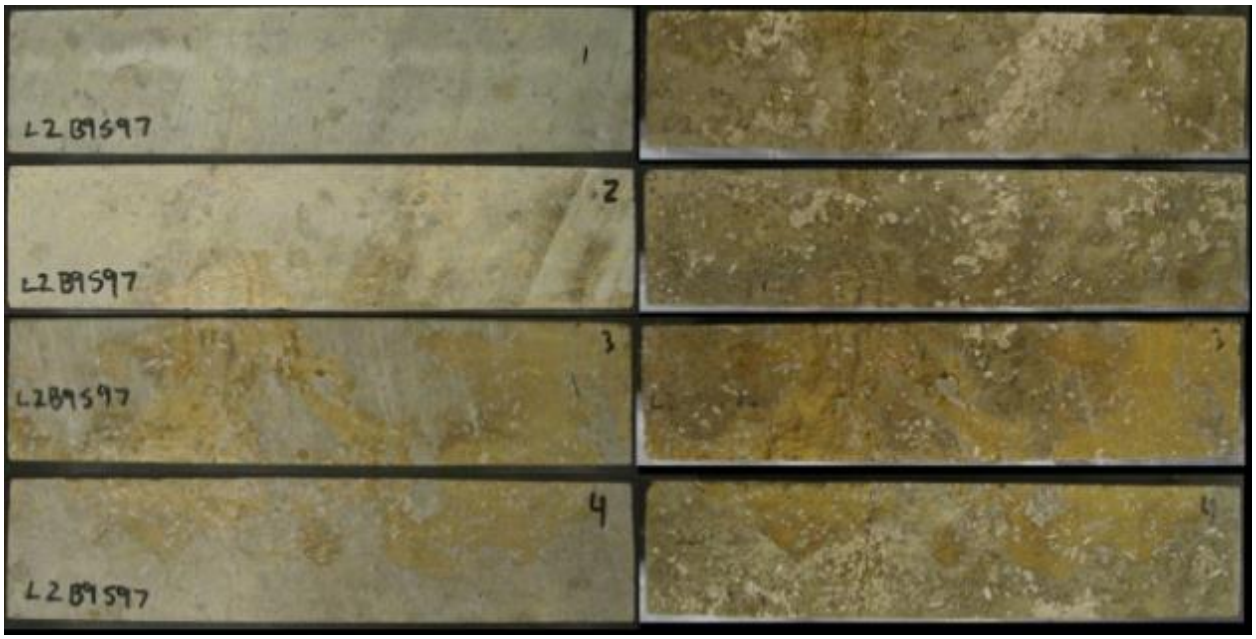

Figure B.50: L2 Sample 97 in Rock Salt Brine

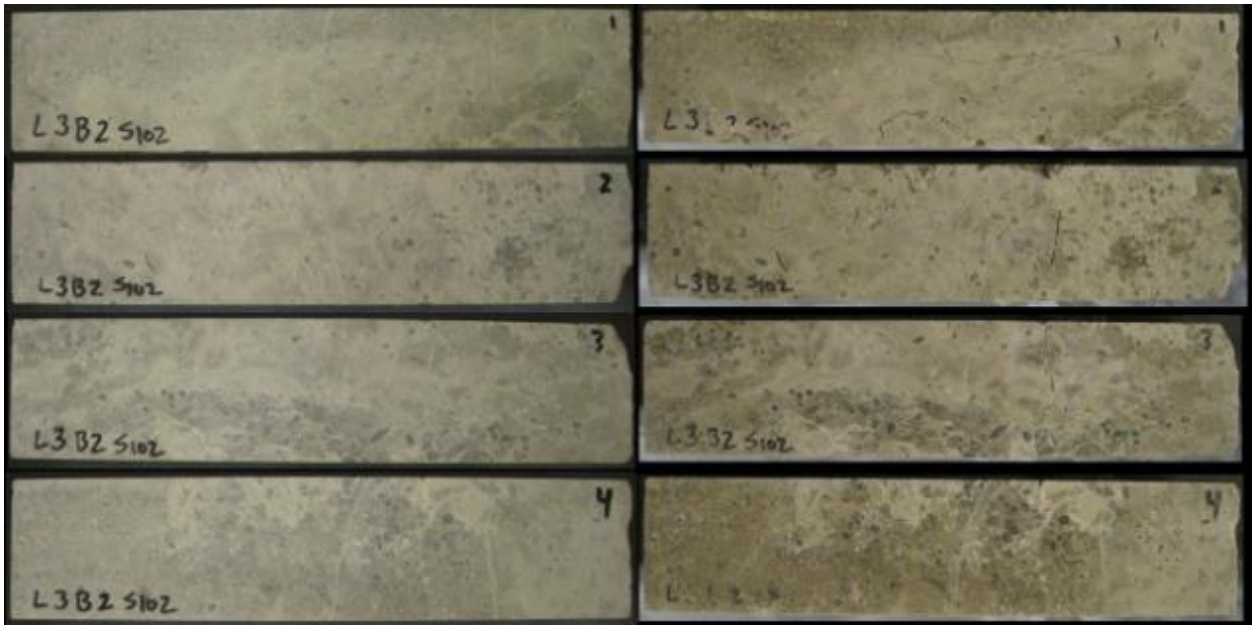

Figure B.51: L3 Sample 102 in Rock Salt Brine

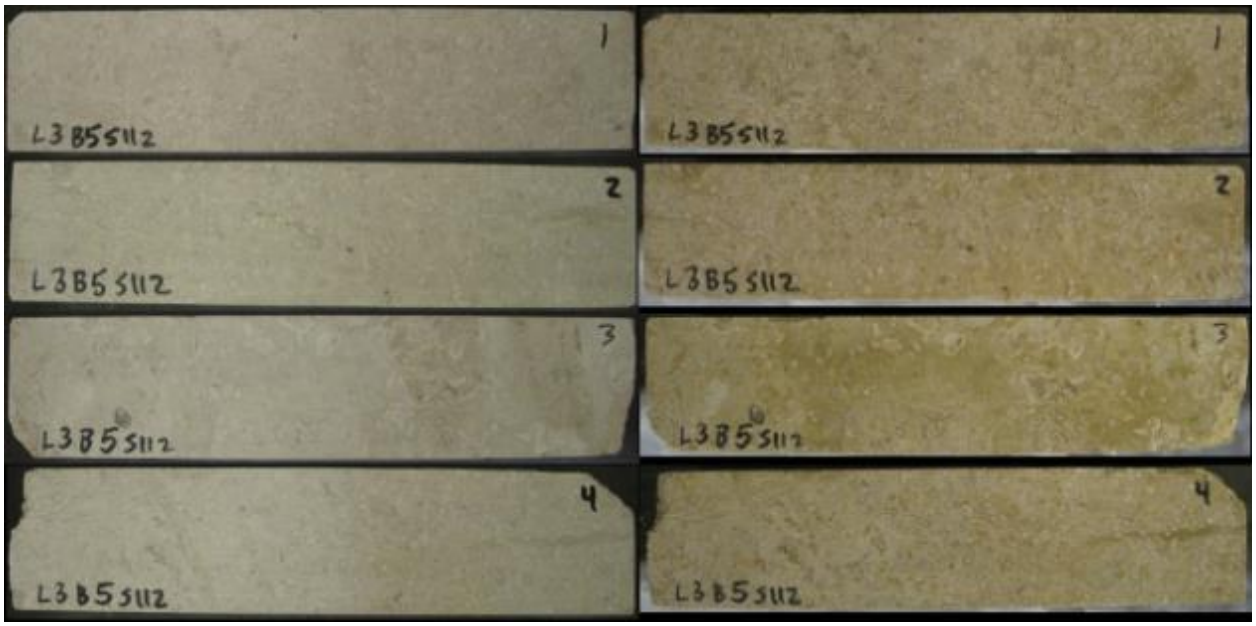

Figure B.52: L3 Sample 112 in Rock Salt Brine

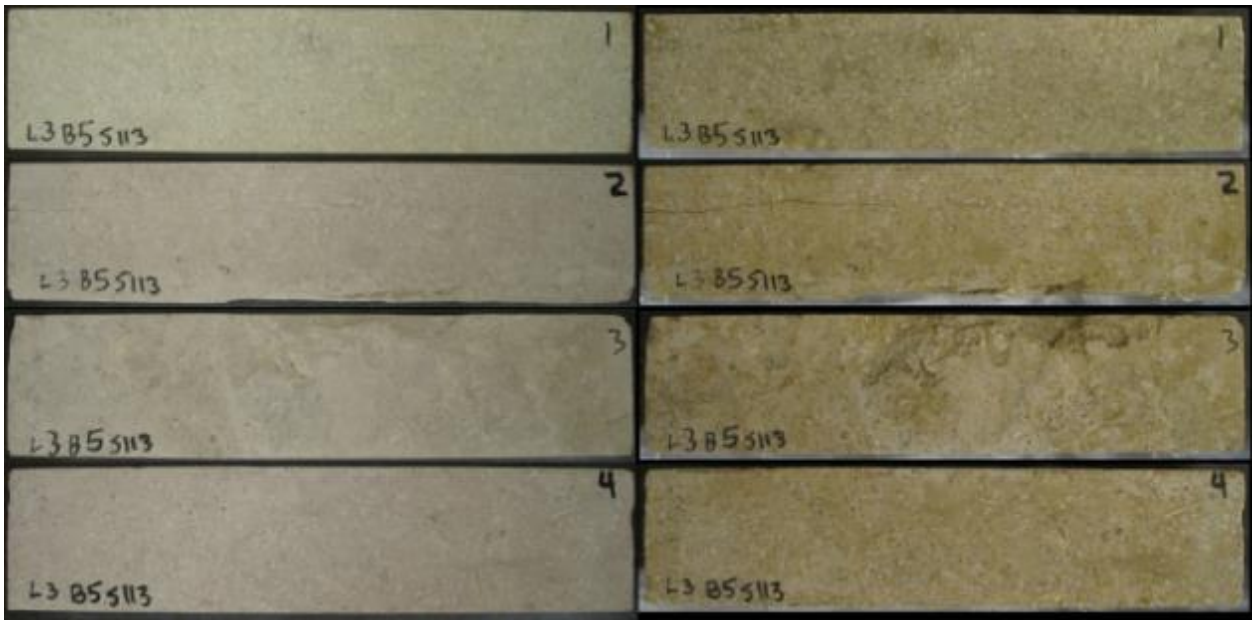

Figure B.53: L3 Sample 113 in Rock Salt Brine

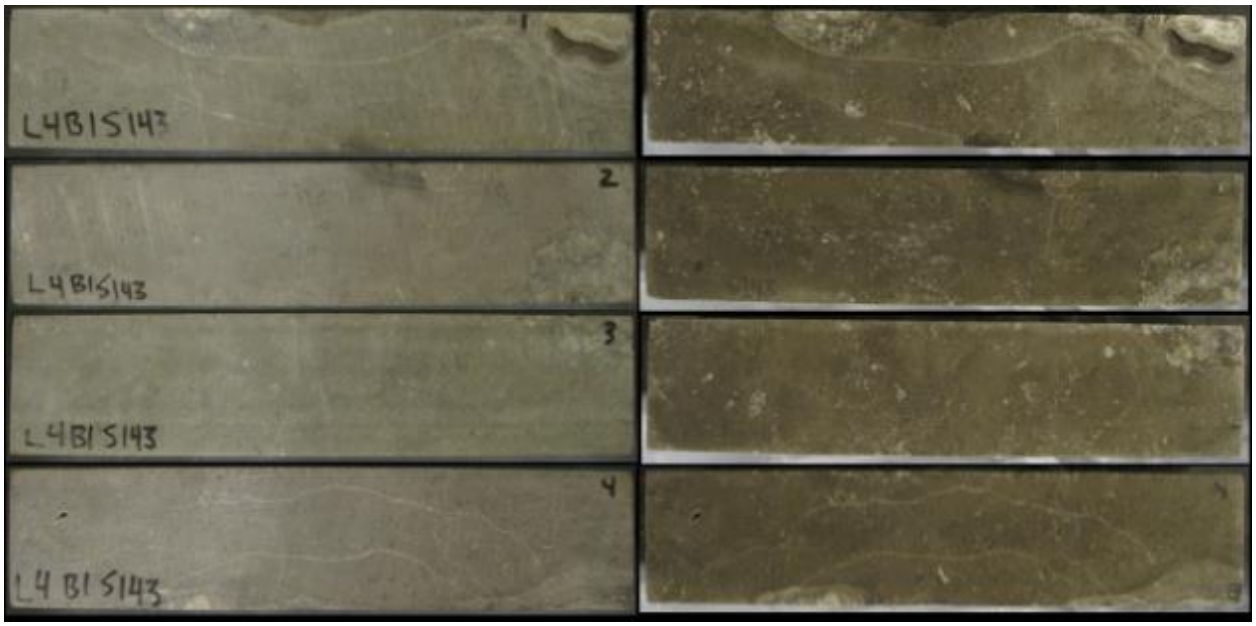

Figure B.54: L4 Sample 143 in Rock Salt Brine

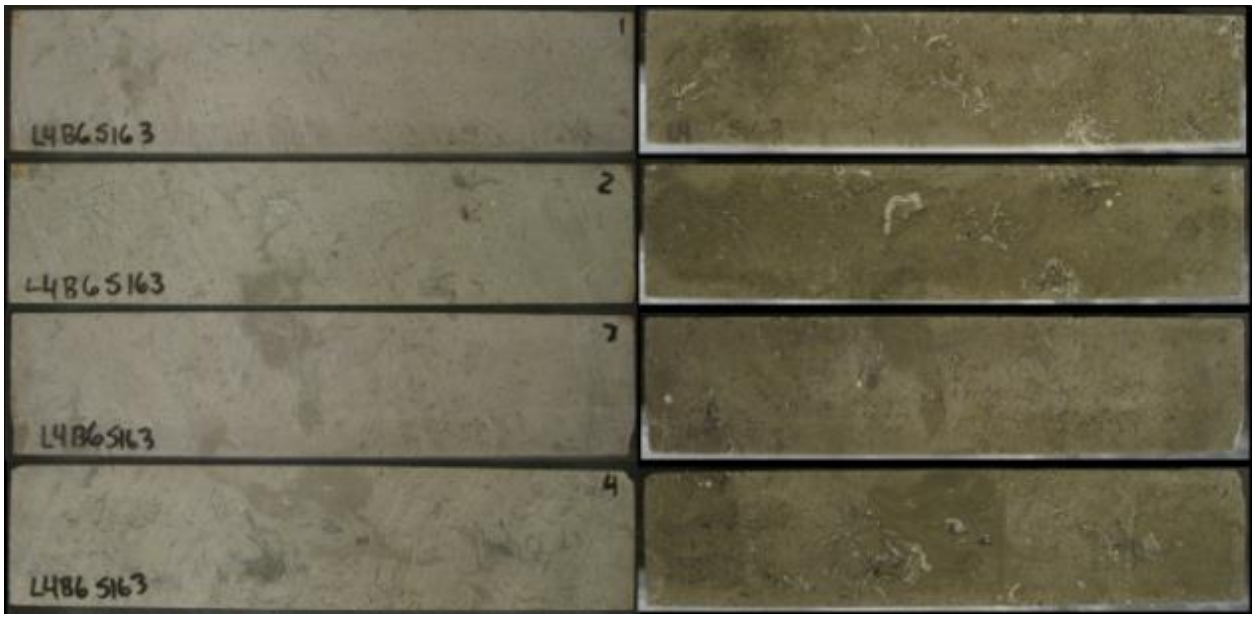

Figure B.55: L4 Sample 163 in Rock Salt Brine

Figure B.56: L4 Sample 175 in Rock Salt Brine

Appendix C: Concrete Prism Wet-Dry Samples

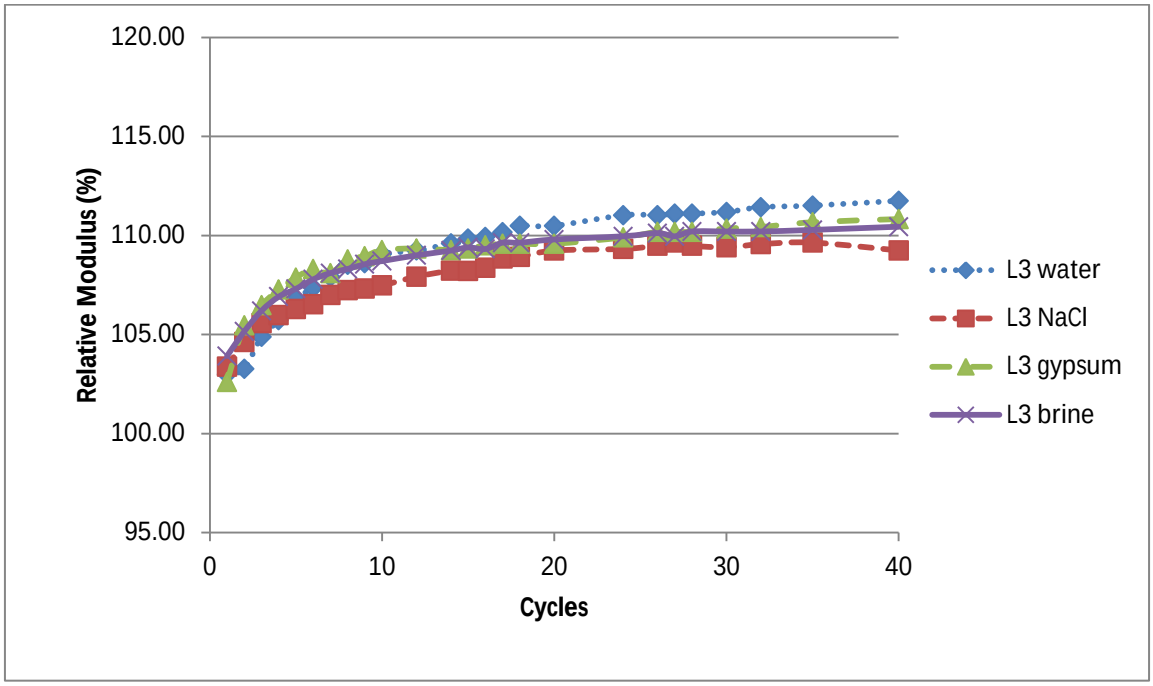

Figure C.1: Average Relative Modulus of L3 Concrete Prisms

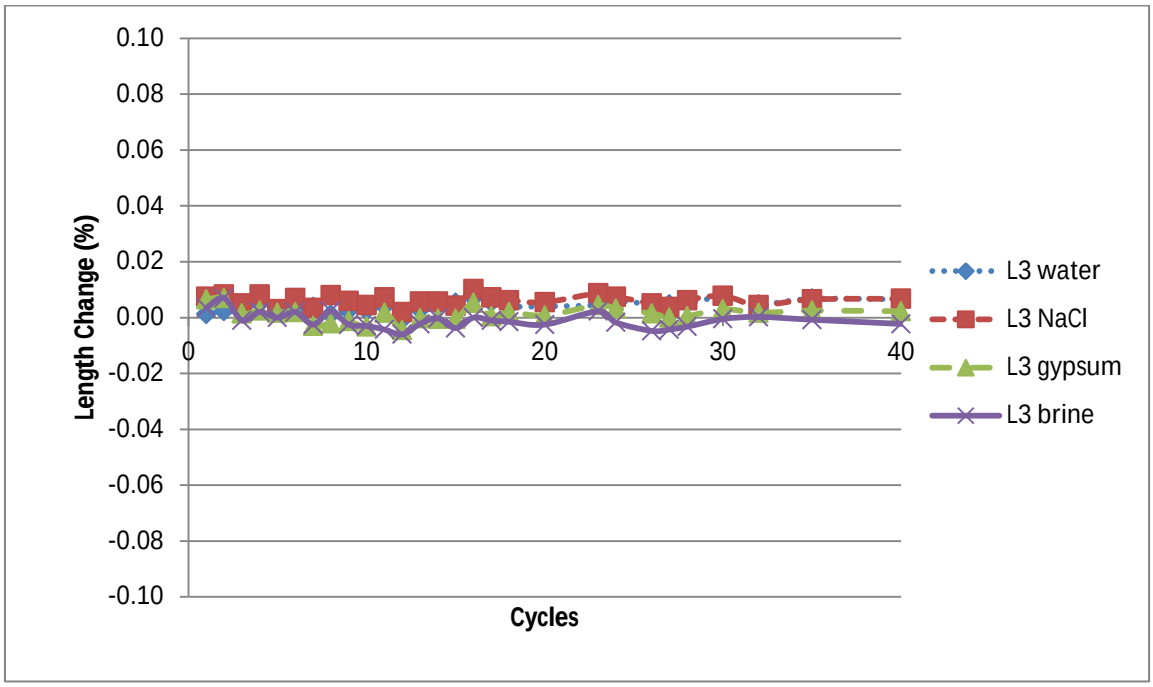

Figure C.2: Average Length Change of L3 Concrete Prisms

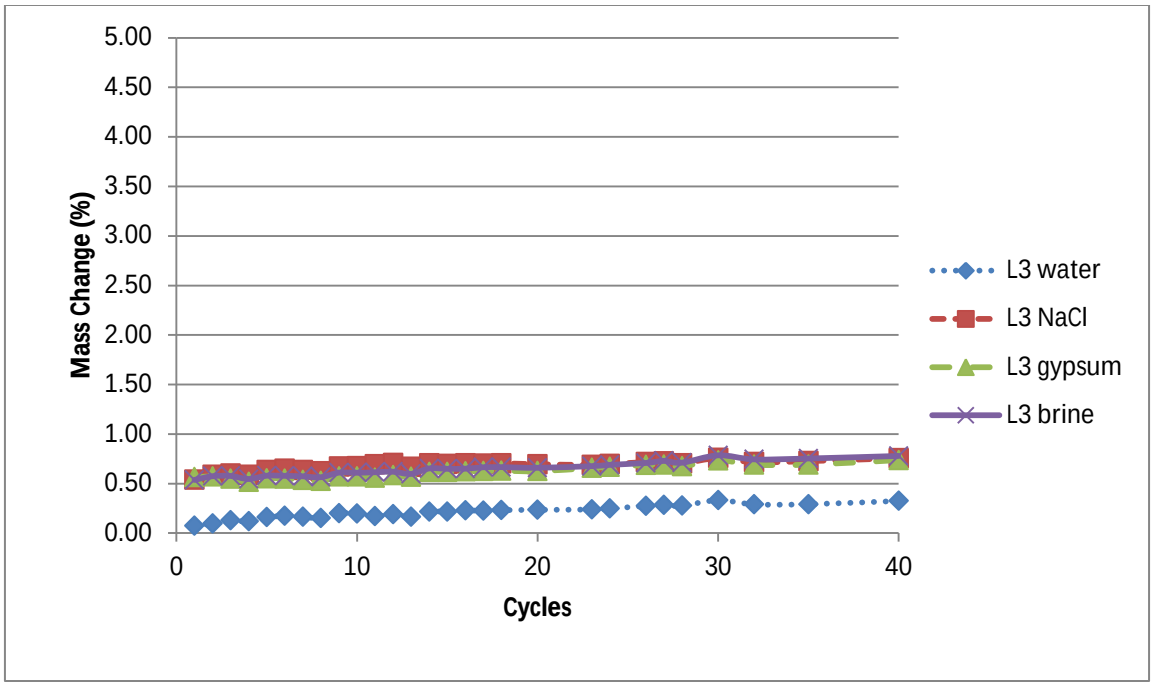

Figure C.3: Average Mass Change of L3 Concrete Prisms

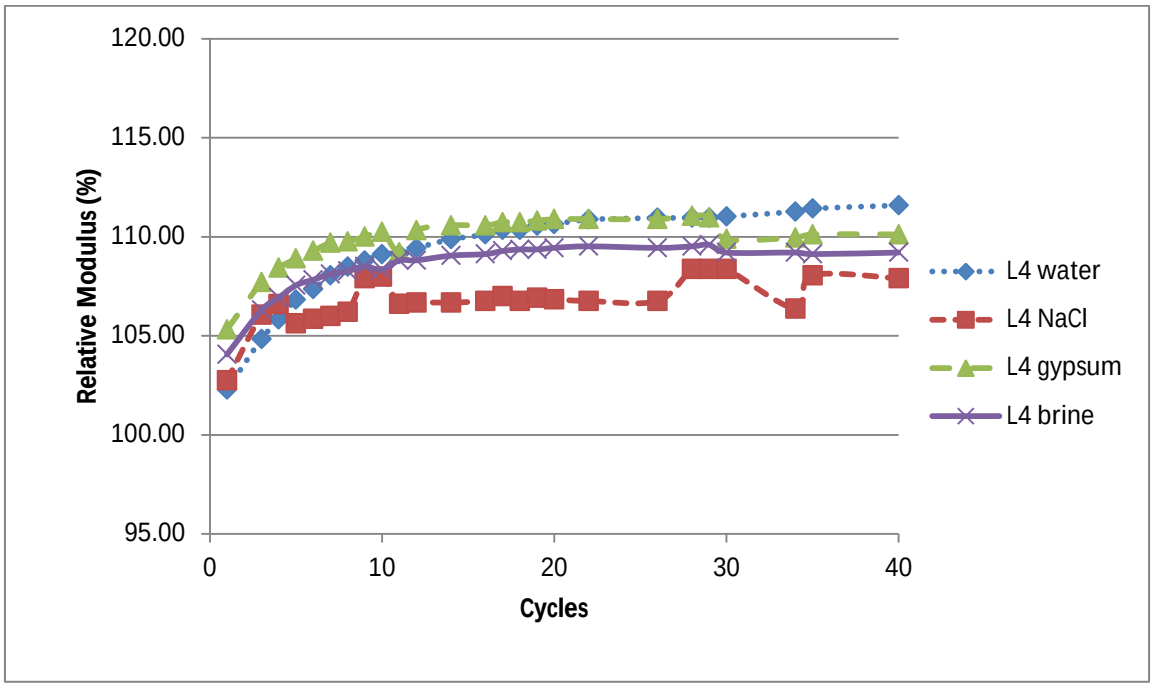

Figure C.4: Average Relative Modulus of L4 Concrete Prisms

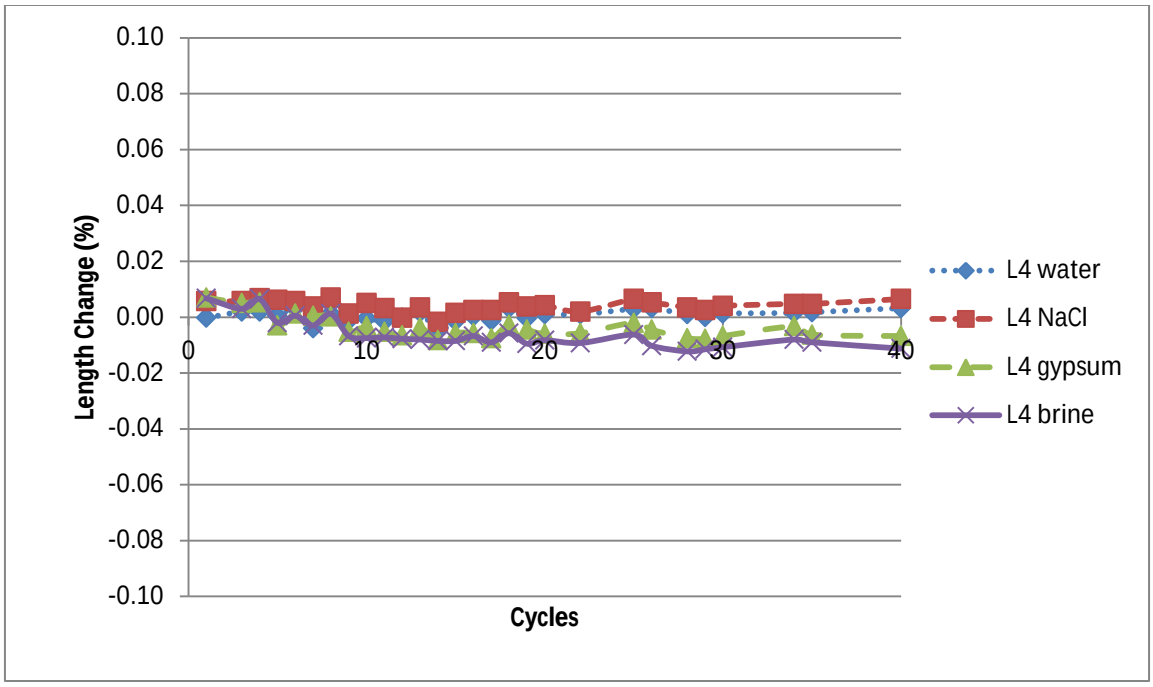

Figure C.5: Average Length Change of L4 Concrete Prisms

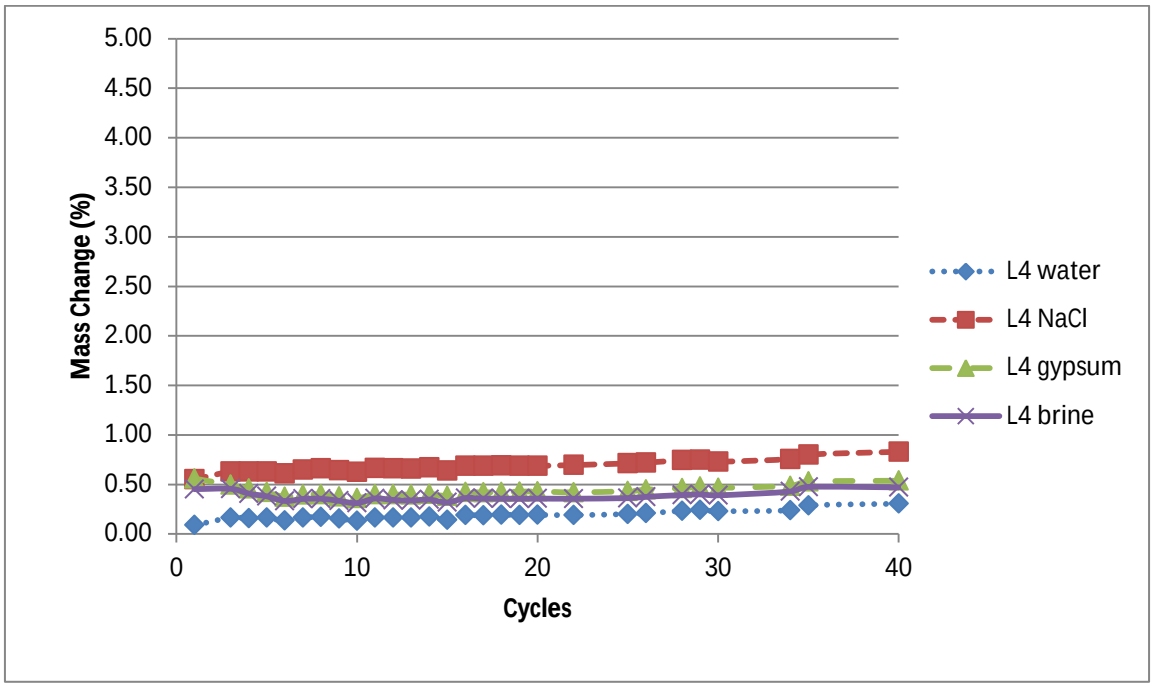

Figure C.6: Average Mass Change of L4 Concrete Prisms

The following figures show concrete prisms before and after completion of 40 wet-dry cycles in various solutions. Each figure shows on the left four prism faces before the start of wet-

dry cycling. The right side of each figure shows the corresponding prism faces after completion of wet-dry cycling. Samples were photographed at the end of the last drying stage with no steps taken to rinse salt from the sample surfaces.

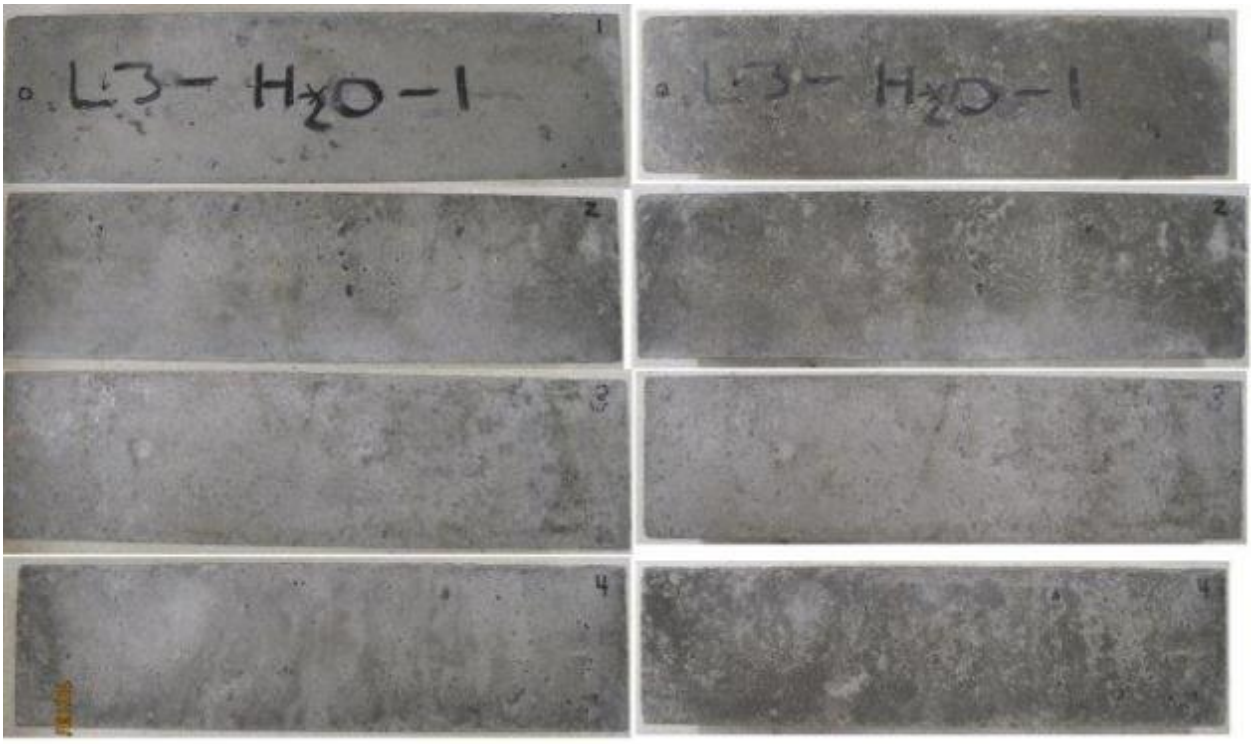

Figure C.7: First L3 Prism in Water

Figure C.8: Second L3 Prism in Water

Figure C.9: First L4 Prism in Water

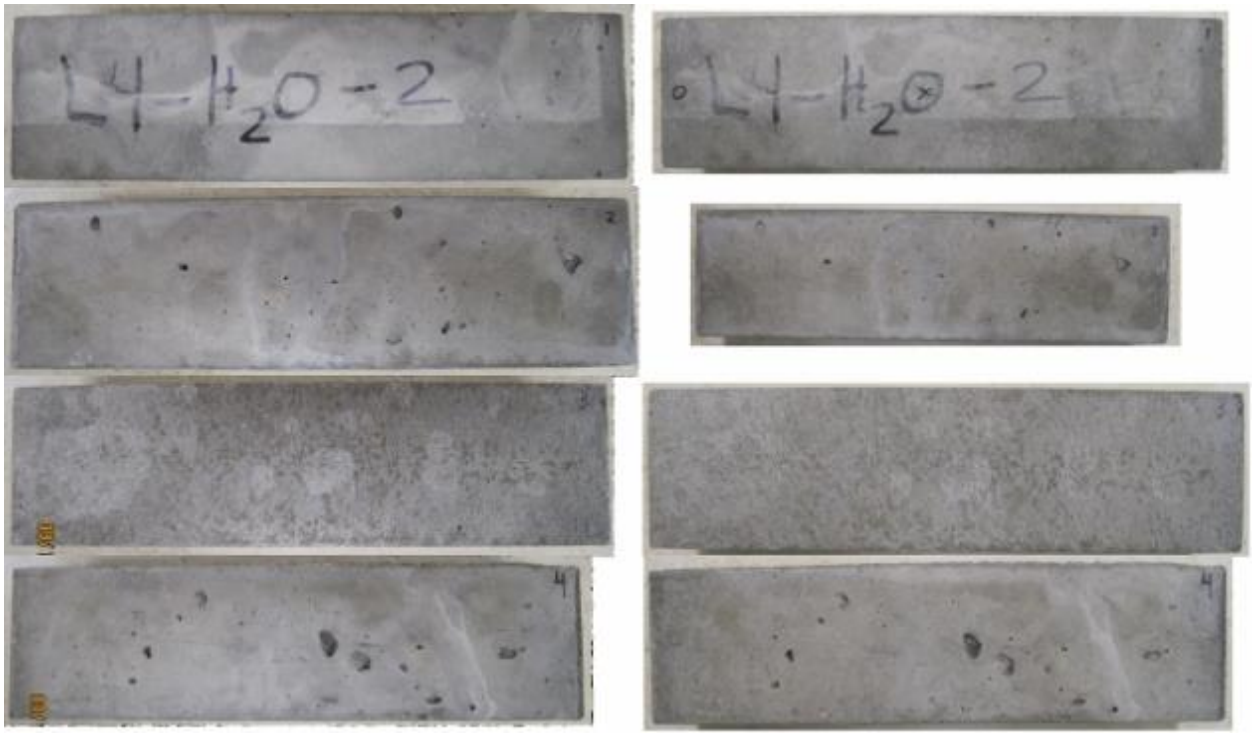

Figure C.10: Second L4 Prism in Water

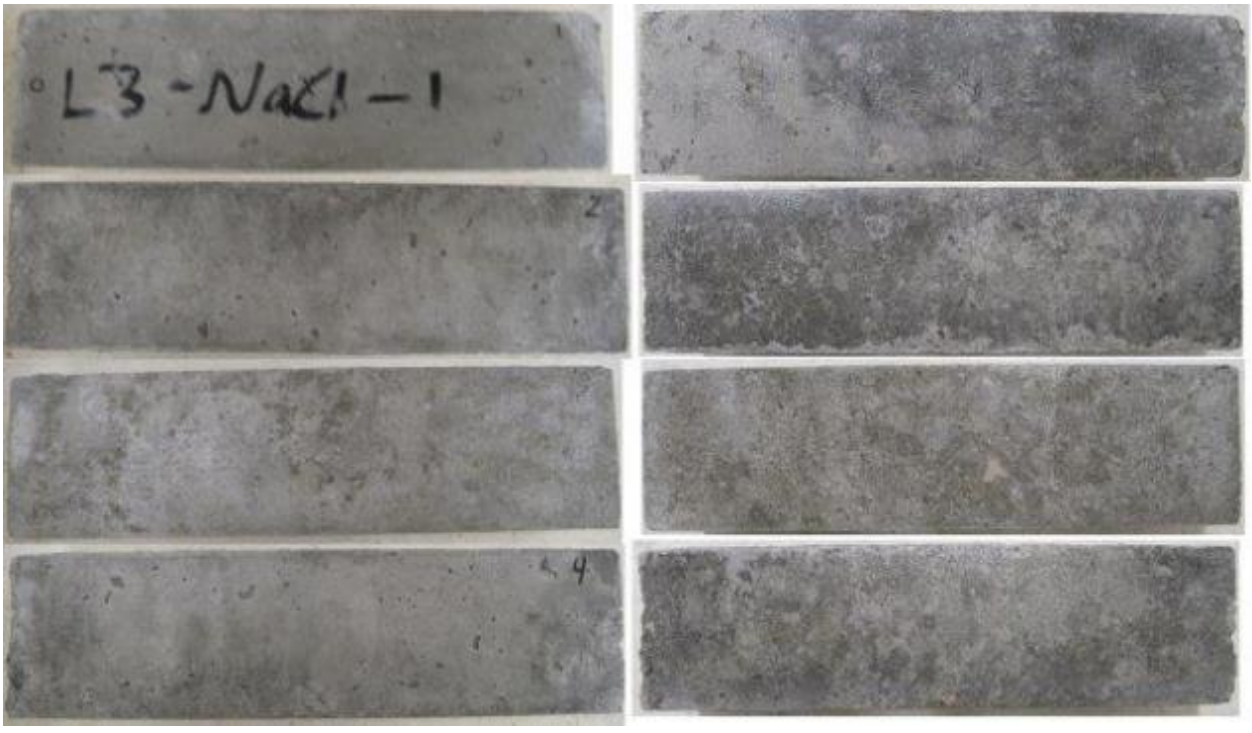

Figure C.11: First L3 Prism in NaCl

Figure C.12: Second L3 Prism in NaCl

Figure C.13: First L4 Prism in NaCl

Figure C.14: Second L4 Prism in NaCl

Figure C.15: First L3 Prism in Gypsum

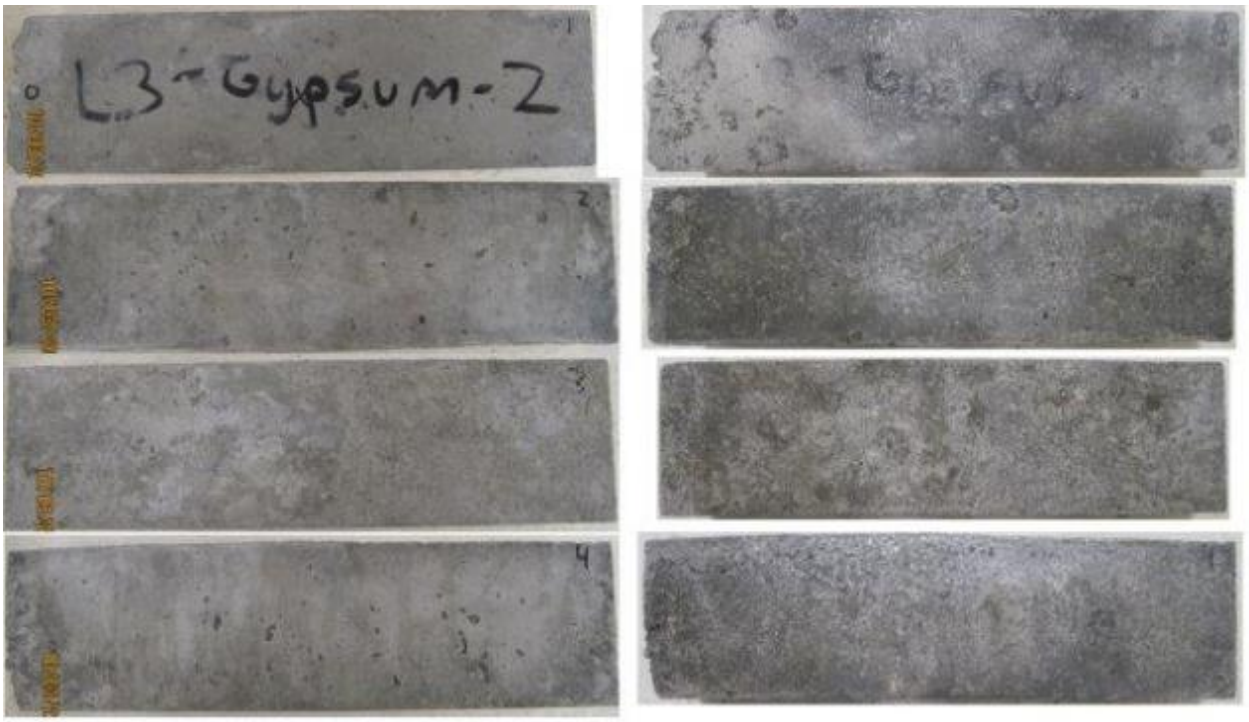

Figure C.16: Second L3 Prism in Gypsum

Figure C.17: First L4 Prism in Gypsum

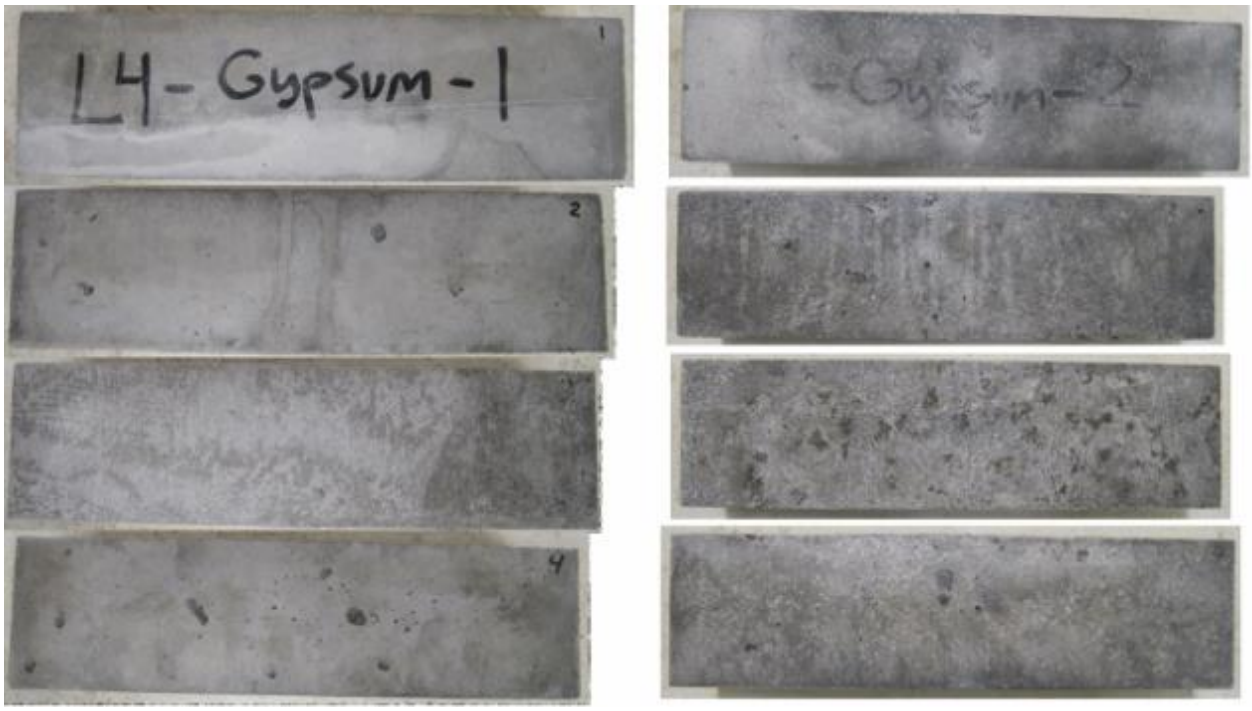

Figure C.18: Second L4 Prism in Gypsum

Figure C.19: First L3 Prism in Brine

Figure C.20: Second L3 Prism in Brine

Figure C.21: First L4 Prism in Rock Salt Brine

Figure C.22: Second L4 Prism in Rock Salt Brine

Appendix D: Limestone Prism Freeze-Thaw Samples

Figure D.1: Unidentifiable Prism After Salt-Frost Exposure

Figure D.2 shows L4 sample 146 before and after freeze-thaw cycling. Significant material was lost, although in a non-uniform manner. This particular prism was cut so that the exterior of the source rock was very near the sample corner on the right side. Fragmentation that occurred at this location during freezing and thawing may indicate lower stone quality at the stone's surface.

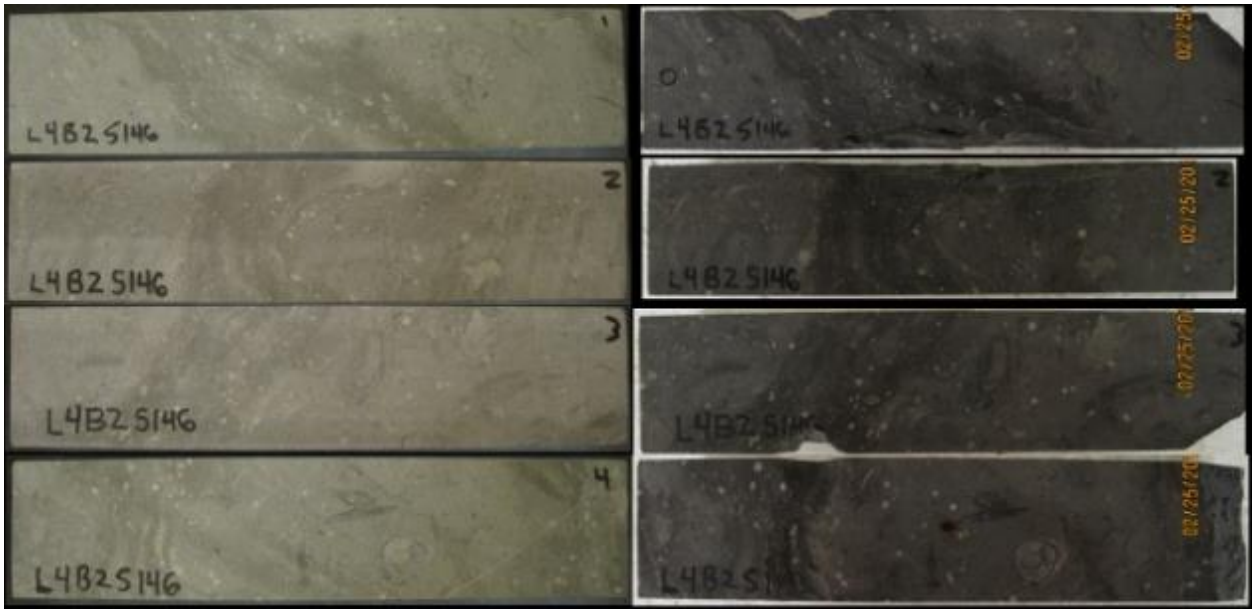

Figure D.2: L4 Sample 146 After Salt-Frost Exposure

Figure D.3 shows L4 sample 153 before and after freeze-thaw cycling. Scaling and loss of material is observable, with varying performance over different areas of the prism.

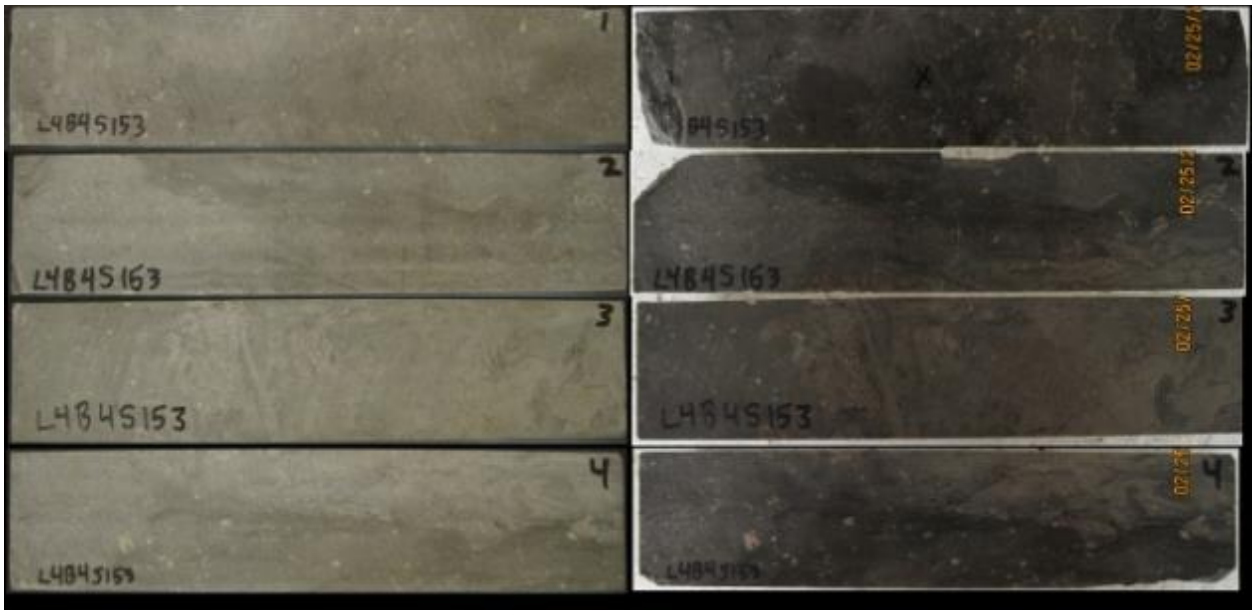

Figure D.3: L4 Sample 153 After Salt-Frost Exposure

Figure D.4 shows L4 sample 187 before and after freeze-thaw cycling, showing that some of the sample was susceptible to frost damage.

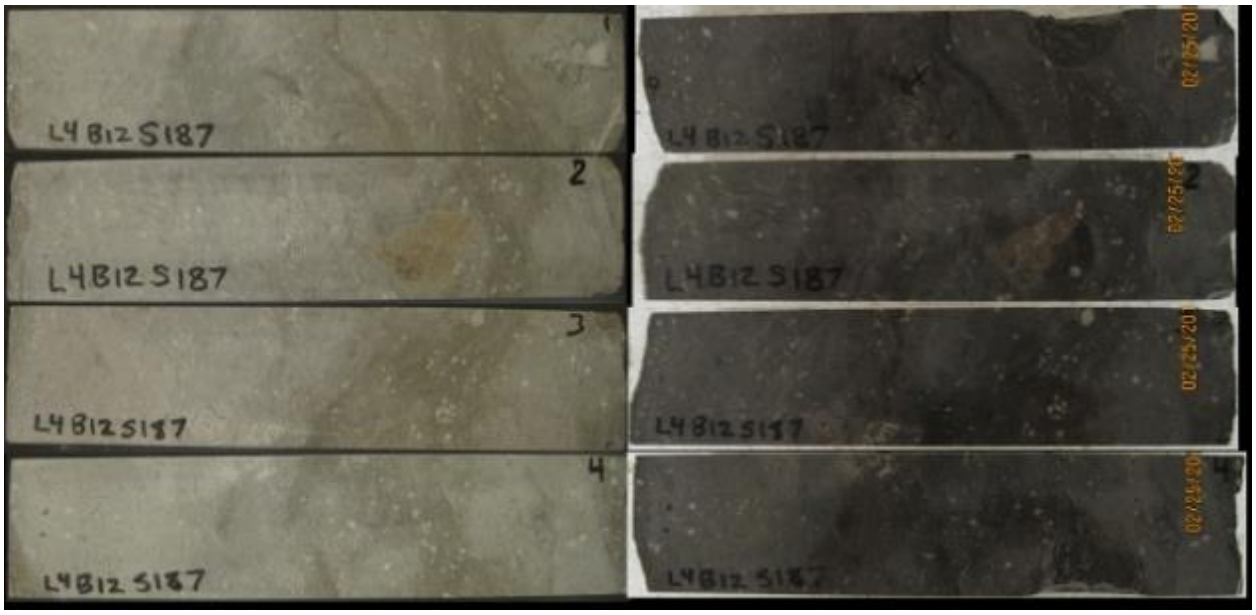

Figure D.4: L4 Sample 187 After Salt-Frost Exposure

Figure D.5 shows L4 sample 189. The sample was cut from a rock that was not quite long enough for a perfect 2x2x9 in. prism. The stone split at a visible lamination in the prism.

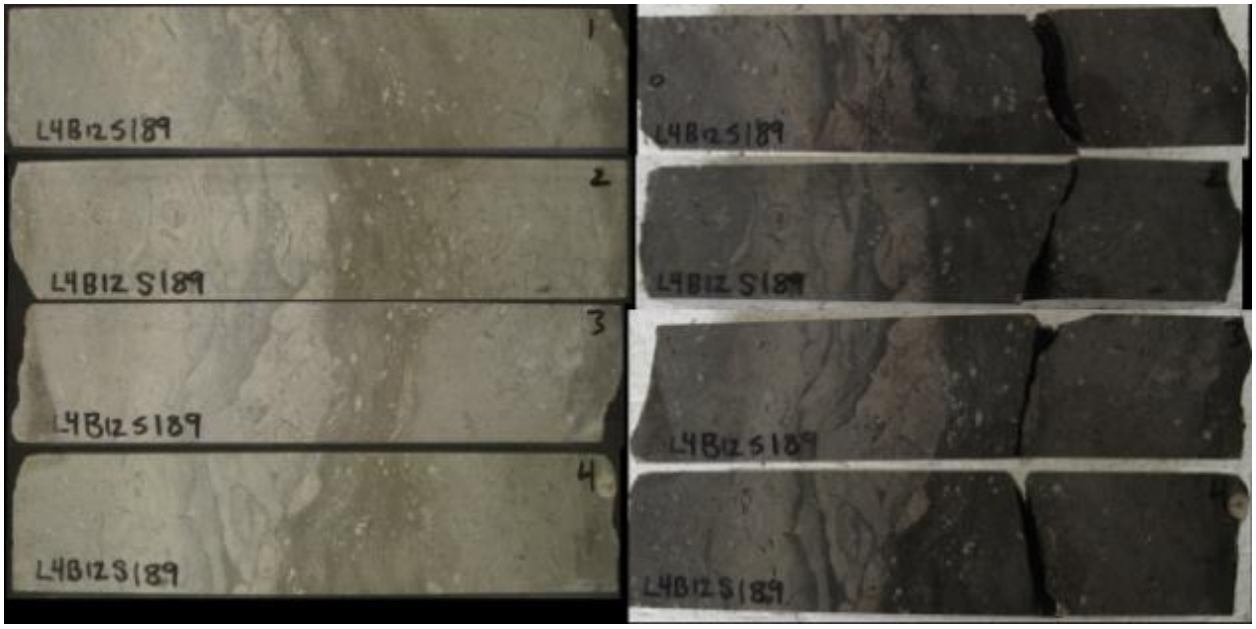

Figure D.5: L4 Sample 189 After Salt-Frost Exposure

Figure D.6 shows L4 sample 199, the only prism that showed no visual damage from the test.

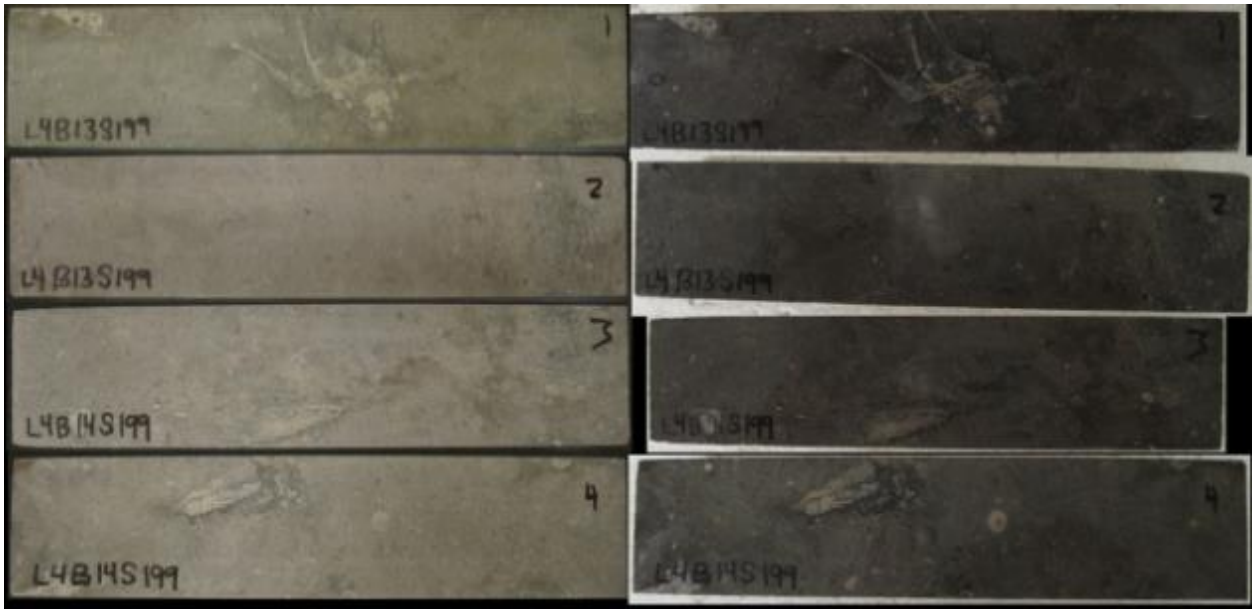

Figure D.6: L4 Sample 199 After Salt-Frost Exposure

Figure D.7 shows L4 sample 212, which split along a crack mid-height on the stone. Scaling and fragmentation also occurred in this sample.

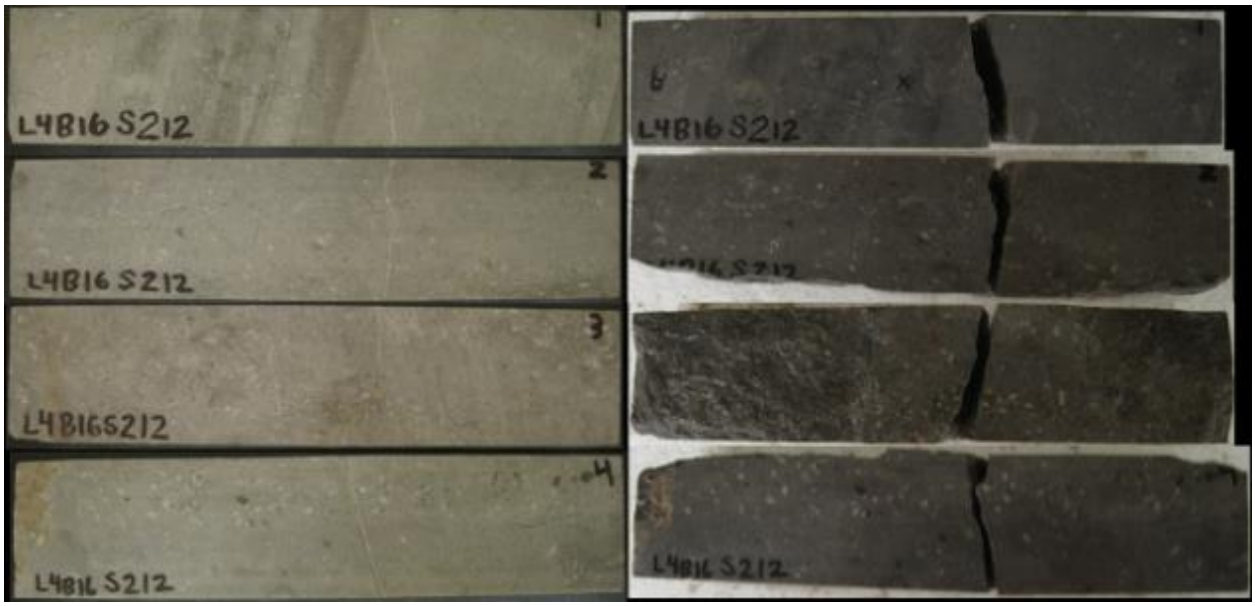

Figure D.7: L4 Sample 212 After Salt-Frost Exposure

Appendix E: Phase I Salt-Treated Aggregate Results

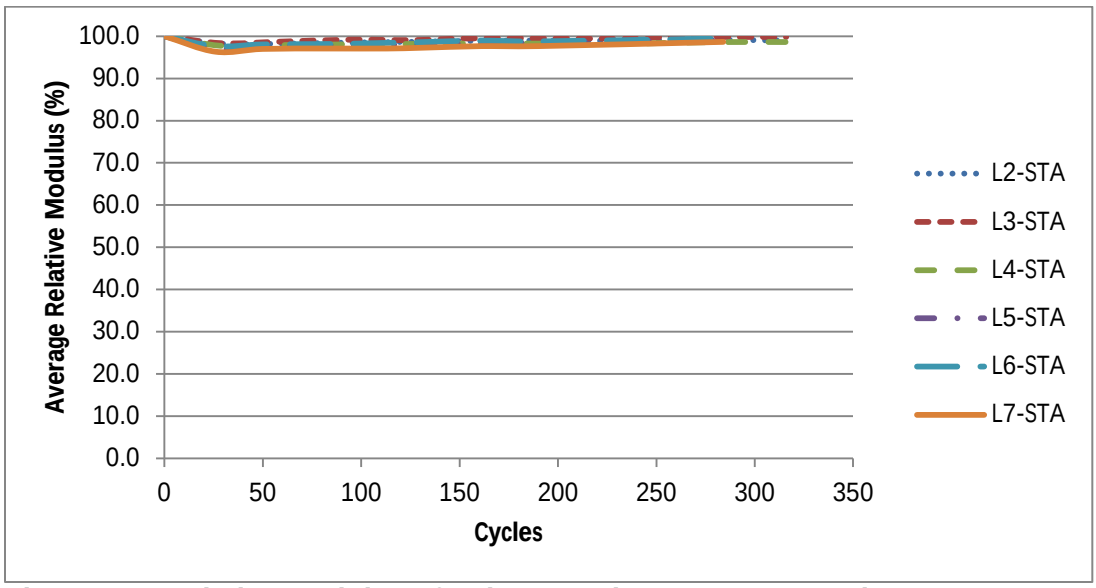

Figure E.1: Relative Modulus of Salt-Treated Aggregate Samples

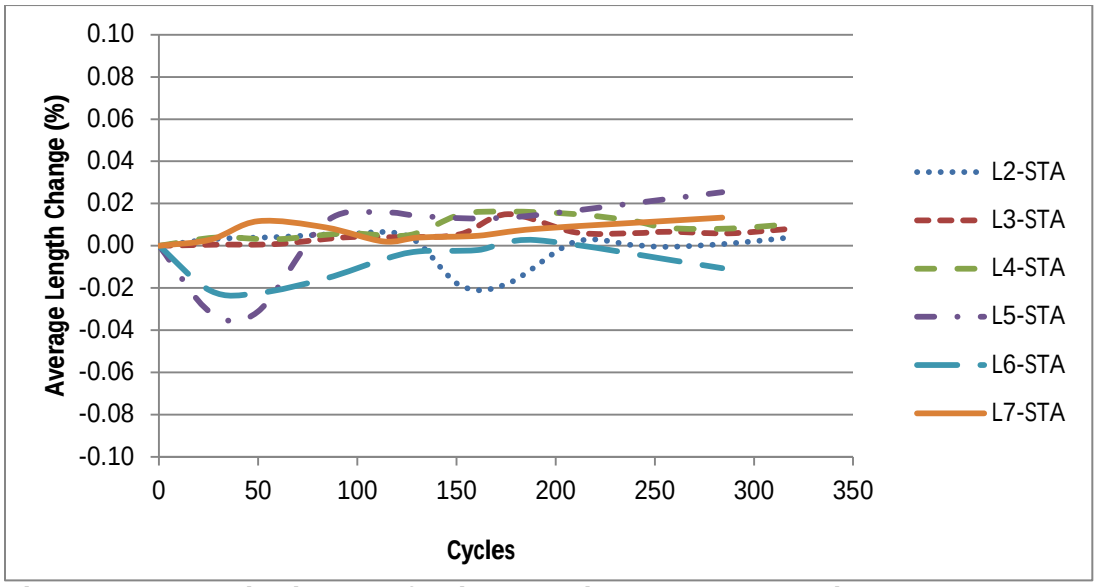

Figure E.2: Length Change of Salt-Treated Aggregate Samples

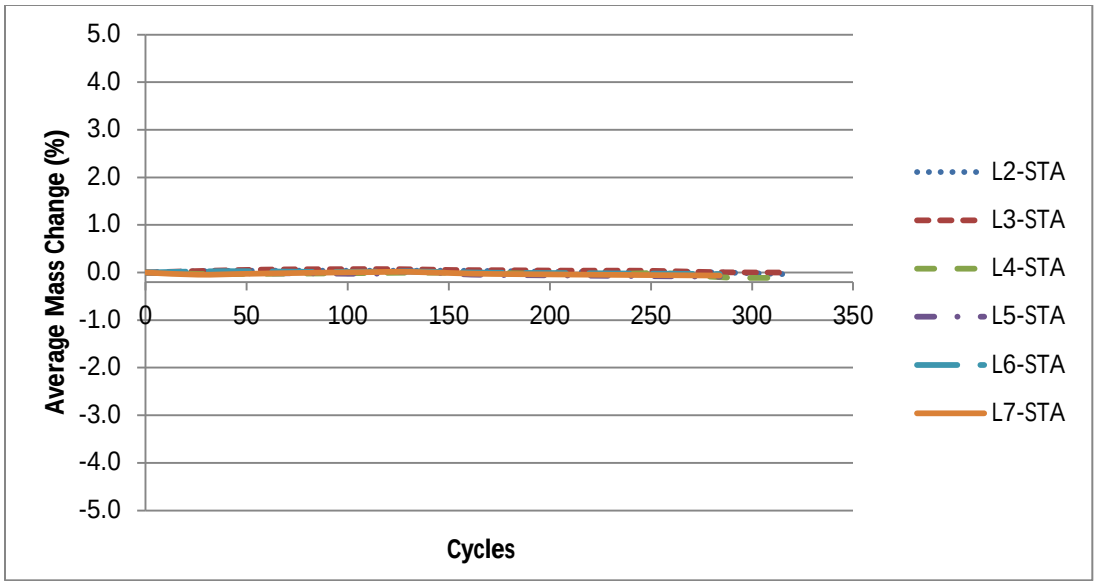

Figure E.3: Average Mass Change of Salt-Treated Aggregate Samples

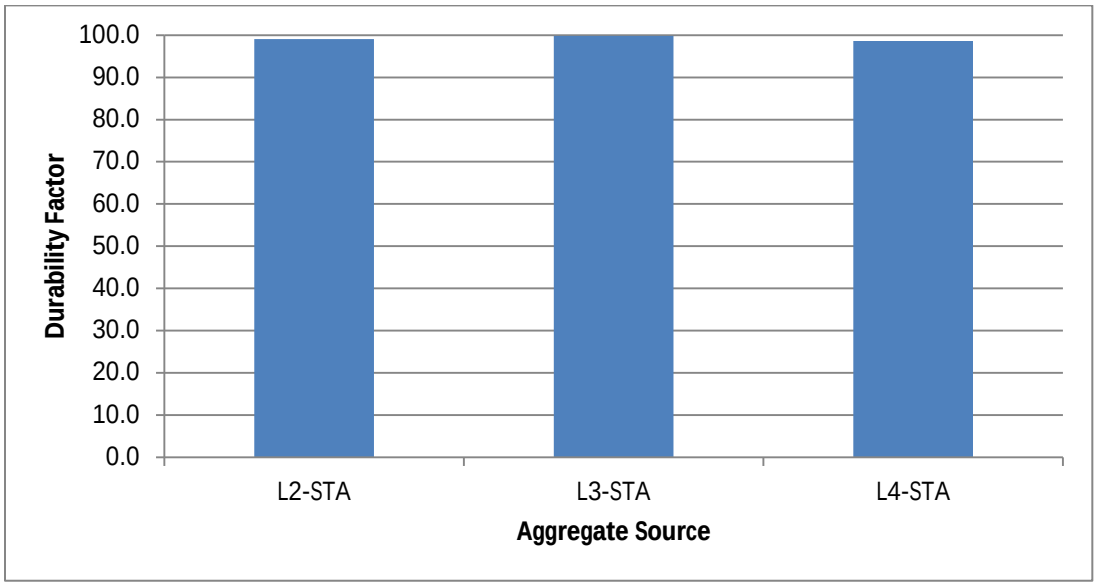

Figure E.4: Durability Factors of Salt-Treated Aggregate Samples

Appendix F: Half-Immersed Sample Results

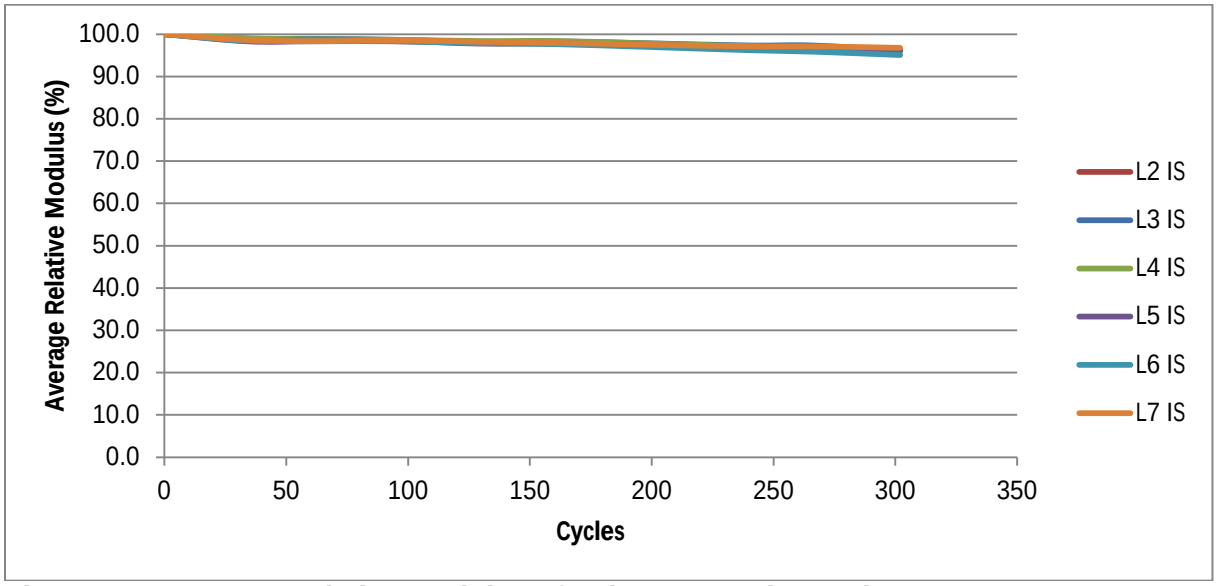

Figure F.1: Average Relative Modulus of Salt-Immersed Samples

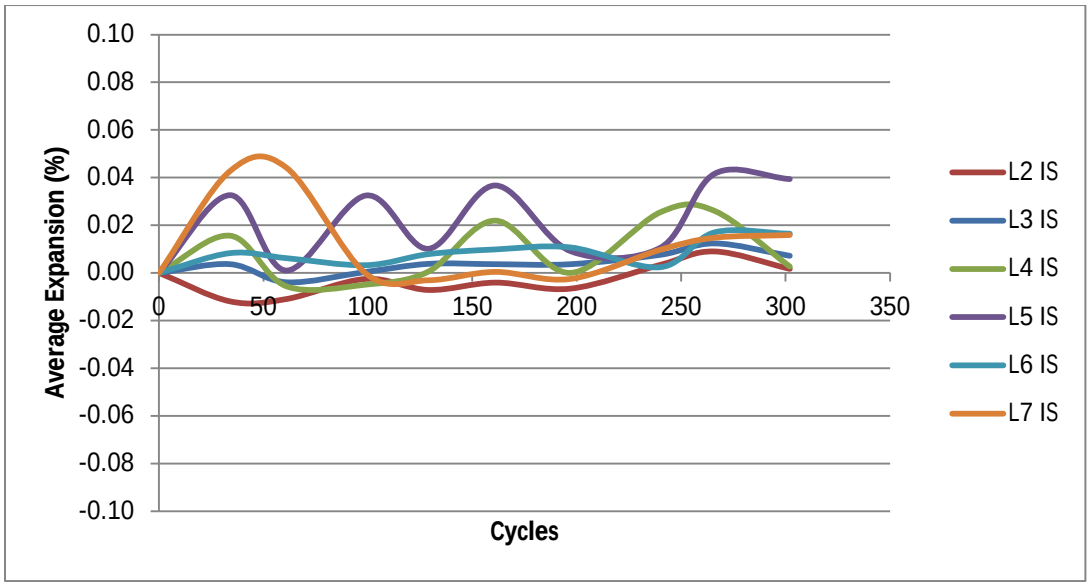

Figure F.2: Average Length Change of Salt-Immersed Samples

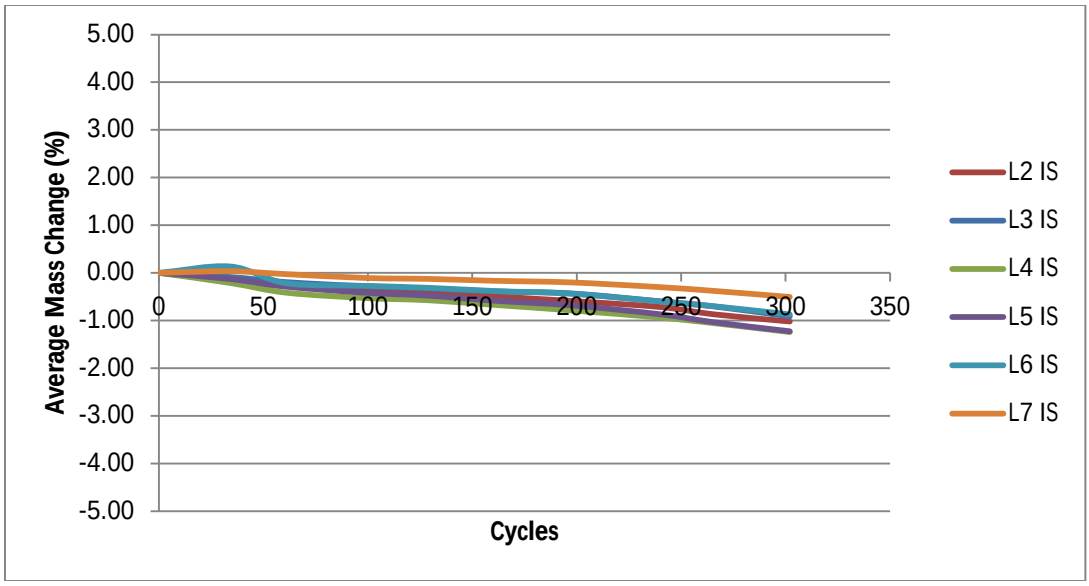

Figure F.3: Average Mass Change of Salt-Immersed Samples

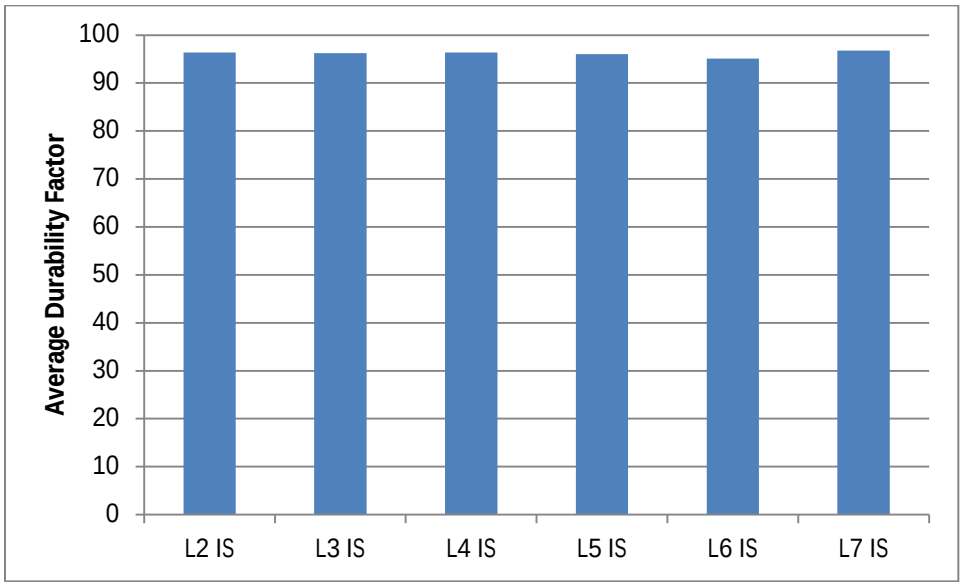

Figure F.4: Durability Factors of Salt-Immersed Samples

Figure F.5: L2 Half-Immersed Concrete Prism

Figure F.6: L3 Half-Immersed Concrete Prism

Appendix G: Phase II ASTM C666 Results

Average changes in concrete prism mass for each aggregate set are plotted in Figures G.1a through G.1l.

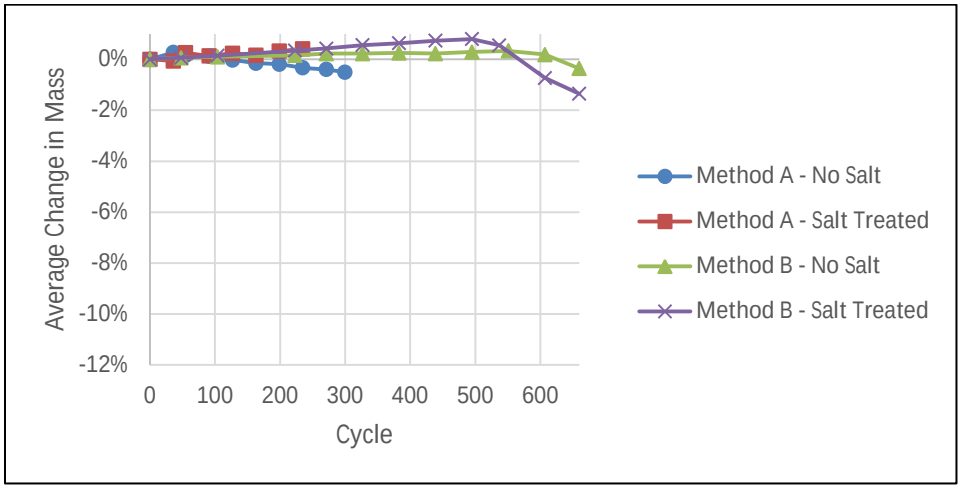

Figure G.1a: Average Change in Mass: Penny's Aggregates Samples

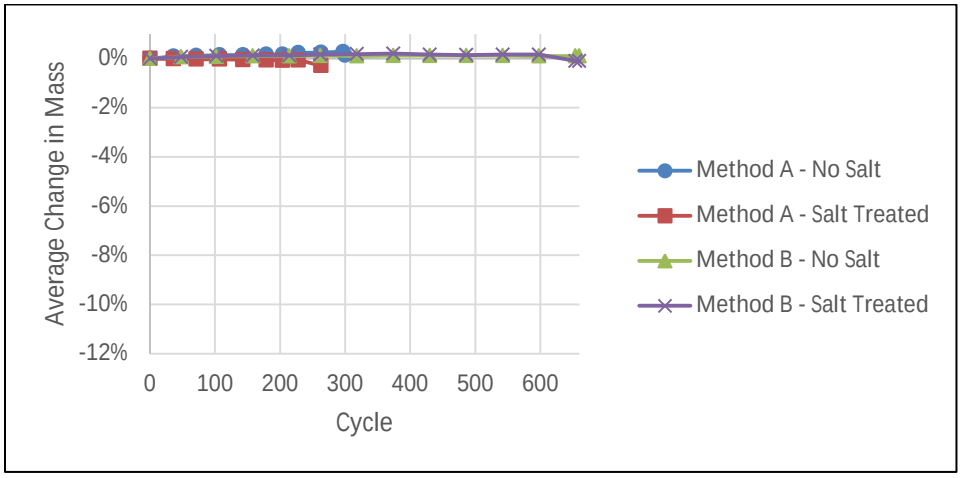

Figure G.1b: Average Change in Mass: Eastern Colorado Aggregates Samples

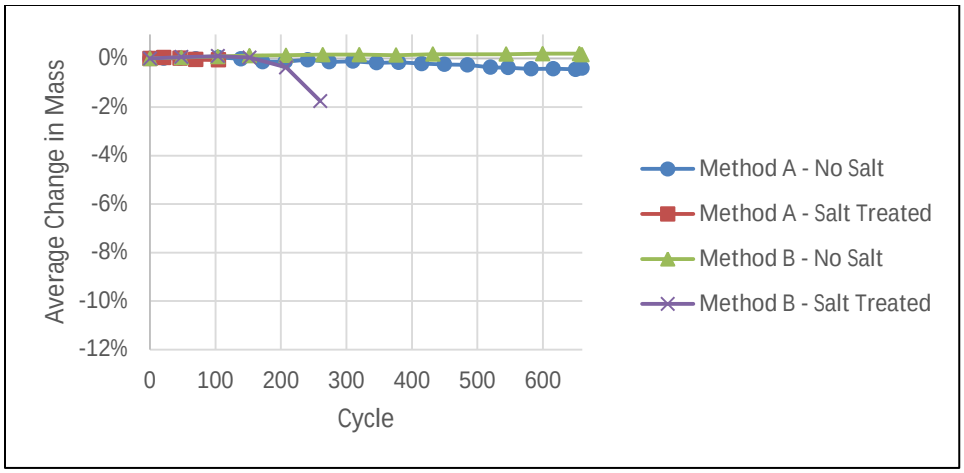

Figure G.1c: Average Change in Mass: Jasper Stone Samples

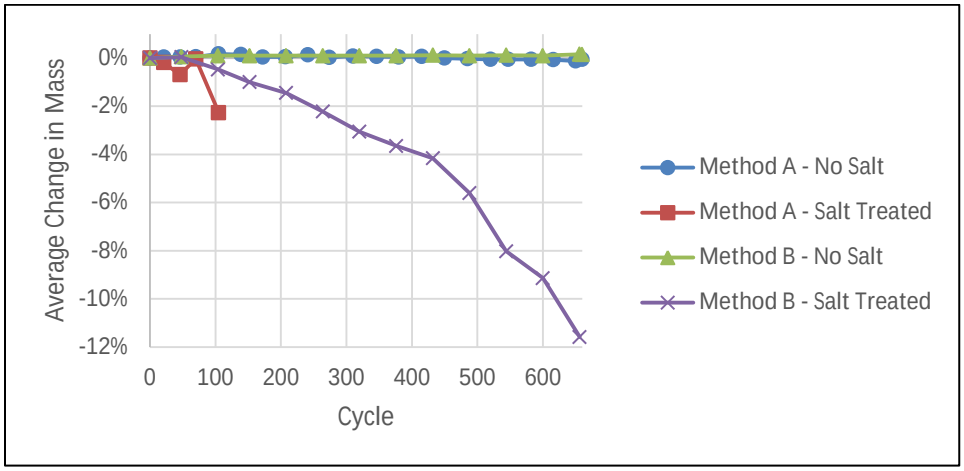

Figure G.1d: Average Change in Mass: Bayer Construction Samples

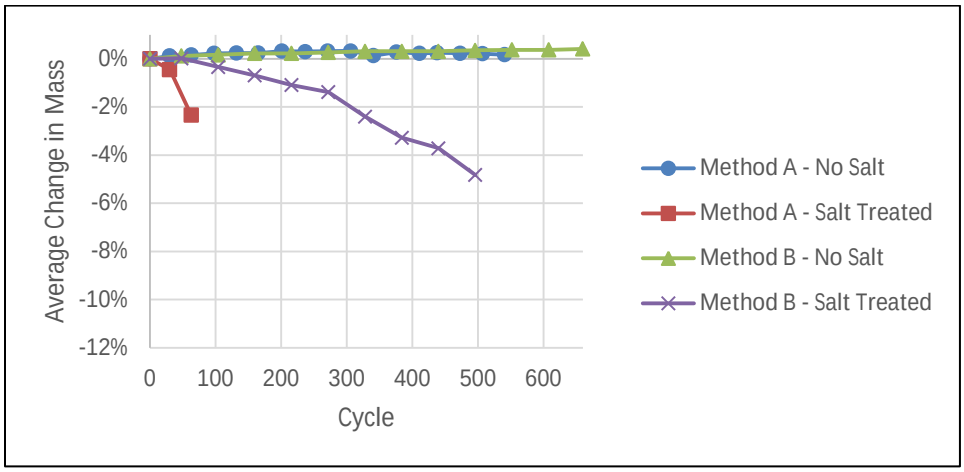

Figure G.1e: Average Change in Mass: Hamm WB Samples

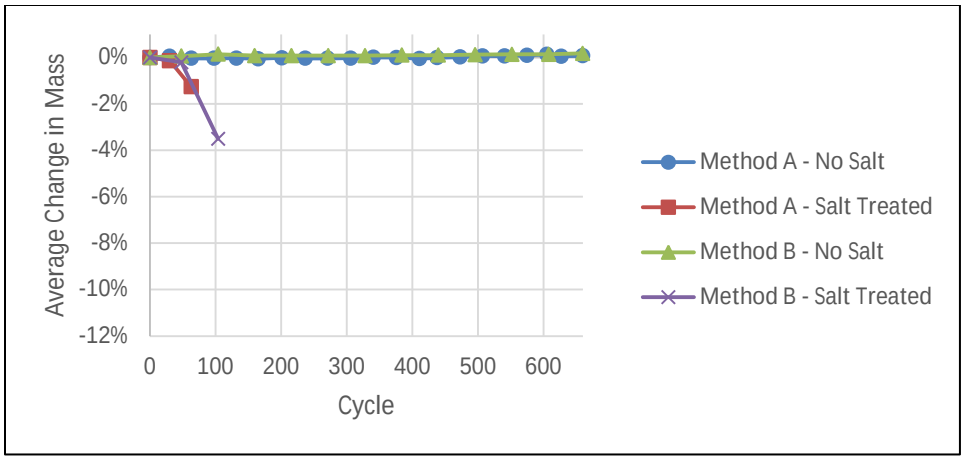

Figure G.1f: Average Change in Mass: Mid-States Materials - Edgerton Samples

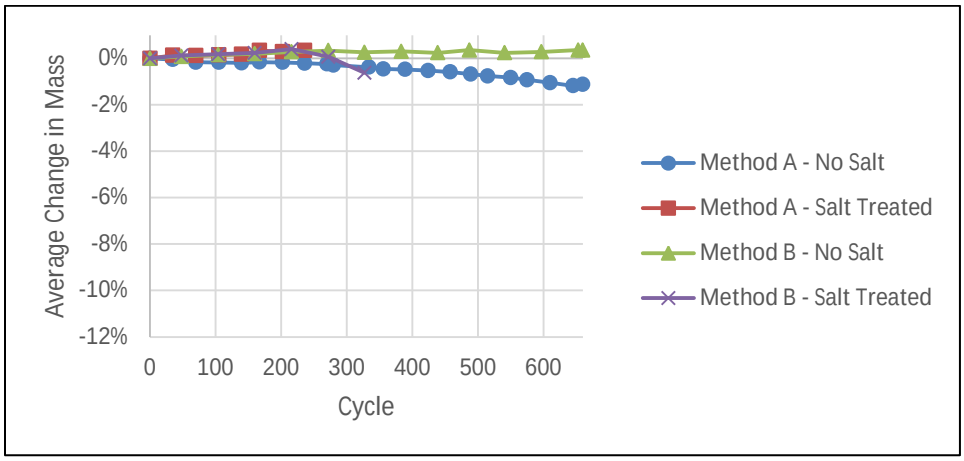

Figure G.1g: Average Change in Mass: Mid-States Materials - Plummer's Creek Samples Rock Bluff Bed

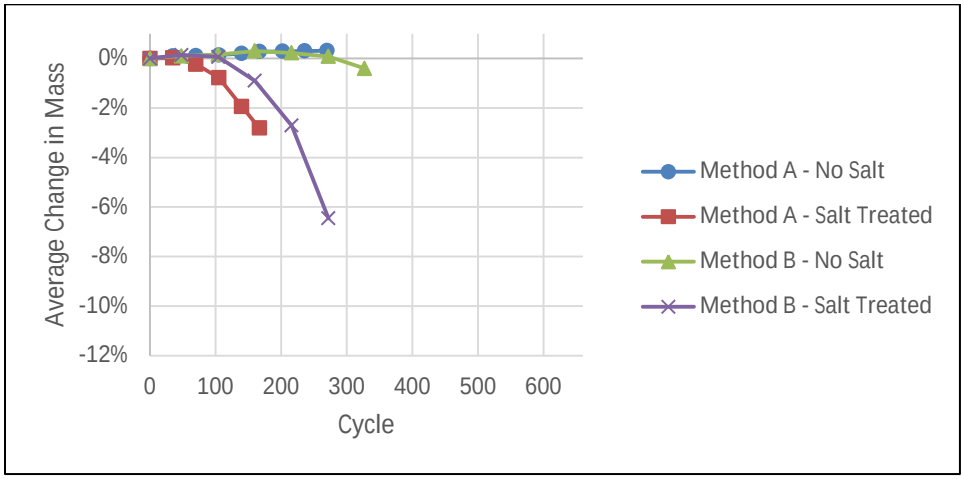

Figure G.1h: Average Change in Mass: Mid-States Materials - Plummer's Creek Samples Avoca Bed

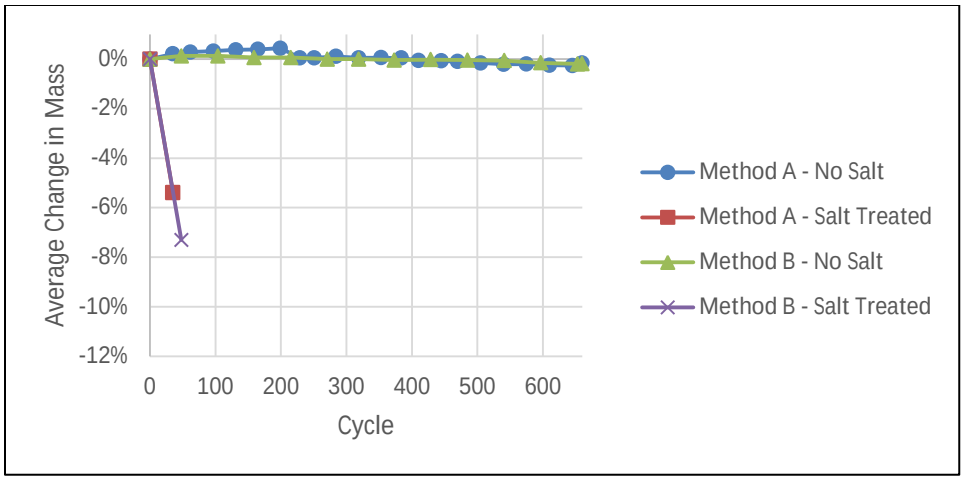

Figure G.1i: Average Change in Mass: Florence Samples

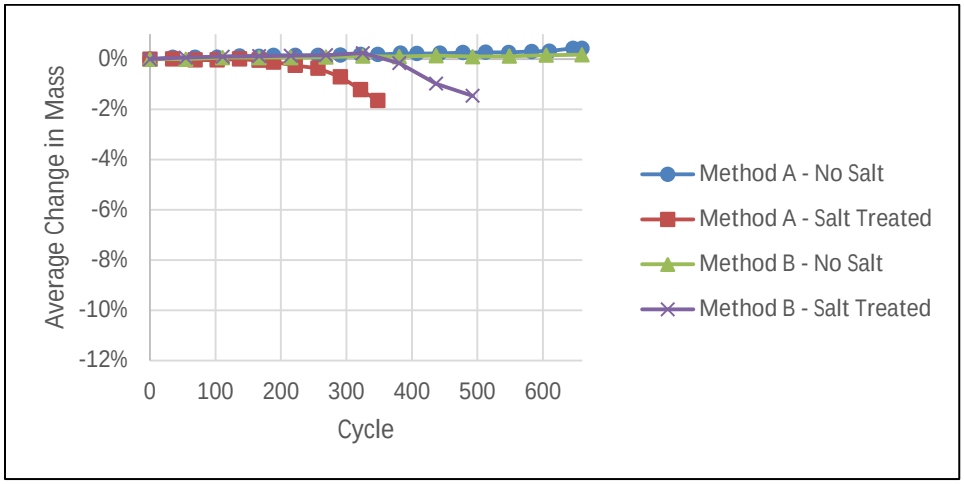

Figure G.1j: Average Change in Mass: Midwest Minerals - Parsons Samples

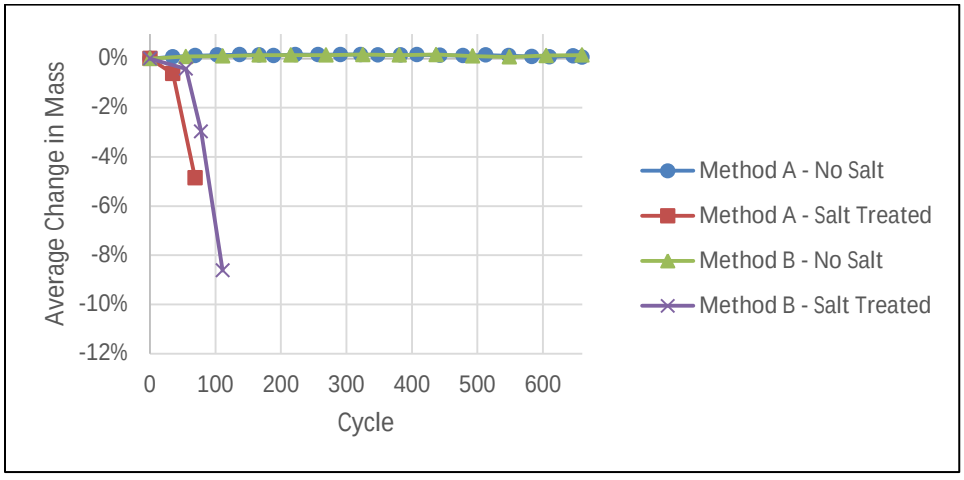

Figure G.1k: Average Change in Mass: Midwest Minerals - Fort Scott Samples

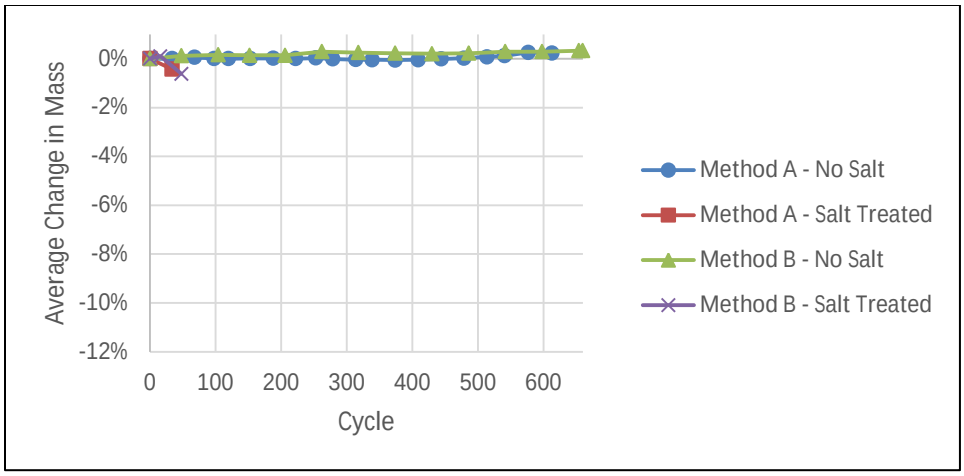

Figure G.1l: Average Change in Mass: Cornejo Stone Samples

The figures above illustrate that the most significant mass loss generally occurs in the salt-treated samples subject to method A testing. Surface scaling prominently contributes to this mass loss and can be seen in Figure G.2.

Figure G.2: Surface Scaling of Florence Aggregate Sample

Average concrete prism expansion for each aggregate set is plotted in Figures G.3a through G.3l.

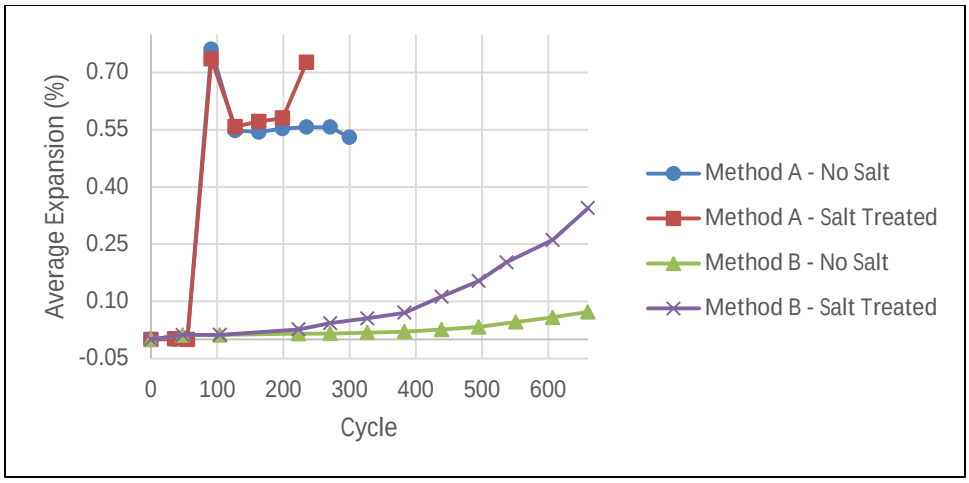

Figure G.3a: Average Expansion: Penny's Aggregates Samples

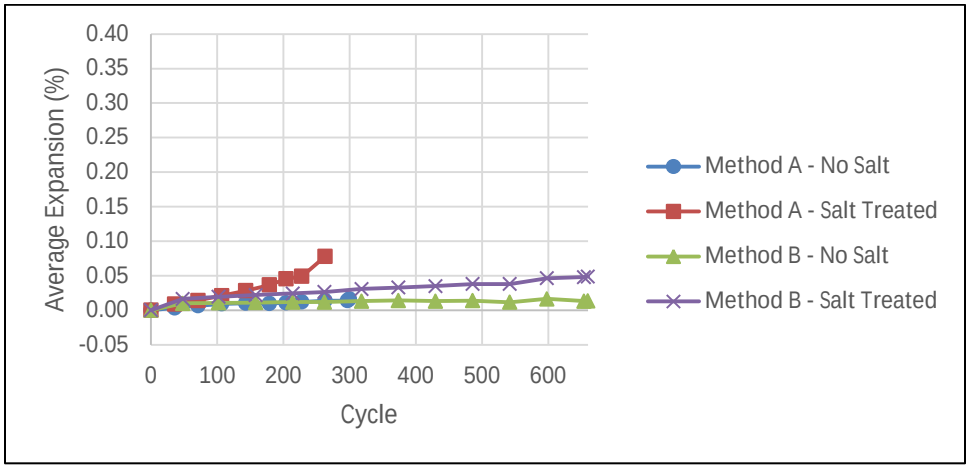

Figure G.3b: Average Expansion: Eastern Colorado Aggregates Samples

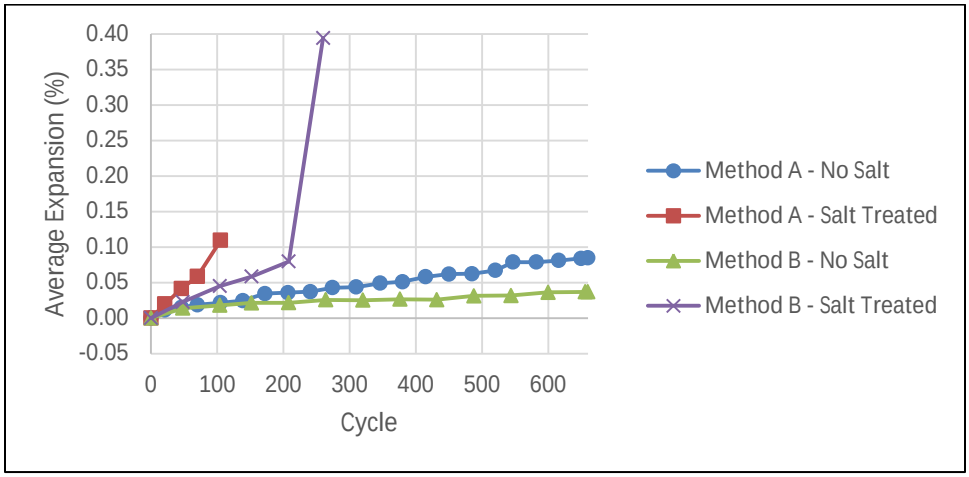

Figure G.3c: Average Expansion: Jasper Stone Samples

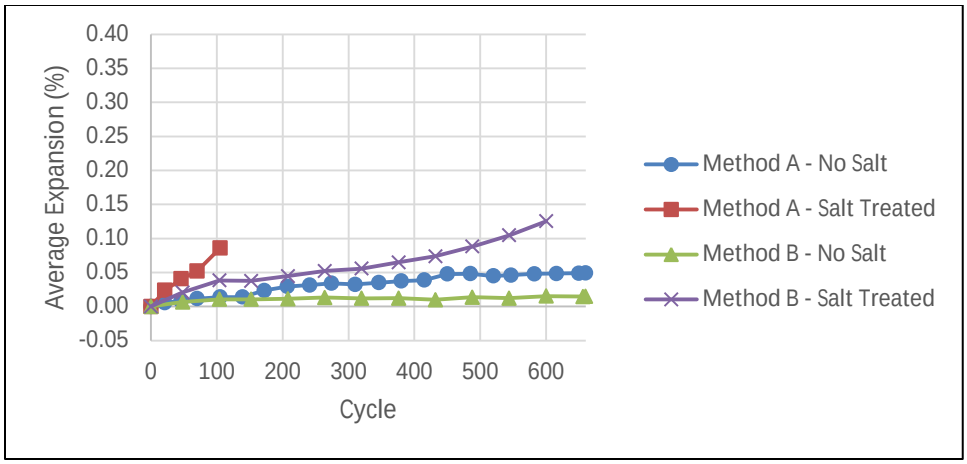

Figure G.3d: Average Expansion: Bayer Construction Samples

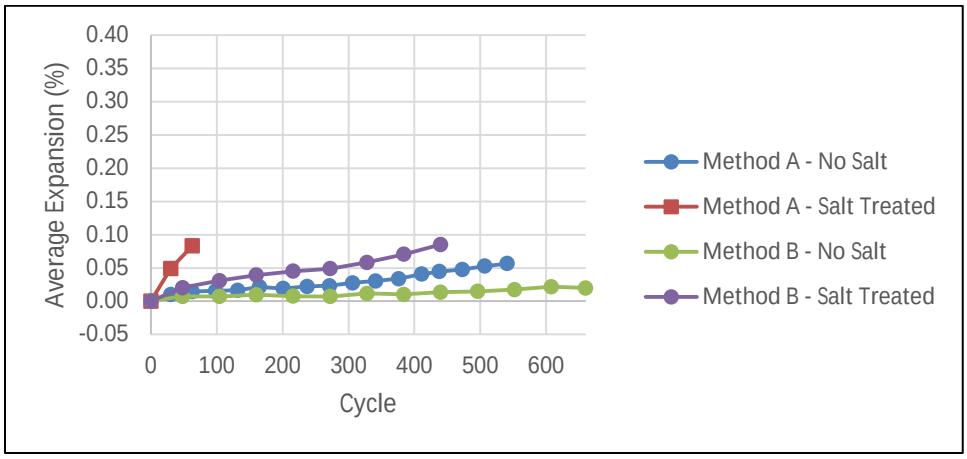

Figure G.3e: Average Expansion: Hamm WB Samples

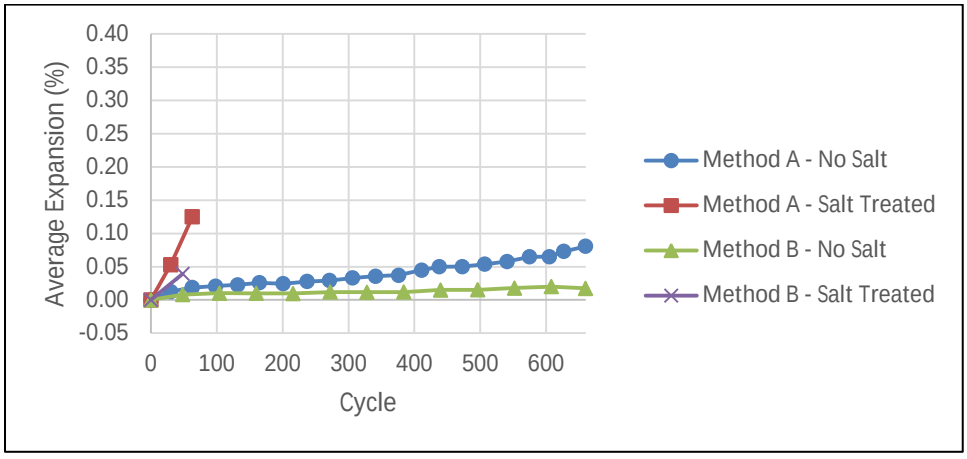

Figure G.3f: Average Expansion: Mid-States Materials - Edgerton Samples

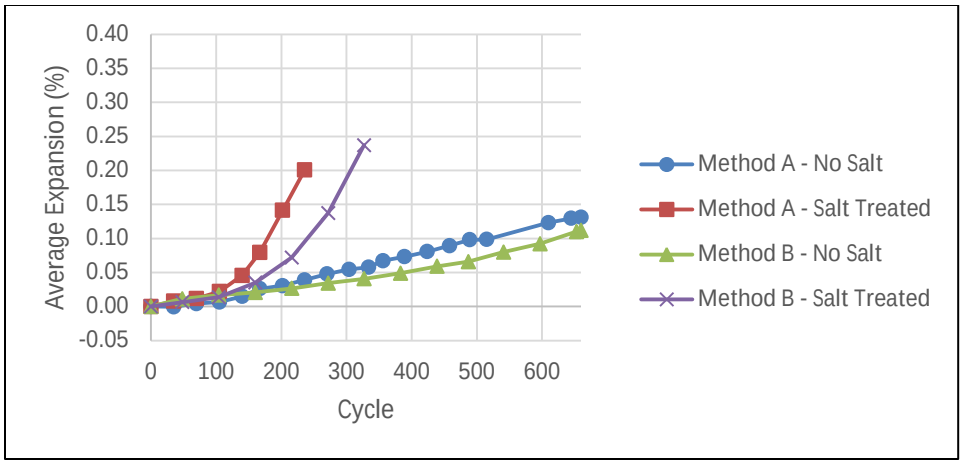

Figure G.3g: Average Expansion: Mid-States Materials - Plummer's Creek Samples, Rock Bluff Bed

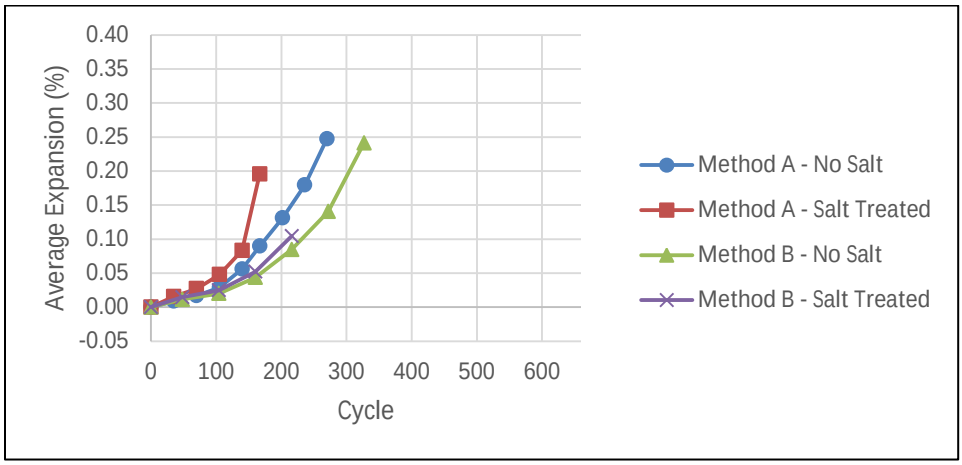

Figure G.3h: Average Expansion: Mid-States Materials - Plummer's Creek Samples, Avoca Bed

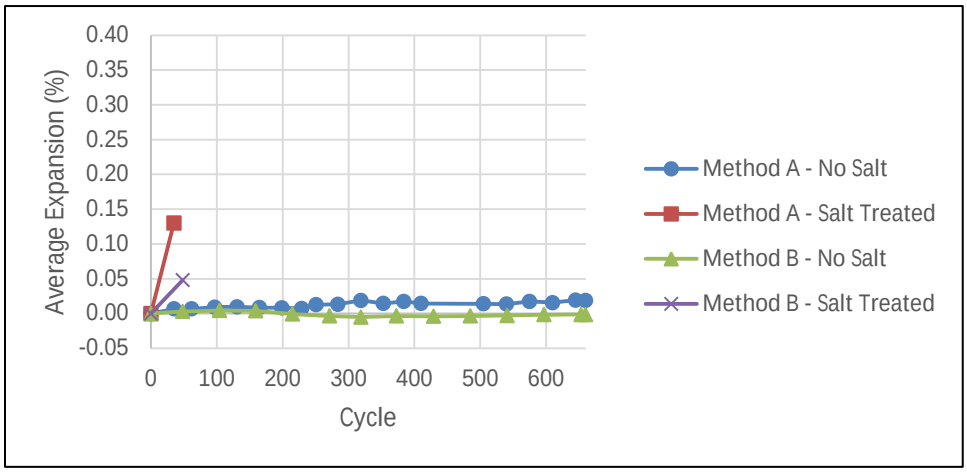

Figure G.3i: Average Expansion: Florence Samples

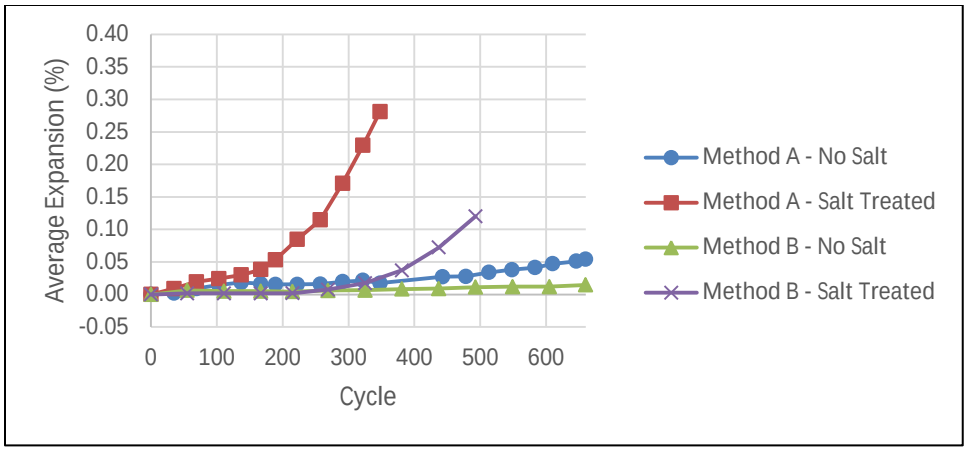

Figure G.3j: Average Expansion: Midwest Minerals - Parsons Samples

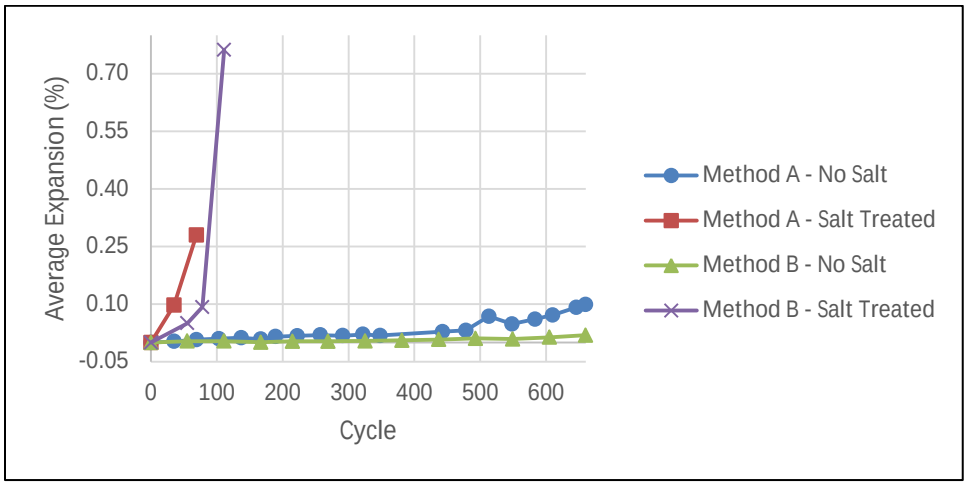

Figure G.3k: Average Expansion: Midwest Minerals - Fort Scott Samples

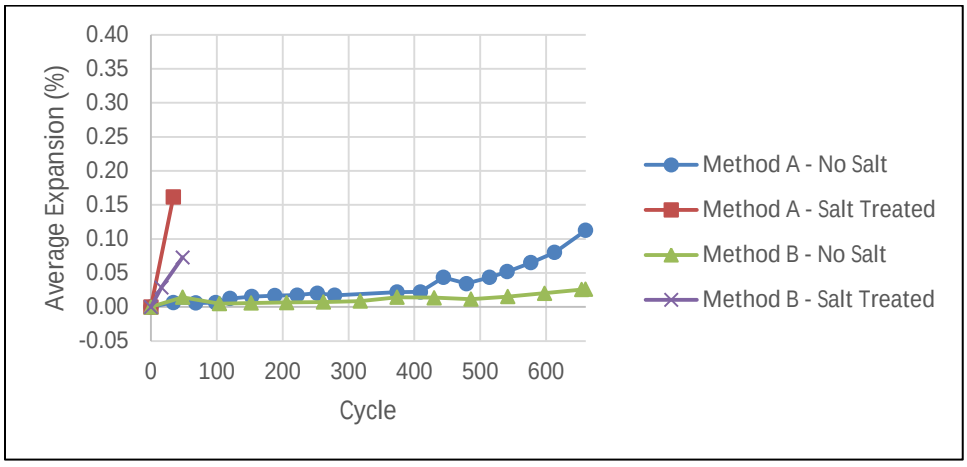

Figure G.3l: Average Expansion: Cornejo Stone Samples

Average relative dynamic modulus of elasticity (RDME) for each aggregate set is plotted in Figures G.4a through G.4l.

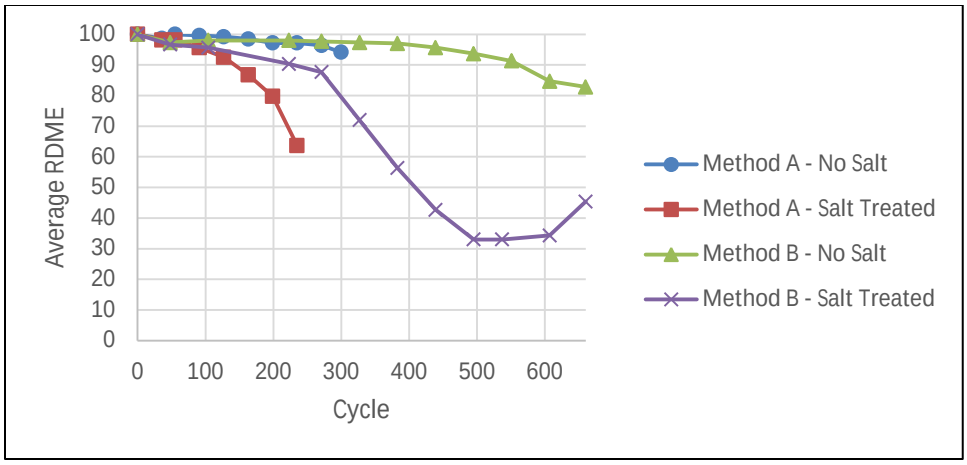

Figure G.4a: Average RDME: Penny's Aggregates Samples

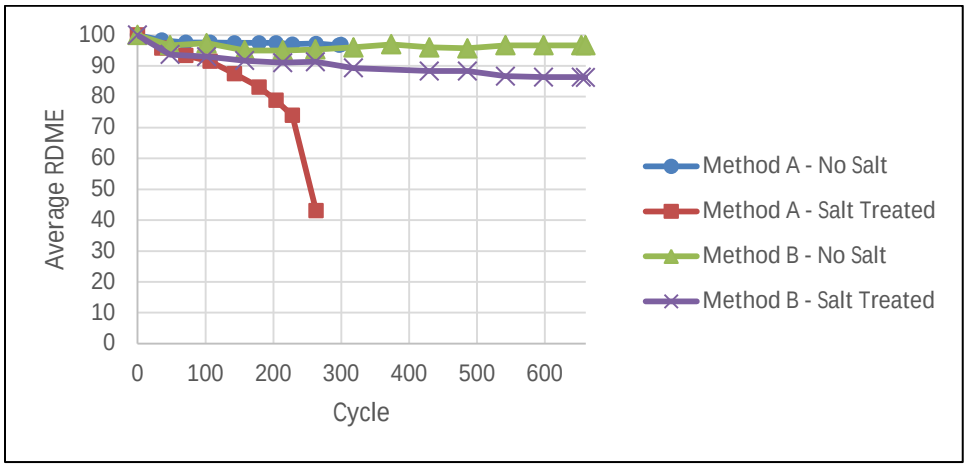

Figure G.4b: Average RDME: Eastern Colorado Aggregates Samples

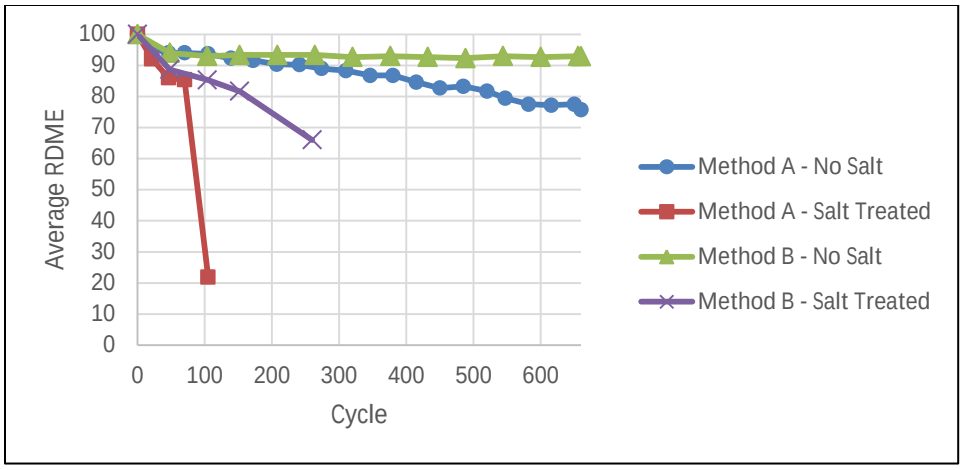

Figure G.4c: Average RDME: Jasper Stone Samples

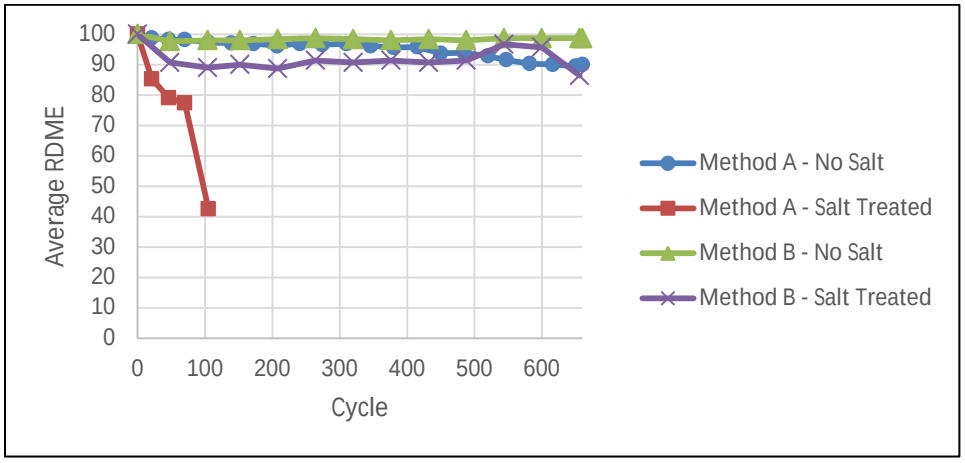

Figure G.4d: Average RDME: Bayer Construction Samples

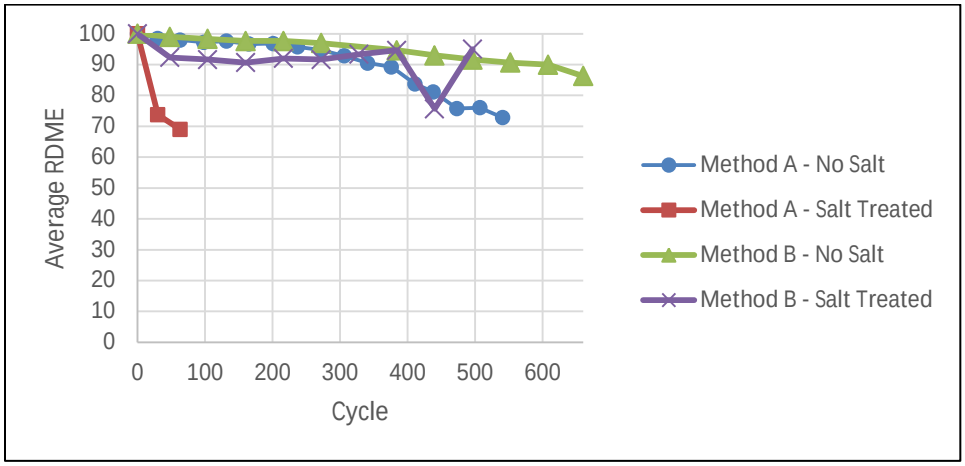

Figure G.4e: Average RDME: Hamm WB Samples

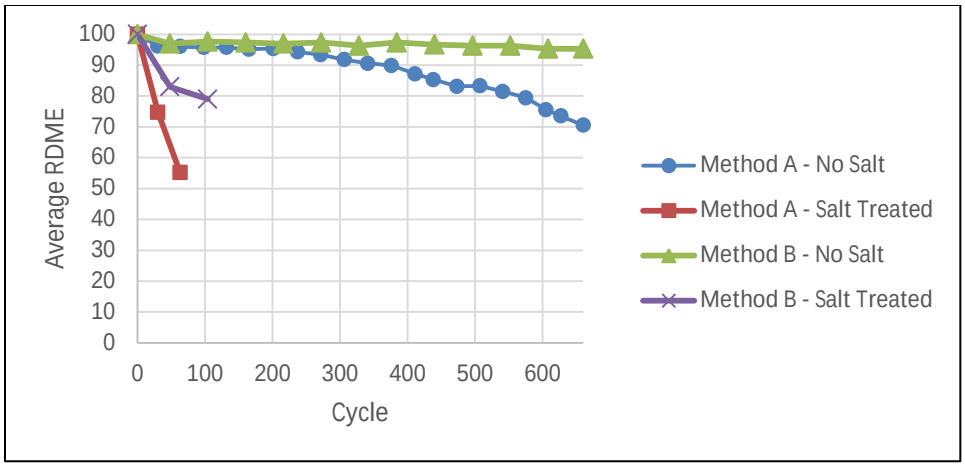

Figure G.4f: Average RDME: Mid-States Materials - Edgerton Samples

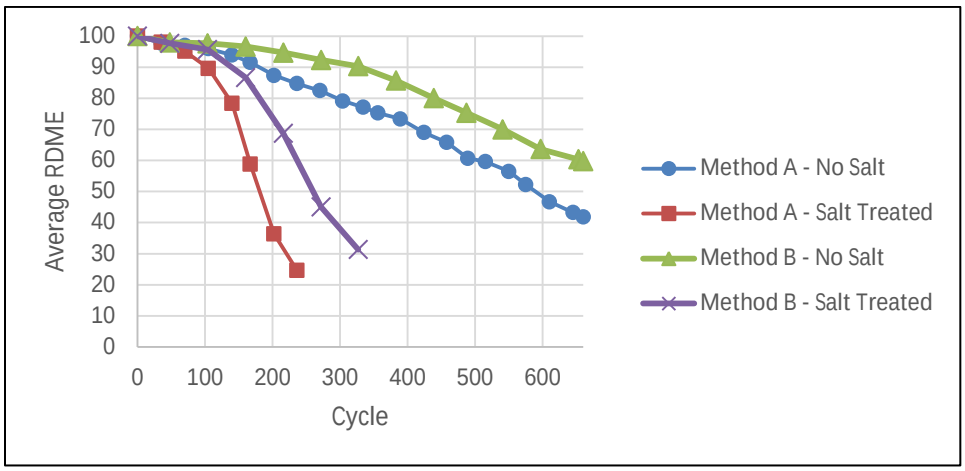

Figure G.4g: Average RDME: Mid-States Materials - Plummer's Creek Samples, Rock Bluff Bed

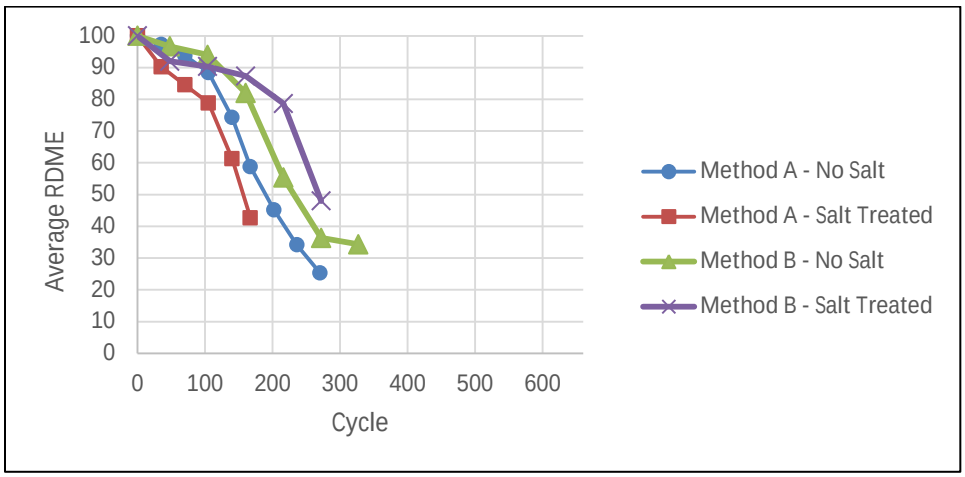

Figure G.4h: Average RDME: Mid-States Materials - Plummer's Creek Samples, Avoca Bed

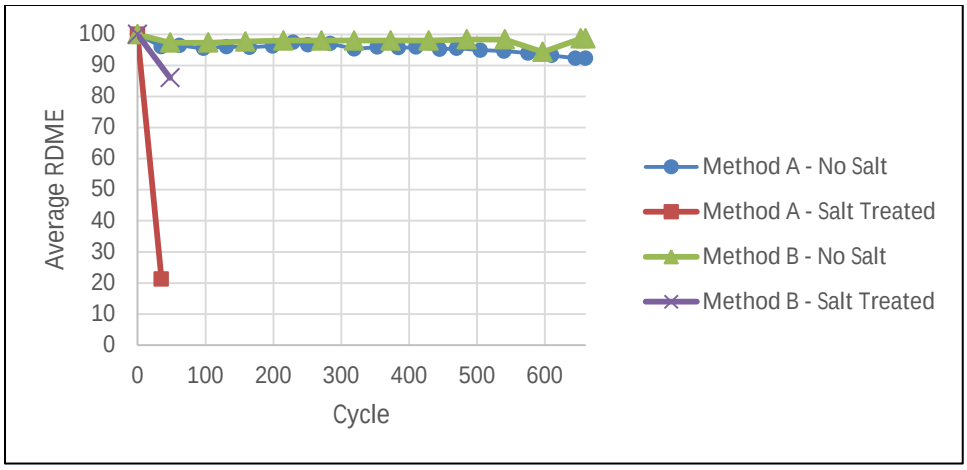

Figure G.4i: Average RDME: Florence Samples

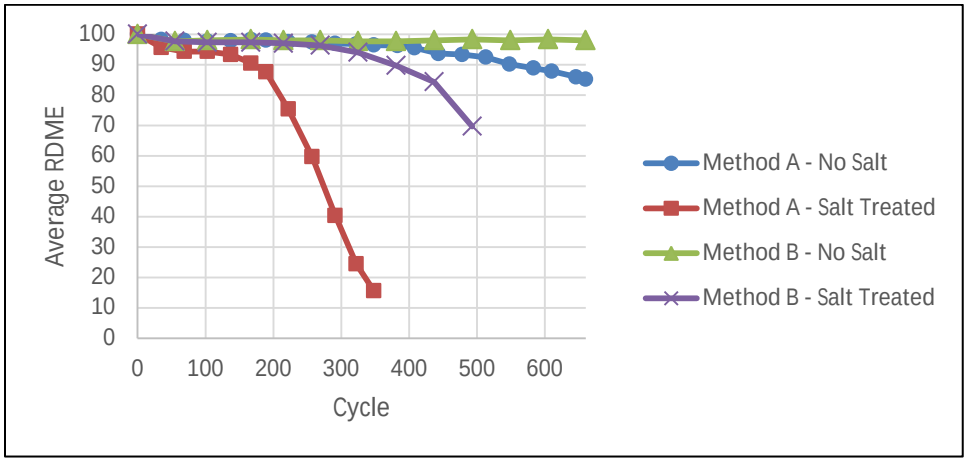

Figure G.4j: Average RDME: Midwest Minerals - Parsons Samples

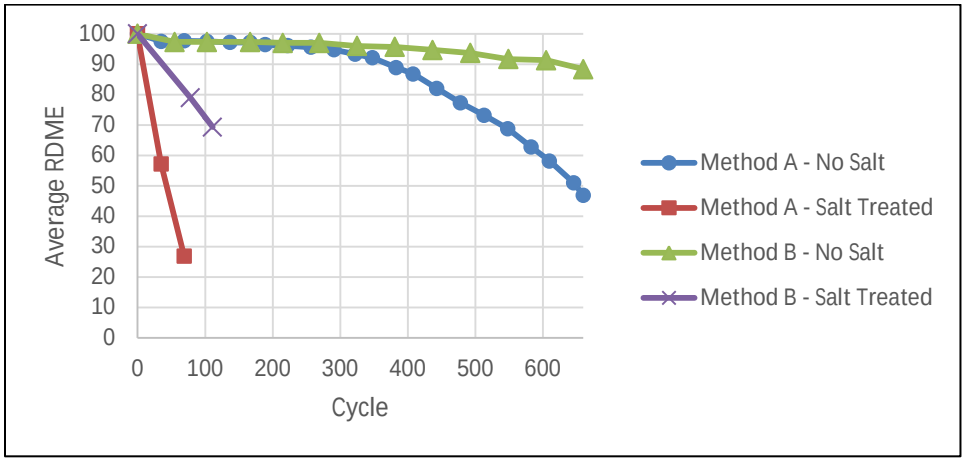

Figure G.4k: Average RDME: Midwest Minerals - Fort Scott Samples

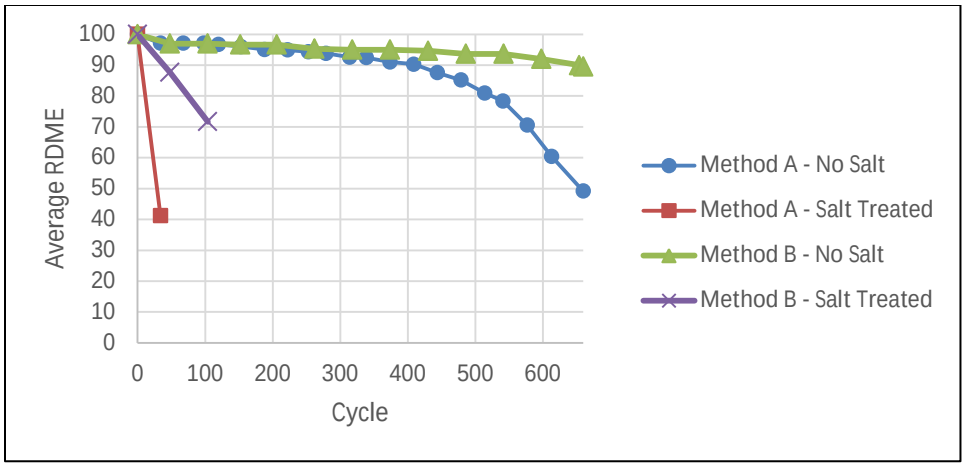

Figure G.4l: Average RDME: Cornejo Stone Samples

Appendix H: Permissions

The following is the copyright permission to reuse a figure from Darwin et al. (2008):

Dear Mr. Varner,

Thank you for your inquiry regarding the use of ACI-copyrighted material. You have ACI's permission to reuse the attached figure. Because rights for the figure were released to ACI upon publication, there is no need to also obtain permission from the authors. Please provide a statement similar to "Reprinted with permission from the American Concrete Institute," and credit the original authors, as appropriate.

Please let me know if you require any further documentation of this permission, or if you have any questions or concerns.

Best Regards,

Ashley

Ms. Ashley A. Poirier
Associate Editor
American Concrete Institute
38800 Country Club Drive
Farmington Hills, MI 48331 USA
Phone: (248) 848-3753
Fax: (248) 848-3701
E-mail: Journals.Manuscripts@concrete.org
Website: http://mc.manuscriptcentral.com/aci

From: Jonathan Varner <jvarner@k-state.edu>
To: Journals.manuscripts@concrete.org
Date: 07/30/2013 02:00 PM
Subject: Copyright permission for figure from report "Effects of Deicers on Concrete Deterioration"

Hello,

My name is Jon Varner and I am a graduate student at Kansas State University under Dr. Kyle Riding in the Civil Engineering Department. I am writing to ask permission to use the attached figure in my Master's thesis and the report for the Kansas DOT based on the research included in my thesis.

The citation for the article is as follows:

Darwin, D., Browning, J., Gong, L., and Hughes, S.R. (2007). "Effects of Deicers on Concrete Deterioration." ACI Materials Journal, 105(6), 622-627

The figure attached is from the full report rather than the article itself. Would the authors' permission be required as well?

Thank you,

Jon Varner

The following is the copyright permission to reuse a figure from Dubberke and Marks (1985):

Dear Mr. Varner:

The Transportation Research Board grants permission to reproduce one figure from the paper, "The Effect of Deicing Salt on Aggregate Durability," by W. Dubberke and V. Marks, in your Master's thesis, as identified in your request of July 30, 2013, subject to the following conditions:

1. Please cite paper publication in Transportation Research Record 1031 , Figure 5,

p. 30. Copyright, National Academy of Sciences, Washington, D.C., 1985.

2. Please acknowledge that the material is reproduced with permission of the Transportation Research Board.

3. None of this material may be presented to imply endorsement by TRB of a product, method, practice, or policy.

Every success with your Master's thesis. Please let me know if you have any questions.

Sincerely,

Javy Awan

Director of Publications
Transportation Research Board

Phyllis Barber
Transportation Research Board
Publications Office
202 334-2972 phone
202 334-3495 fax
pbarber@nas.edu

-----Original Message-----

From: Jonathan Varner [mailto:jvarner@k-state.edu]

Sent: Tuesday, July 30, 2013 1:35 PM

To: Barber, Phyllis

Subject: TRR Journal Online Copyright Question

Hello,

My name is Jon Varner and I am a graduate student at Kansas State University. I am writing to ask permission to use the attached figure in my Master's thesis and the report for the Kansas DOT based on the research included in my thesis.

The following is the citation for the source article of the figure:

Dubberke, W. and Marks, V. (1985). “The Effect of Deicing Salt on Aggregate Durability.” Transportation Research Record, No. 1031, 27-34

Is permission of the authors required as well?

Thank you,

Jon Varner

K-TRAN

KANSAS TRANSPORTATION RESEARCH AND NEW-DEVELOPMENT PROGRAM

AD ASTRA PER ASPERA

Kansas

Department of Transportation